Comparative studies on the cultivation of *Xanthomonas campestris* in submerged culture for the production of xanthan using the traditional industrial stirred tank reactor and a novel oscillatory baffled bioreactor

Ebtihaj J. Jambi

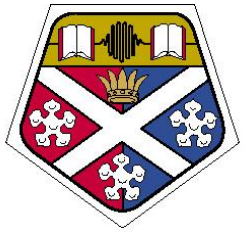

Thesis submitted for the degree of Doctor of Philosophy
On the completion of research in the
Strathclyde Fermentation Centre
Strathclyde Institute of Pharmacy and Biomedical Sciences
University of Strathclyde
Glasgow, Scotland

2012

Abstract

Xanthan is a well-known extracellular polysaccharide, produced by a Gram negative bacterium *Xanthomonas campestris* (*X. campestris*) under aerobic conditions. Solutions of xanthan exhibit high viscosities and non-Newtonian behaviour even at low concentrations. This biopolymer has a wide range of valuable commercial and industrial applications, for example; it can be used as a food thickening agent and a stabilizer in some other industries. Traditionally the production of xanthan has predominantly been performed in stirred tank fermenter (STR).

This study sought to compare the cultivation of the bacterium, *X. campestris* for the production of the viscous biopolymer xanthan gum in two different reactor systems, a novel oscillatory baffled reactor (OBR) and the conventional industry workhorse, the stirred tank reactor (STR).

Overall biopolymer production occurred at similar rates in the well stirred and aerated STRs, albeit at the cost of higher energy inputs for mixing and aeration. Despite much previous literature promoting the use of the OBR for transporting and reacting very viscous systems, this was the first actual study attempting to investigate the use of the OBR for a highly viscous non-Newtonian fermentation process. The experimental results show that xanthan production was similar in the OBR than in the STR, the OBR is however readily suitable for the cultivation of xanthan. The probable reasons for the inability of the OBR to match the production rates of the STR may well lie in the complex nature of this fermentation process. Unlike a

previous study on pullulan production (Gaidhani 2004) where the OBR outperformed the STR, *X. campestris* initially needs high oxygen transfer rates and the OBR, although it provides good bulk mixing and low energy consumption, seemed unable to equal the STR in this respect, especially in a very viscous system. The result shows that xanthan production in the OBR was similar to the equivalent process in the STR.

In order to attempt to improve the OBR a number of technical modifications were made including a novel sparger design to improve gas dispersal. These were not successful in improving xanthan production. Similarly, attempts to achieve improvements via wider amplitude ranges led to damage to the equipment.

The conclusion was that significant improvements to the physical robustness of the OBR were necessary before it could be successfully used to process highly viscous bio-fluids.

Acknowledgment

I would like to express my sincere gratitude to my supervisors, Professor Brian McNeil and Dr. Linda Harvey, for their continuous support, encouragement and guidance throughout my studies at University of Strathclyde It was a great pleasure for me to conduct this dissertation under their supervision words fall short to express my regards and respect towards them. I am deeply indebted to Professor Xiong-Wei Ni who provided us the OBR and the constructive comments during my dissertation time.

I cannot thank enough all my colleagues and friends from different countries and cultures for making these years in Glasgow unique and unforgettable. Thank you all for creating such a pleasant and friendly atmosphere, inside and outside the lab. Special thanks to Manal Eshelli, Tantima Kumlung, Ioannis Voulgaris, Peter Gardner, Ivo Kretzers, Melissa Black and Dr. Mariana Fazenda, I am also thankful to the lab technician, Walter McEwan, for the excellent technical support and many others need special thanks for always being helpful and technical support for making the OBR running and the experimental set-up. Special thanks to Dr Bassem Sabaa for offering the MW estimation.

I would like to share this moment of happiness with my family. I feel a deep sense of gratitude for my father Jamaludeen Jambi, who emphasized the importance of education and encouraged me to pursue the highest levels of education. I am deeply indebted to my uncle Abadi Falemban who formed part of my vision and taught me the values of hard work by his own example. I am grateful for my Mum, sisters, brother, nieces, nephews, aunties and uncle for giving me the sense and the value of the family. I am also thankful to my friends in Glasgow and in sweet SUMSA you were my family here in Glasgow. Special thanks go to my Dr Zino for the encouragement and patience through all my post studies in Glasgow.
Finally I would like to thank King Abdulaziz University in Jeddah for the funding provided throughout this study.

Copyright declaration

Abbreviations

Abbreviations

ALR	Air lift reactor
CPBR	Centrifugal packed-bed reactor
DCU	Digital control unit
DCW	Dry cell weight
DOT	Dissolved oxygen tension
EOR	Enhanced oil recovery
ESP	Extra-cellular polysaccharides or exopolysaccharides
FDA	Food and drug administration
GPC	Gel permeation chromatography
ICIS	International construction information society
LLS	Laser light scattering
LRT	Large rushton turbine
NRRL	Northern regional research laboratories
OBC	Oscillatory baffled column
OBR	Oscillatory baffled Reactor
OFN	Oxygen free nitrogen
PBS	Phosphate buffered saline
PID	Proportional integral derivative
PJR	Plunging jet reactor
PMD	Prochem maxflo T
RPC	Reciprocating plate column
SEC	Size exclusion chromatography
SRGT	Scaba 6S RGT
SRT	Standard rushton turbine
STR	Stirred tank reactor
UV	Ultra violet
v/v	Volume per volume

w/v	Weight per volume
X. campestris	*Xanthomonas campestris* species as indicated
YM	Yeast malt

Nomenclatures

λ	Wave length (nm)
C_D	Discharge coefficient
D	Column diameter (m)
D/T	Diameter tank ratio
D.O	Dissolved oxygen
D_S	Diameter of impeller (m)
f	Frequency (Hz)
IV	Intrinsic viscosity (dl/g)
Mn	Number average molecular weight (kDa)
Mw	Weight average molecular weight (kDa)
Mw/Mn	Polydispersity
N	Rotational speed of the impeller (rpm)
N_b	Number of baffles per unit length
P/V	Power density kW/m^3
P_o	Number power of the impeller
Rh	Hydrodynamic radius (nm)
rpm	Revolutions Per Minute
rx	Growth rate (g/l/h)
St	Strouhal number
V_v	Volume (m^3)
x_o	Amplitude (m)
α	Ratio of effective baffle area to tube area
μ	Fluid viscosity (kg/m/s)
μm	Micro mole
ρ	Fluid density (kg/m^3)
ω	Angular frequency (rad/s)

Chemicals

$CaCO_3$	Calcium carbonate
$FeCl_3.6H_2O$	Ferric chloride hexahydrate
H_3BO_3	Boric acid
HCl	Hydrochloric acid
KH_2PO_4	Potassium di-hydrogen phosphate
$MgCl_2.6H_2O$	Magnesium chloride hexahydrate
Na_2SO_4	Sodium sulphate
NaOH	Sodium hydroxide
NH_4NO_3	Ammonium nitrate
ZnO	Zinc oxide

List of figures

List of Tables

List of Content

Chapter 1

Introduction

1 Introduction

Natural gums are carbohydrate polymers or polysaccharides of natural origin and can be called biopolymers. The biopolymers have a number of unique chemical and physical properties mainly the capability of causing an increase in viscosity when added in the solution even at small concentrations. In the industry they are used as thickening agents, gelling agents, emulsifying agents, stabilizers, adhesives, binding agents, crystallisation inhibitors, clarifying agents, encapsulating agents, flocculating agents, swelling agents, foam stabilizers. They can be produced by biological systems (i.e. micro-organisms, plants and animals) and can be classified according to their origin. They can also be classified as uncharged or ionic polymers (polyelectrolytes).

Terrestrial and marine plant polysaccharides were the first biopolymers discovered, such as gum Arabic, seaweed and carrageenan (Therkelsen, 1995). The quality and quantity of the plant gums are subject to seasonal variation, moreover they are costly and require skilled efforts to cultivate and recover/purify. Many new and useful gums of scientific and commercial interest have been discovered during the second half of the 20^{th} century, which can be obtained more conveniently from microbial sources. A great deal of interest has been shown in the ability of micro-organisms to produce exopolysaccharides (EPS) as potential substitutes for plant derived gums, since they can be produced under controlled conditions from selected species using both renewable and biodegradable sources. These factors have accelerated the use of microbial gums (Steinbuchel and Rhee, 2005). While dextran

was the first microbial polysaccharide to be commercialized, and to receive approval for food use, several such microbial polymers such as gellan, welan and xanthan now have a variety of commercial uses (Baird *et al.,* 1983).

Microbial polysaccharides, which serve different functions in a microbial cell, may be broadly grouped into three types:

- Extra-cellular polysaccharides or exopolysaccharides (EPS), which can be found either as capsule that envelopes the microbial cell or as an amorphous mass (slime) which is secreted and accumulates outside the cell wall
- Structural polysaccharides, which can be part of the cell wall itself
- Intracellular polysaccharides, which may represent storage compounds for carbon and energy for the cell (Moo-Young, 1985).

Xanthan gum is an extracellular microbial polysaccharide of great commercial significance and was discovered in the late 1950s at the northern regional research laboratories (NRRL) of the United States Department of Agriculture, in the course of a screening operation which aimed at identifying micro-organisms that produced water-soluble gums of commercial interests. The polysaccharide xanthan gum is a secondary metabolite of the plant pathogenic bacterium *Xanthomonas campestris* (NRRL B-1459) (Rogovin *et al*., 1961).

During the 1960s extensive research was carried out in several industrial laboratories. Xanthan gum first became available commercially in the US in 1964. Toxicological studies showed that xanthan gum is non-toxic and does not inhibit

growth or cause skin or eye irritation, on this basis, the US food and drug administration (FDA) and generally recognized as safe (GRAS) approved its use as a food additive without any specific quantity limitation (Kennedy and Bradshaw, 1984). Later on the EU approved it for use in foods under the E number E415 in 1982. Today ICIS listed over 140 companies as making xanthan gum. The major producers of xanthan gum are Merck, Pfizer and Archer Daniels Mills (ADM) in the United States, CP Kelco in UK Danisco in Danmark, Rhone Poulenc in France, and Jungbunzlauer in Austria, the major xanthan gum producer in China is Deosen. Annual volumes worldwide were estimated to be about 35,000 tons in 2001 (Steinbuchel and Rhee, 2005) and currently 40-50,000 tons per year. Xanthan gum market is increasing significantly because the biopolymer has a versatile properties and application in deferent industrial fields such as food, pharmaceuticals, agriculture, oil drilling and enhanced oil recovery (See Table 2.1).

The production of xanthan gum from *Xanthomonas campestris* generally involves the uptake of carbon source (glucose in the present study), oxygen and other nutrients from the medium to produce exopolysaccharide (EPS). This envelopes the microbial cell as a capsule for protection, which leads to an increase in the medium viscosity, and hence a decrease in the mass transfer of nutrients and oxygen to the cell leading to the decrease in the overall productivity.

In order to increase the productivity of xanthan gum and other biopolymers a large number of bioreactors have been invented to meet the increasing market

demands. The stirred tank reactor (STR) technology is still the most commonly used in xanthan gum production.

In the present study a relatively new reactor technology called oscillatory baffled reactor (OBR) will be examined, it is based on the superimposing periodic fluid oscillation onto a cylindrical tube containing evenly spaced orifice baffles and is a very different mixing technology from STR.

1.1 Motivation and objective of this work

This study is a continuing study started by the use a relatively new reactor the OBR in the bioprocesses (Gaidhani, 2004).

The objectives for this study are:

• To design and fabricate of a fully functional oscillatory baffled reactor (OBR) to produce a highly viscous biopolymer such as xanthan gum, as recommended in the previous study.

• To compare the performance of the two different fermenter types when used for a high viscosity process such as xanthan. In addition, to quantitatively analyse and describe of major nutrients cells growth and biopolymer production and compare the power consumption and the yield in both OBR and STR fermenters.

• To characterise the product molecular weight and relate this to power consumption in both OBR and STR.

1.2 Structure of the Thesis

This thesis is divided into six chapters and its structure is as follows. Following the introduction, Chapter 2 presents a literature review of the relevant reactors and xanthan synthesis. The design and setup of the OBR, as well as the modifications that have been done to the OBR will be described in Chapter 3, together with the materials and methods of laboratory procedures for cultivating the microorganism and monitoring fermentation progress. In Chapter 4, xanthan fermentation process in the shake flasks, the STR and the OBR and the effects of various operating parameters on growth and production are shown, and the results are compared and discussed in Chapter 5. Chapter 6 presents main conclusions of this work and suggestions for future work. In addition, a calibration graph of glucose is given in Appendix.

.

Chapter 2

Literature review

2 Literature Review

This chapter reviews the background literature that is relevant to the characterization of production of xanthan gum in various reactors and an OBR. It is divided into two parts: Section 2.1 Reactors and Section 2.2 Xanthan gum production.

2.1 Bioreactors

2.1.1 Introduction

The production of xanthan gum has been studied extensively in several industrial laboratories since the early sixties covering both batch and continuous operations culminating in semi-commercial production. Generally, batch production has been proven to work successfully instead of continuous production (Rogovin, and Cadmus, 1961; Silman and Rogovin, 1970; Moraine and Rogovin 1973; Leela and Sharma, 2000; Garcia-Ochoa *et al.*, 2000). Substantial commercial production began in early 1964. However, corresponding to the increased demands of industrial processes a large number of bioreactor types have been designed, however few are used in the bioprocessing industry.

Production of xanthan gum by the micro-organism *X. campestris* is accompanied by increased viscosities of the fermentation medium during growth and production phases. Often the medium becomes highly non-Newtonian in character as the process progresses, thus the selection of suitable and economical mixing mechanisms places additional constraints on reactor operation. There have been many attempts to increase xanthan productivity and lower energy costs by using new agitation designs, different impellers and new types or reactors (See below).

2.1.2 Stirred Tanks Reactor (STR)

Stirred tank reactor (STR) technology is still the workhorse of the fermentation and bio-processing industries worldwide, and has been utilised since the 1940s. These fermenters, even though they are considered to be well-characterized reactor types, are acknowledged to have a number of drawbacks or limitations (Misra and Barnett, 1987; Popovic and Robinson, 1993; Wang and McNeil, 1992; Rossi, 2001).

In general, these drawbacks worsen as scale of operation increases and with the rise in apparent viscosity of the process fluid. Among the drawbacks are: the high running costs due to continuous mechanical agitation, ineffective mass and momentum transfer in regions of the process fluid, and the possible occurrence of static and anoxic regions distant from the impeller zones (Solomon *et al.,* 1981; Funahashi *et al.,* 1987a, b, 1988a, b; Peters *et al.*, 1989, 1992; Saeed and Ein-Mozaffari, 2008). Furthermore, there may be a tendency to gas (air) channelling, leading to inadequate gas dispersion for viscous system such as xanthan (Charles, 1985; Atkinson and Mavituna, 1991; Scragg, 1991). Therefore, ideally broth homogeneity (good bulk mixing) is important to maintain optimal levels of dissolved oxygen, temperature and mass transfer throughout the reactor. By contrast, the agitation of non-Newtonian fluids such as xanthan in STR can result in the formation of a zone around the impeller of significant motion (called a cavern) with stagnant regions elsewhere. This size of the cavern is governed by the properties of the fermentation broth, power input, agitator design and speed as can be seen in figure

2.1 (Elson *et al.*, 1986; Elson, 1990; Galindo and Nienow, 1992, 1993; Jaworski *et al.*, 1994; Amanullah *et al*., 1998a; Liu *et al.*, 2010).

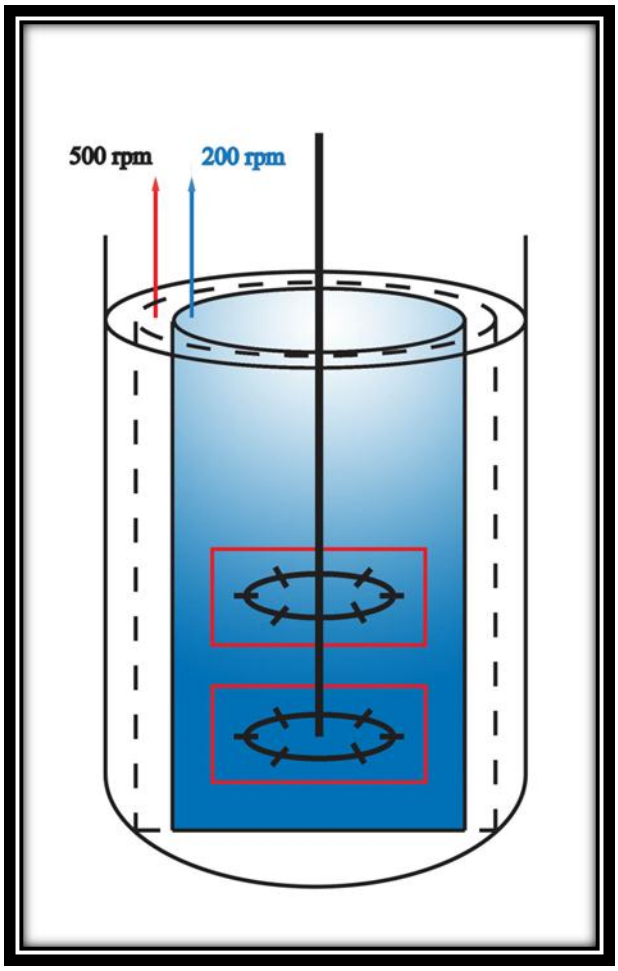

Figure 2.1: Illustration of decreasing oxygen availability with decreasing cavern size at 200 rpm compared with 5000 rpm. Note that dissolved oxygen occurs only within the caverns zone (Amanullah *et al*., 1998a).

The typical (STR) mainly consists of a glass or stainless steel vessel with side ports for pH, dissolved oxygen and temperature probes, as will be described in detail in chapter 3 Materials and methods. Different types of impellers can be used in the STR system as shown in figure 2.2. As in many industrial scale fermentation

processes, xanthan production has typically utilized radial flow impellers, such as turbines. Standard Rushton turbines (SRT) (In this study D/T ratio was 0.5) and the impellers are generally located on the stirrer shaft at a spacing of around one third tank diameter apart.

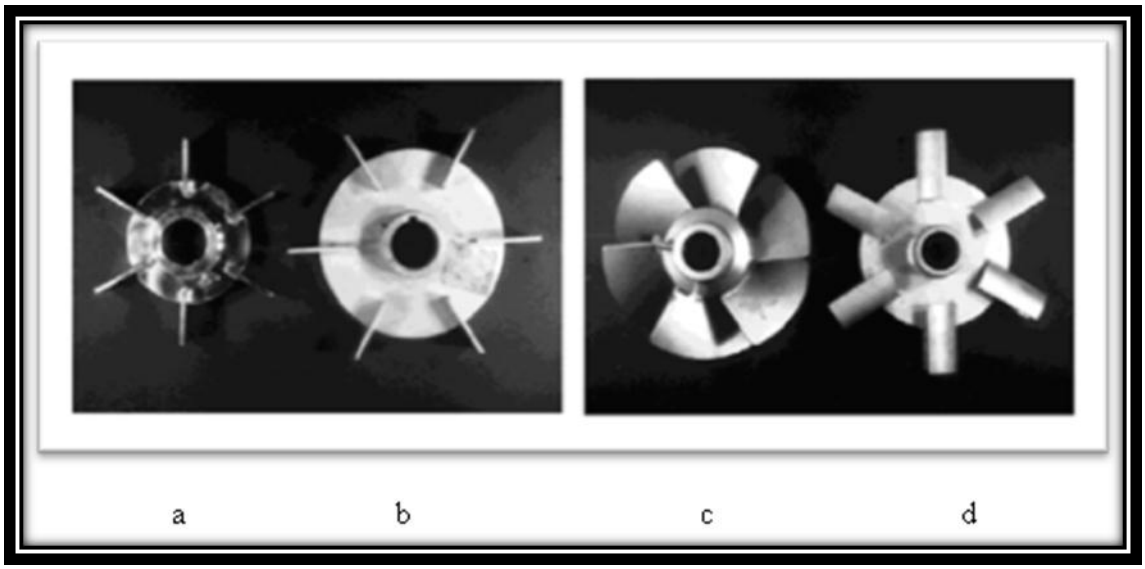

Figure 2.2: Different types of impellers (a) Standard Rushton Turbine (SRT), (b) Large Rushton Turbine (LRT), (c) Prochem Maxflo T (PMD), and (d) Scaba 6SRGT (SRGT) (Amanullah *et al*., 1998b).

From the literatures in small scales, standard rushton turbine (SRT) with D/T ratio of 0.33-0.5 typically used on an industrial scale are the most common impellers used for agitation in xanthan gum production because they have traditionally been extensively studied and are considered to be good at gas dispersion (Oldshue., 1960; Vant Riet and Smith, 1975; Solomon *et al.*, 1981; Nienow *et al.*, 1983; Amanullah *et al*., 1998b). Usually mass transport rates govern the aerobic bioprocess overall rate. In addition, the oxygen transfer rate has been often chosen as the main criterion for scaling-up and as a consequence the D/T ratios vary with the scale-up to ensure the gas dispersion and bulk binding in scaling up The disadvantages of this impeller,

especially in viscous broths, include its relatively large power consumption (Nienow and Elson, 1988). Due to the radial nature of the flow pattern, poor top to bottom mixing in multiple impeller systems leading to stratification (Solomon *et al.,* 1981; Kuboi and Nienow, 1986).

In 1998 Amanullah *et al.* studied the influence of different impeller types, at pilot scale, on the production of xanthan gum. They demonstrated that the agitator performance and the extent of bulk blending in xanthan fermentations is dependent on the properties of the fluid, power input, and agitator design is regarded as one of the limiting factors in the fermentation process. None of these criterions favoured the use of the standard rushton turbine; therefore they suggested that there are strong grounds to retrofit these STRs with either larger diameter impellers of similar design or with novel agitators.

An earlier study had also shown that as a result of the tendency to form caverns, two small SRT were much more energy efficient than a single impeller for bulk blending in non-Newtonian fluids (Solomon *et al.,* 1981). (In the present study two SRT with D/T ratio of 0.5 were used).

2.1.3 Other Reactors types

2.1.3.1 Air Lift Reactor (ALR)

Improvements in fermentation performance may be achieved by a better understanding of the limitations of bioreactors. From the findings of some of the

studies above, the need for alternative reactors is apparent for processing viscous fermentation fluids.

There has been a search for simpler, less expensive reactors, and especially in the processing of highly viscous non-Newtonian fluids, a large number of bioreactor types have been developed, in line with an increasing demand for the product over time.

One reactor type in which the reaction medium is kept mixed and gassed by introduction of air or another gas (mixture) at the base of a column is the air lift reactor (ALR); which often consists of a simple tower type reactor similar to bubble column reactors. ALR contain either inner draft tube (this kind is called "air-lift bioreactor with an internal loop) or external draft tube (this kind is called "air-lift bioreactor with an external loop) that make the recirculation loops increase bulk mixing, gas retention time, within a small reactor volume as shown in figure 2.3. Overall the use of non-mechanical agitation contributes to a reduction in energy consumption. In general the ALR is attractive for slow reactions such as the cultivation of some biological organisms and waste water treatment, but is also considered a poorly characterised reactor system. However such low-cost reactors in term of power consumption have been previously shown to be at least the equal of STR in the production of a range of exopolysaccharides (Wang and McNeil, 1992; Kang *et al.*, 2001). On the other hand Suh *et al.*, (1991) traced the poor performance of the air lift relative to STR in the production of xanthan gum to the lack of any

oxygen supply in the downcomer section, thus exposing the cultures to significant periods of oxygen limitation.

2.1.3.2 Plunging Jet Reactor (PJR)

In 1991 Zaidi *et al.*, used a plunging jet reactor (PJR) (Figure 2.4) for the production of the xanthan from *X. campestris*. The results showed similar specific growth rates to those in other reactor types at lower specific power inputs. They reported that the microorganism was not affected by the pump shear forces furthermore the oxygen sorption efficiency was better in the jet reactor, and this overcompensated for the effects of poor mixing in the wall region at high xanthan concentrations. On the other hand at higher gum concentrations low heat transfer rates in the fermenter walls resulted in poor mixing outside the plume region. This could lead to local oxygen limitation in dead zones.

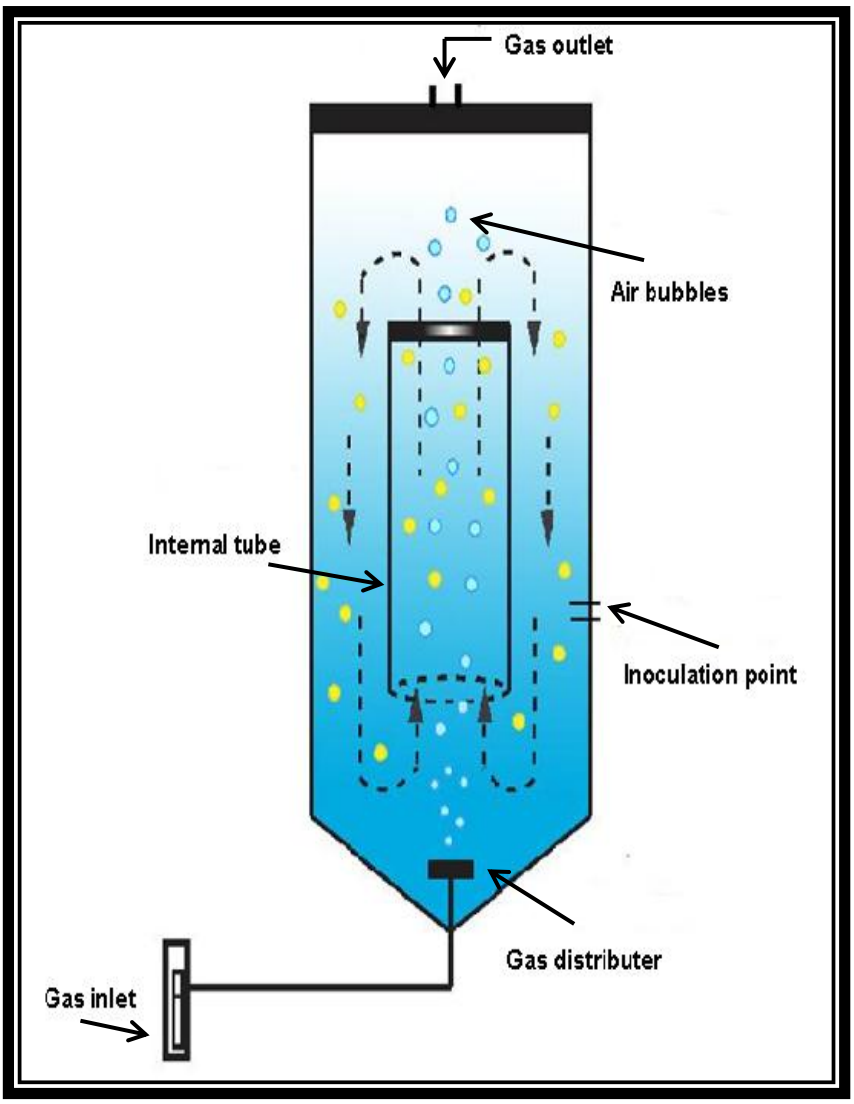

Figure 2.3: Schematic presentation of the experimental Air Lift Rector (ALR) with internal recirculation loop.

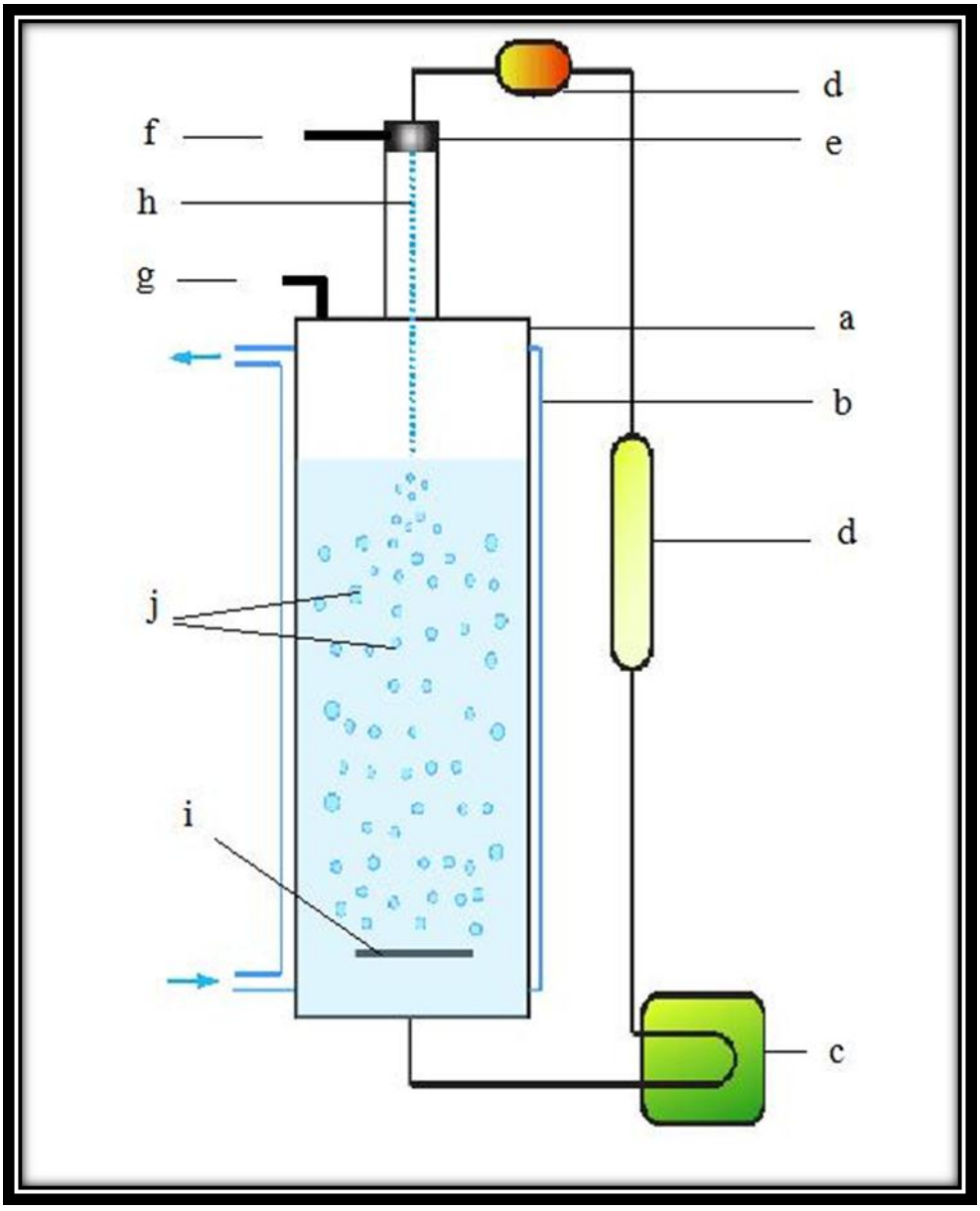

Figure 2.4: Schematic presentation of the experimental Plunging Jet Reactor (PJR). (a) Vessel. (b) Cooling jacket. (c) Peristaltic pump. (d) Damper. (e) Magnetic inductive flowmeter. (f) Nozzle. (g) Gas inlet. (h) Gas outlet. (i) Plunging liquid jet. (j) Baffle. (k) Gas bubbles.

2.1.3.3 Centrifugal Packed-Bed Reactor (CPBR)

The centrifugal packed-bed reactor (CPBR) has been developed by Yang *et al.* in 1996. It was used for the production of xanthan gum from *X. campestris*. The cells were immobilised by attaching them to a rotating fibrous matrix surface. Yang examined different woven materials; cotton towel, cotton fabric, and 50% cotton and 50% polyester. The medium broth was continuously pumped through the rotating fibrous matrix to ensure good contact between the gas, medium and cells. The results showed that rough cotton was the preferred material, and the cells adsorbed faster to cotton than to polyester fibres. Almost all cells were removed from the fermentation broth, thus enhancing product recovery (Yang *et al*., 1996). The CPBR and cell adsorption method has been developed further for continuous operation in other types of study. Extensions to the application of such immobilised systems include axial-flow hollow fibre cell culture bioreactors, the continuous fibrous-bed bioreactor and the ceramic membrane reactor (Brotherton *et al*., 1996 and Chen *et al.*, 2002).

2.1.4 Oscillatory Baffled Reactor (OBR)

For this study a relatively new reactor technology was used, the oscillatory baffled reactor (OBR). Oscillatory flow has been studied since (1935) when van Dijck proposed the reciprocating plate column (RPC) for liquid- liquid extraction. Pulsation of the fluid in the column gave much-improved dispersed phase mixing, efficient fluid mixing and a narrow residence time distribution, therefore RPC has evolved significantly both in the extraction and in some gas- liquid applications area (Lo and Prochazka, 1983; Baird *et al.*, 1994).

Several plate designs have been reported but the Karr RPC (Karr, 1959) has been the most successful one. It consisted of multi-perforated plates with many circular perforations of several diameters mounted on vertical shafts and moved from above by an electro-mechanical oscillator as shown in figure 2.5.

Since then, research interest focused on oscillatory flow in a smooth tube for many years. However, in 1989 researchers at Cambridge University found that improved radial mixing and narrow residence time distributions in the vessel could be achieved by the combination of periodically spaced orifice baffles along the length of a tube, with a net flow superimposed and a reversing oscillatory component. The baffle edges increase the radial mixing in the tube through the formation of eddies resulting in significant enhancement in processes (Brunold *et al.,* 1989; Dickens *et al.,* 1989; Mackley and Ni, 1991, 1993)

Flow in this device was found to produce sharp or near plug flow residence time distribution leading to enhanced heat transfer, gas-liquid mass transfer and good solid-liquid suspension with respect to the stirred tank (Dickens *et al.,* 1989; Mackley *et al.,* 1990; Mackley and Ni, 1991,1993; Ni, 1994; Ni *et al.,* 1995a; Ni *et al.,* 1996).

In the current study the OBR was used as described in the materials and methods chapter 3

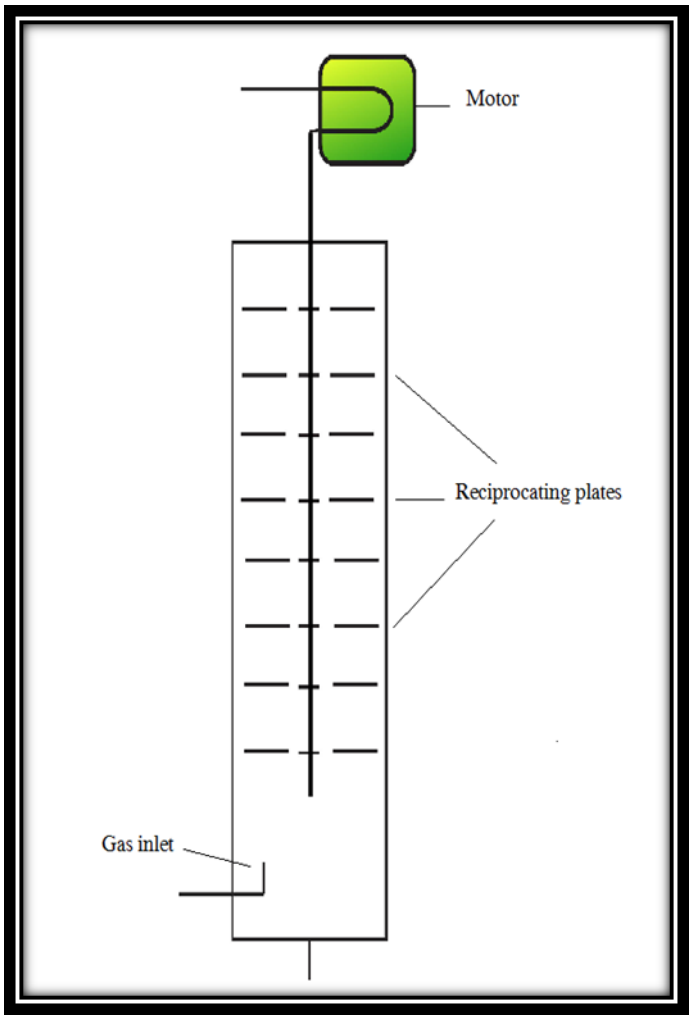

Figure 2.5: Traditional reciprocating plate column (Karr column)

2.1.4.1 Mixing

The basis of the OBR technology is a tubular reactor with the presence of annular-baffles. The mixing mechanisms in a baffled cell are controlled by the geometrical configuration of the baffles and the oscillation conditions. The fluid mechanics

within an oscillatory baffled tube can be described by two dimensionless parameters. The first is called the Reynolds number:

- The oscillatory Reynolds number Re_o: is characterises the intensity of mixing applied to the column and defined as:

$$\mathrm{Re}_o = \frac{\rho x_o \omega D}{\mu} \tag{2.1}$$

The Reynolds number Re_o is the indicator of the relative importance of inertial and viscous forces in steady flow. However, in oscillation (unsteady) flow, the relative importance of these two forces is not constant, and an additional parameter is used to describe the flow, called the Strouhal number St

- The Strouhal number St: is the ratio of column diameter to stroke length, measuring the effective eddy propagation and defined as:

$$St = \frac{D}{4\pi x_o} \tag{2.2}$$

where D is the column diameter (m), x_o is the peak to peak amplitude of oscillation (equal to half the stroke) (m), ρ is the fluid density (Kg/m), ω the

angular frequency (rad/s), **f** is frequency of oscillation (Hz), and **μ** is the fluid viscosity (kg/m/s). Attempts to revise these parameters and include the orifice diameter in the equations have been proposed and discussed by Ni and Gough (1997).

The mechanism of fluid mixing in the oscillatory baffled flow is that with each oscillation, if a liquid is pushed up through the tube, fluid near the wall of the tube is pushed up into upstream and eddies will be created around the baffles as the flow accelerates enabling significant radial motion On flow reversal, these eddies are ejected into the centre of the tube and new eddies will be created on the opposite side thus intense eddy mixing can be achieved between baffles as shown in figure 2.6.

Each flow reversal generates new eddies, which are subsequently pumped into the centre of the tube leading to chaotic mixing where fluid forces near the walls are as strong as those in the centre of the column (Figure 2.7). In this way, the intensity of eddy generation and cessation can precisely be controlled by fine tuning the oscillatory conditions. The correct combination of oscillation amplitude and frequency creates a well-mixed regime in respect of intensity of mixing, axial dispersion (Brunold *et al.,* 1989) and other transfer processes (Mackley *et al.,* 1994; Mackley and Stonestreet, 1995). Many geometrical parameters have been examined for these systems, such as a baffle spacing of 1.5 times column diameter (Brunold *et al.,* 1989). Mackay *et al.* (1991) suggested orifice baffles with no gap between the wall of the column and the baffles, Ni *et al.,* (1998b) and Ni and Stevenson, (1999) tried a 22% baffle free area and a baffle width of 3 mm. Most importantly, for

continuous processing, the degree of mixing can be controlled independently of the changes in net flow rate through the tube.

2.1.4.2 Mass transfer

In xanthan gum production dissolved oxygen concentration is the limiting nutrient and the oxygen mass transfer rate (OTR) can be considered the controlling step rate for the overall process. This is because xanthan fermentation is accompanied by a dramatic increase of the viscosity of the broth, which produces a significant decrease of oxygen mass transfer rate because of the extracellular accumulation of the biopolymer. The oxygen mass transfer rate in a fermenter depends on several factors, such as the geometry of the fermenter, the broth properties, the air flow rate, the mixing speed, etc. (Garcia-Ochoa 2000).

This implies that whatever reactor system is to be used for xanthan production must be capable of high oxygen transfer rates in a viscous medium. Since systems like the ALR tend to be low shear and have modest OTR it is easy to see why industry still uses the STR.

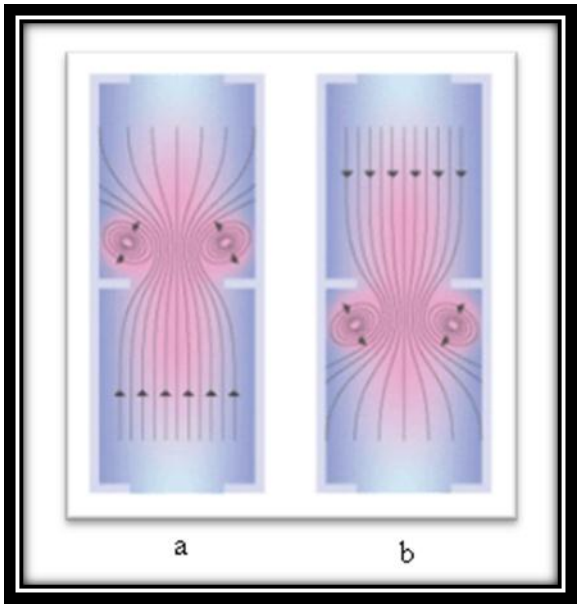

Figure 2.6: The mixing mechanism in the oscillatory baffled flow (a) upstroke and (b) down stroke (NiTech Solutions Ltd).

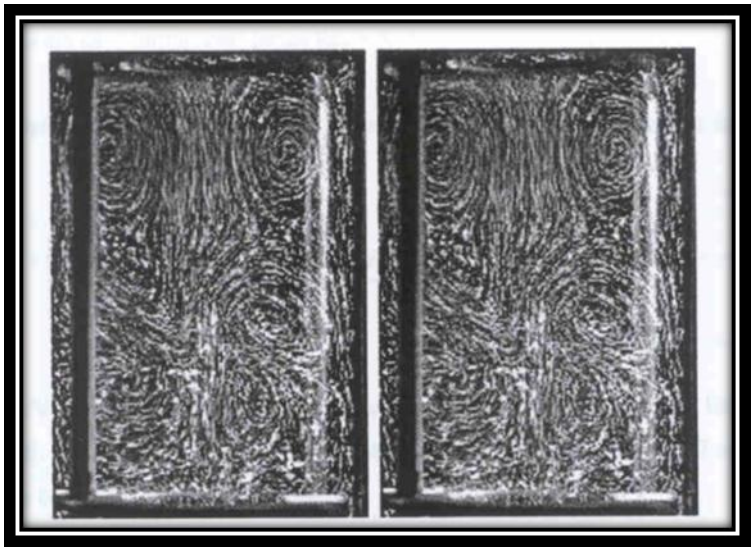

Figure 2.7: Chaotic mixing achieved in OBR (NiTech Solutions Ltd).

2.2 Xanthomonas campestris

2.2.1 Pathogenicity

The genus *Xanthomonas* (from Gk. *xanthos* 'yellow' and *monas* 'entity') is a genus subdivision of the *Pseudomonaceae* family consisting of 20 plant-associated species, many of which cause important diseases of crops and ornamentals. Individual species comprise multiple pathogenic variants (pathovars, pv.). Monocotyledonous and dicotyledonous plants species, including fruit and nut trees, solanaceous and brassicaceous plants, and cereals are susceptible to infection by strains of the genus *Xanthomonas* (Hayward 1993). Some plants of the family *Brassicaceae* of agricultural interest for example, cabbage, broccoli, and cauliflower are attacked by *X. campestris*, whereas *X. alfalfae*, is pathogenic on alfalfa, bean, and peas. *X. albilineans*, causes leaf scald of sugar cane and *X. fragaria* causes leaf spot disease of strawberry. *X. ampelina* causes a canker disease of grapevine as can be seen in figure 2.8 (Leyns *et al.*, 1984).

Van den Mooter *et al*., (1987) proposed that the genus *Xanthomonas* contains the following eight species: *X. albilineans, X. axonopodis, X. campestris, X. fragariae,X. graminis,X. maltophilia, X. oryzae, and X. populi.* Dye *et al.* (1980) described *X. campestris* as the most complex of these species because it has been subdivided into 123 pathovars.

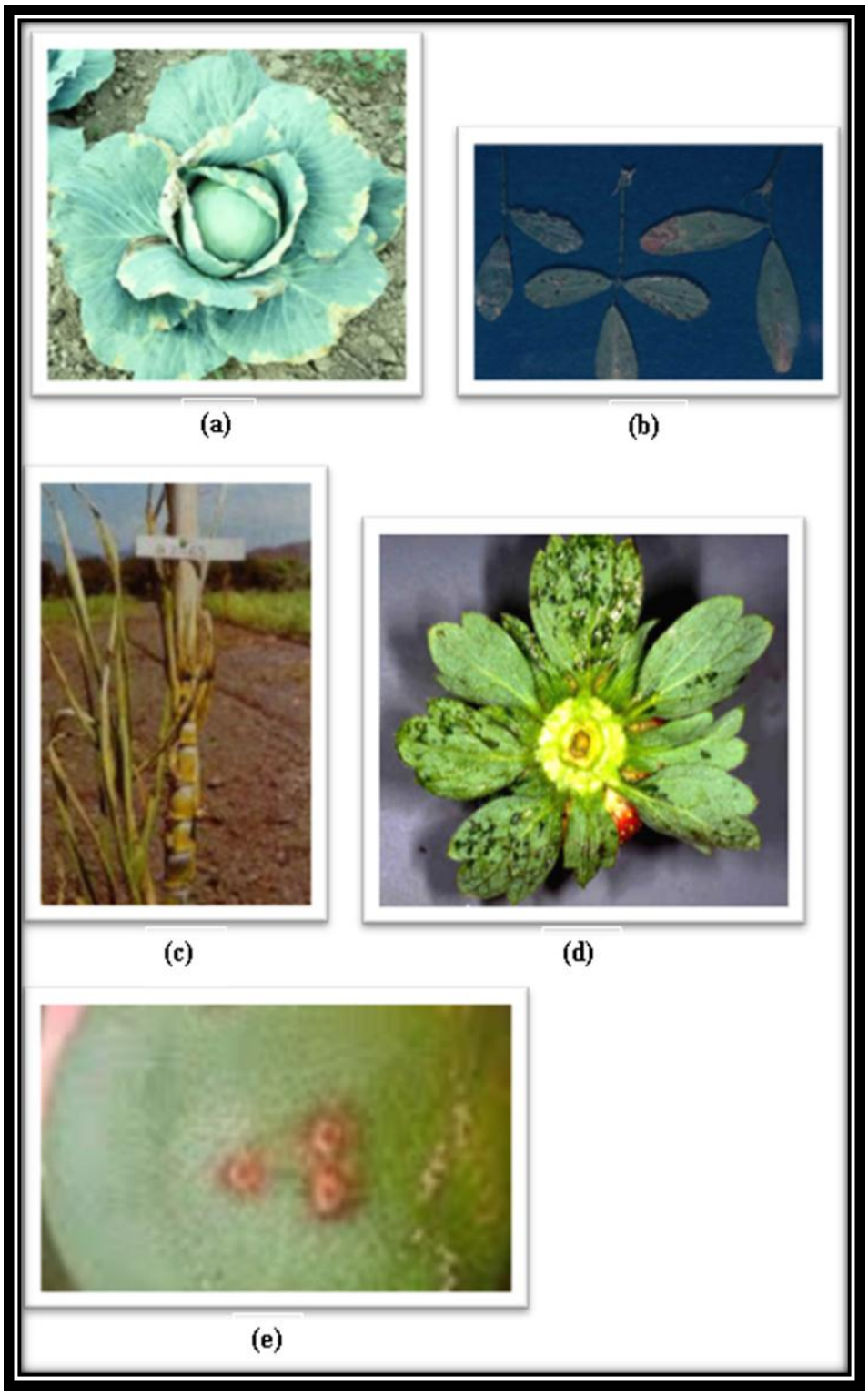

Figure 2.8: Plants disease caused by *Xanthomnas* species (a) *X. campestris*, (b) *X. alfalfae*, (c) *X. albilineans*, (d) *X. fragaria* and (e) *X. ampelina.*

2.2.2 Genome sequence of *X. campestris*

In *Xanthomonas campestris* many genes which are involved in xanthan biosynthesis have been identified, isolated and characterized. The biosynthesis of the polysaccharide is directed by a cluster of 12 genes, *gumB* to *gumM* are expressed as a single operon from a promoter which is located upstream of the first gene (Crescenzi *et al.,* 1989 and Vojnov *et al.,* 1998). Seven gene cluster products not linked to the genes which are required for the synthesis of the sugar nucleotide precursors are required to form the complete acylated repeating unit. Xanthan synthesis is activated by the gene product of a cluster of at least five genes (Tang *et al.,* 1991). Vojnov *et al,* (1998) showed that *gumB* and *gumC* are both involved in the translocation of xanthan across the bacterial membranes. Steinbuchel and Rhee, (2005) have constructed a physical map of the *X. campestris* chromosome, the location of eight loci involved in xanthan gum synthesis and four loci, which may be involved in gum polymerization, secretion and regulation were determined. Several mutants of *X. campestris* were identified showing increased viscosity and/or gum production after UV treatment (Rodrigues and Aguilar, 1997). Genetically modified (GM) bacteria were used to produce xanthan gum other than *X. campestris.* Polloch *et al.* (1997) have cloned 12 genes coding for the assembly, acetylation, pyruvylation, polymerization and secretion of the polysaccharide xanthan gum in *Sphingomonas.* The recombinant genes were sufficient for synthesis of xanthan gum and the polysaccharide was largely indistinguishable both structurally and functionally from the native xanthan gum.

2.2.3 Morphology

The pathogenic diversity of *Xanthomonas* contrasts with a characteristic uniformity with regard to morphology and physiology. *X. campestris* is Gram negative rod-shaped, round-ended, and varies in length from approximately 0.7 to 2.0 μm and in width from 0.4 to 0.7 μm. *X. campestris* species are motile by a single polar flagellum (Figure 2.9).

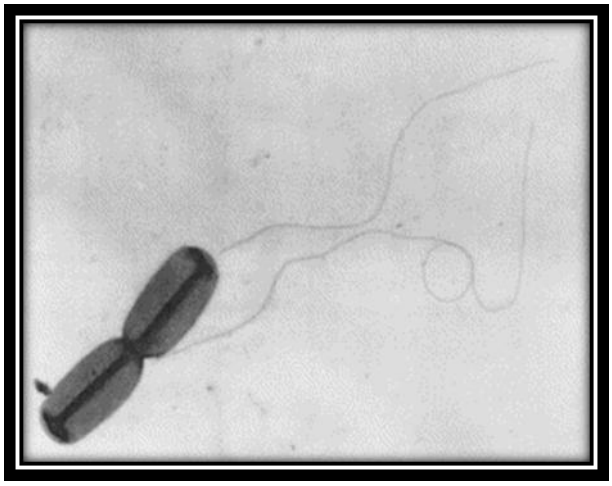

Figure 2.9: *X. campestris* cell with polar flagellum (Garcia-Ochoa *et al*., 2000).

The micro-organism is chemoorganotrophic and an obligate aerobe with a strictly respiratory metabolism where molecular oxygen is the electron acceptor. The bacterium is never fermentative and cannot denitrify. Moreover, it is catalase-positive and oxidase-negative (Bradbury, 1984). The vast majority are also yellow pigmented, due to the production of photoprotector carotenoids, membrane-bound, brominated aryl-polyene pigments called xanthomonadins shown in figure 2.10 (Rajagopal *et al*., 1997).

Figure 2.10: *X. campestris* on nutrient agar plate (Garcia-Ochoa *et al*., 2000).

Colonies of *Xanthomonas* are also typically highly mucoid, smooth and viscid on sugar-rich media, but are very resistant to desiccation due to the production of the protective exopolysaccharide xanthan (Sutherland, 1993). *X. campestris pv. campestris* (Xcc) is the most commonly employed micro-organism for industrial production of xanthan which is used extensively in food, cosmetic, and oil industries (Sutherland, 1993; Becker *et al*., 1998). The capsular extracellular polysaccharide xanthan is known to play an important role in pathogenicity for the organism, but is also believed to be important in survival of the bacterium (Dunger *et al.,* 2007), protecting against UV light, freezing, desiccation and bacteriophages by building a physical barrier around the cell (Bretschneider *et al.*, 1989; Dow and Daniels, 1994; Rajeshwari and Sonti, 2000; Dow *et al.*, 2003; Crossman and Dow, 2004; Blanch *et al.*, 2008). Capsular EPS are often ionic and as such function as an ion-exchanger to concentrate nutrient molecules around bacteria (Whitfied, 1988). In general, the bacterium is not able to catabolize its own extra-cellular polysaccharide, and therefore xanthan gum is not usable as a reserve energy source. Several strain variations of *X.*

campestris have been observed, and grown on standard laboratory media both in continuous cultures and batch cultures (Silman and Rogovin, 1970 and Cadmus *et al*., 1976).

2.3 Xanthan gum

2.3.1 Chemical structure

Xanthan gum is a natural extracellular polysaccharide (Su *et al.,* 2003) with very high molecular weight ranging between 2 and 50 × 106 Daltons (Dintzis *et al.,* 1970). This wide range of molecular weight is due to the association between polymer chains that results in aggregation. The structure and molecular weight distribution of xanthan variations can be influenced by the fermentation conditions (Garcia-Ochoa *et al*., 2000). Native xanthan is a hetero-polysaccharide consisting of a cellulosic backbone with a penta-saccharide repeating unit. The main chain consists of two β-D-glucose units linked at the 1-4 position but the unique character of xanthan gum is derived from the tri-saccharide side chain. This chain is composed of (β-D-mannose-(1,4)- β-D-glucuronic acid-(1,2)-α-D-mannose) linked at the C-3 position to every other glucose residue in the main chain. Approximately half of the terminal D-mannose unit contains a pyruvic acid residue linked via a keto group to the 4 and 6 positions, with an unknown distribution; the internal mannose unit linked to the main chain may contain an acetyl group at the position C-6. The repeating unit of xanthan gum is shown in figure 2.11 (Becker A *et al*., 1998; Garcia-Ochoa *et al*., 2000; Steinbuchel and Rhee, 2005).

The glucuronic acid and pyruvic acid groups on the side chains determine the properties of xanthan gum solutions and give xanthan gum its anionic character. The interaction of these trisaccharide side anionic side chains with the polymer backbone

causing a single, double, or triple helix stiff chain, or can result in interaction with other polymer molecules to form a complex (Morris *et al*., 1977; Milas and Rinaudo, 1979).

Usually, the degree of substitution for pyruvate varies between 30 and 40%, whereas for acetate the degree of substitution is as high as 60 - 70% (Smith *et al.*, 1981). There are still deficiencies in our basic knowledge of the influence of reactor type and fermentation conditions on the molecular weight of xanthan and on the product quality.

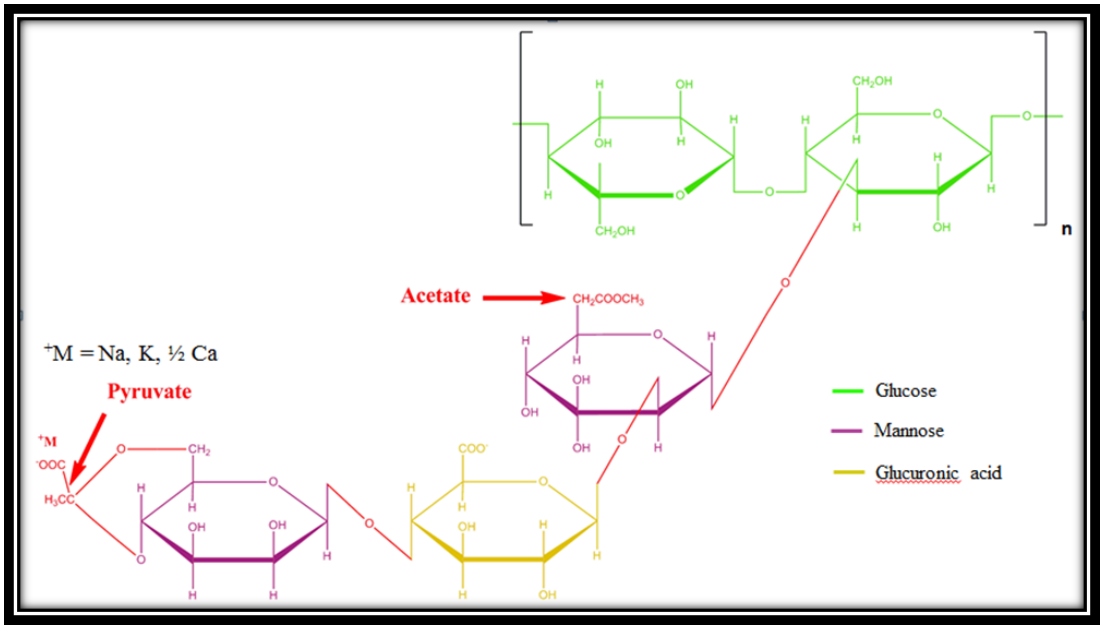

Figure 2.11: The repeating unit of xanthan gum (Garcia-Ochoa *et al*., 2000).

2.3.2 Molecular Weight

Values of xanthan molecular weight (MW) reported in the literature range between 4 and 12 $\times 10^6$ g/mol. There are several reasons making accurate determination of the molecular weight of xanthan difficult including: the very high molecular weight, the stiffness of the molecule and the presence of aggregates. Nonetheless, several techniques have been used to determine the molecular weight of xanthan.

The MW can be determined by different methods, for example, gel permeation chromatography (GPC) is one of the techniques commonly used to determine the molecular weight distribution of xanthan (Lambert et al., 1982; Milas et al., 1985). Most of the molecular weight, structure and conformation studies have been done with commercial xanthan samples. Clearly MW may vary with process time. In 1986 Kulicke and Lehmann performed rheological studies and reported a distinct maximum of the intrinsic viscosity of purified samples taken at different fermentation times. Moreover, they estimated the average molecular weight using laser light scattering (LLS) for the same samples. Xanthan average molecular weight was determined by size exclusion chromatography (SEC) by Herbst et al., (1988) as in the range 7.2-9.3×106 g/mol.

2.3.3 Secondary structure

Two models, a single-strand helix and a double-strand or multi-strand helix, have been proposed, though most authors currently support the idea of a double helix. The

helix is stabilized by non-covalent bonds, such as hydrogen bonds, electrostatic interaction, and steric effects; its structure can be described as a rigid rod (Bindal *et al.*, 2007). Electron microscopy (Milas *et al.*, 1988), optical rotation (Norton *et al.*, 1984), scanning tunnelling microscopy (Gunning *et al*., 1993), force spectroscopy (Li *et al.*, 1999), and atomic force microscopy (Camesano and Wilkinson 2001) studies suggested that the ordered form of xanthan is a single helix (Figure 2.12).

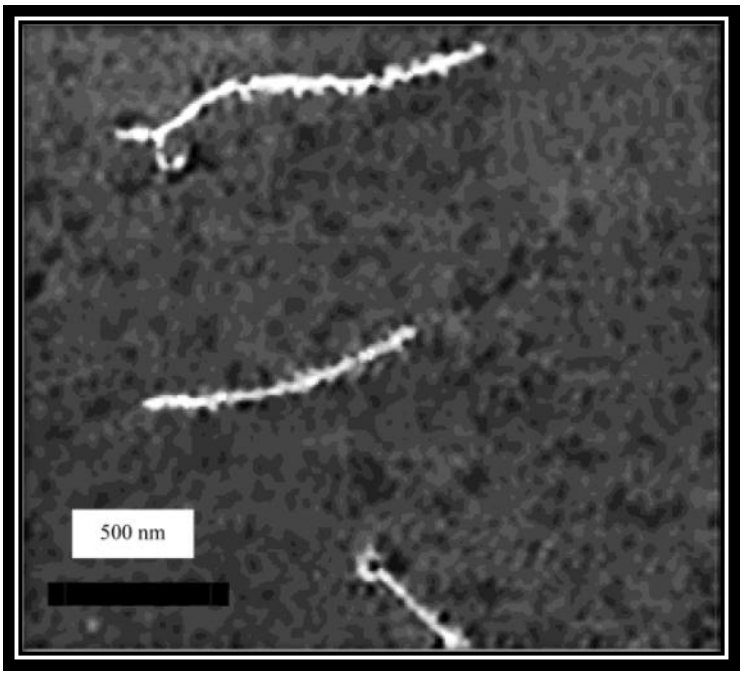

Figure 2.12: AFM Representative image of xanthan in pure water. (Camesano and Wilkinson, 2001).

In addition X-ray diffraction studies suggested that xanthan forms a single-stranded 5-fold helix (Moorhouse *et al.*, 1977). On the other hand the double-stranded model was favoured based on viscometry (Sato *et al*., 1984a), light scattering (Baradossi and Brant, 1982), electron microscopy (Holzwarth and

Prestridge, 1977; Stokke *et al.,* 1986), calorimetry (Paoletti *et al.,* 1983), and combined viscometry and light scattering (Sato *et al*., 1984b).

Rochefort and Middleman (1987) reported that the backbone of xanthan is disordered (or partially ordered in the form of a randomly broken helix) in aqueous solution at 25 °C, but due to the electrostatic repulsions from the charged groups on the side chains the molecule is highly extended. Therefore the molecules may align and associate due to hydrogen bonding to form a weakly structured material and so as the temperature increased the molecule undergoes a transition to coil-like configuration, which causes a dissociation of the molecules that affect the rheological properties (Rochefort and Middleman, 1987). Another factor which can cause the transition is when salt is added to an aqueous solution of xanthan at 25 °C, where a disorder-order transition occurs due to charge screening effects that stabilize the ordered conformation where the backbone takes on a helical conformation and the charged tri-saccharide side chains collapse down onto the backbone (Muller *et al.,* 1986).

The secondary structure of xanthan depends on the conditions under which the molecule is characterized. The molecule undergoes a thermally induced conformational change from a stiff, ordered helical conformation at lower temperature where the side chains are folded-down and associated with the backbone by non-covalent interactions, to a more flexible, disordered structure, where the side chains are project away from the backbone. This conformational transition depends on ionic strength, nature of electrolyte, pH, temperature, xanthan concentration and acetyl and pyruvate constituent contents (Figure 2.13) (Matsuda *et al.,* 2009).

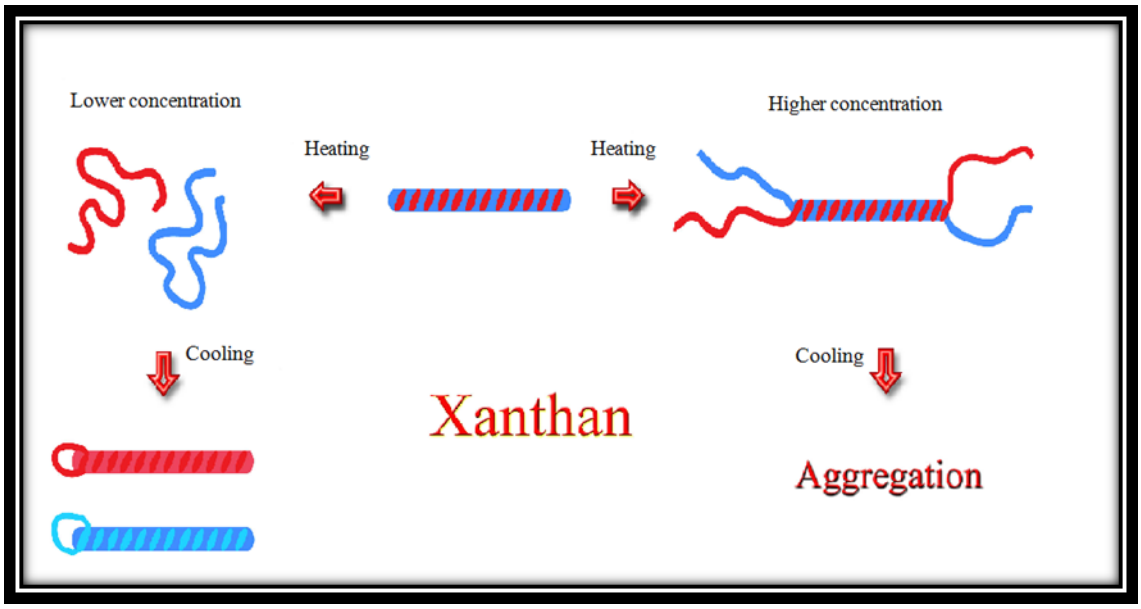

Figure 2.13: Thermal denaturation, re-naturation, and aggregation of a double-helical polysaccharide xanthan in aqueous solution (Matsuda *et al.*, 2009).

2.3.4 Biosynthesis of xanthan

Xanthan gum is produced by *X. campestris* and synthesised intracellularly (Jarman and Pace 1984; Blanch *et al.*, 2008). The path of xanthan gum synthesis is a complicated process similar to the exopolysaccharide synthesis in other Gram-negative bacteria. It is catalysed by a multi-enzyme system and each enzyme possesses a high degree of specificity (Sutherland, 2001). However Sutherland (1977a, b) showed that substrate enters the cell usually by active transport and group translocation involving substrate phosphorylation during the biosynthesis of xanthan gum and other bacterial extracellular polysaccharides. After entry, the substrate is directed to either catabolic pathways or pathways leading to polysaccharide

synthesis. The Entner-Doudoroff pathway is the main route for glucose catabolism in this organism (Whitfield *et al.,* 1982; Becker *et al.*, 1998).

The path of xanthan biosynthesis has been described and reviewed by several authors (Jarman and Pace 1984; Leigh and Coplin, 1992; Becker *et al*., 1998; Sutherland 2001; Blanch *et al.,* 2008). The synthetic pathway can be divided into three parts: initially the uptake of monosaccharide, followed by phosphorylation of the sugar, this phosphorylated substrate is then converted to the various sugar nucleotides (activated carbohydrate donor) required for assembly of the pentasaccharide repeating unit attached to polyisoprenol phosphate from the inner membrane that functions as an acceptor (Ielpi *et al*., 1993).

Xanthan synthesis starts with the construction of the pentasaccharide repeating unit by the sequential addition of monosaccharides from sugar nucleotide diphosphates to poly-isoprenol phosphate lipid acceptor molecule from the inner membrane (Ielpi *et al*., 1993, 2006). The first step of pentasaccharide assembly is the transfer of D-glucose-1-phosphate from UDP-D-glucose to the phosphate lipid carrier. Thereafter, D-mannose and D-glucuronic acid residues are added from GDP-mannose and UDP-glucuronic acid, respectively. An O-acetyl group is donated from acetyl-CoA to the internal mannose residue and pyruvate is donated from phosphoenolpyruvate (PEP) to the terminal mannose. Acetyl CoA and phosphoenol pyruvate are formed through the entner-doudoroff (ED) pathway and enter the tricarboxylic acid cycle (TCA) to produce ATP and NADH (Becker *et al.*, 1998). The quantity of the acetyl and pyruvate residues present in the mannose units in the

side chain of xanthan molecule varies from strain to strain, and is influenced by the fermentation conditions and post-fermentation process (Rinaudo, 2004). Each of the previous steps requires specific substrates and specific enzymes for completion. The final steps of biosynthesis are the release of the polymer from the lipid carrier, the secretion from the cytoplasmic membrane involving the passage across the periplasm and the outer membrane and finally the excretion into the extracellular environment. The process requires an energy source in which ATP is the energy supplier, and a specific transport system. The above system is shown in figure 2.14 (Jarman and Pace 1984; Daniels and Leach, 1993; Becker *et al*., 1998; Letisse *et al.,* 2001).

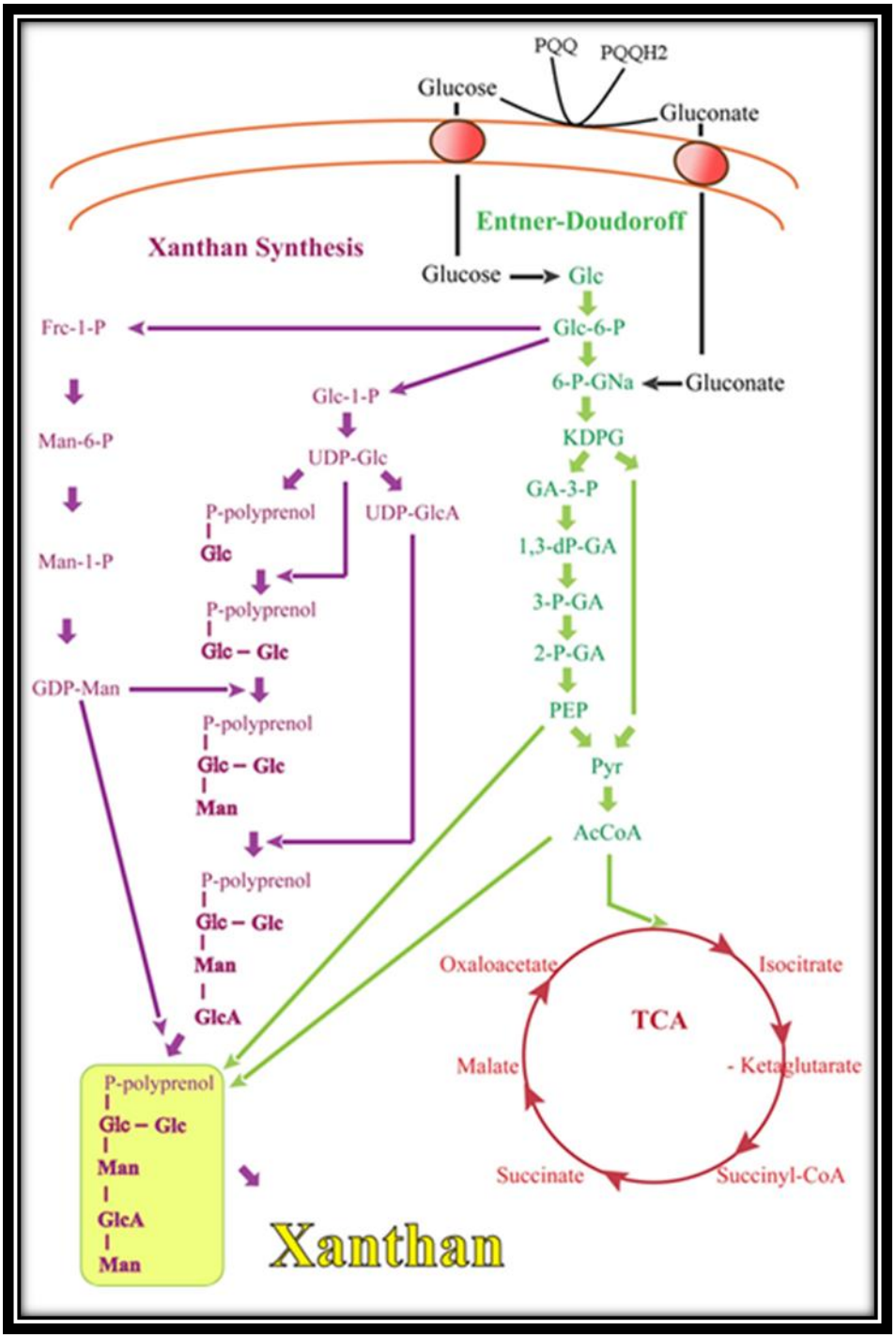

Figure 2.14: Xanthan gum biosynthesis.

2.3.5 Viscosity

Xanthan has a number of unusual rheological properties. It is an acidic polymer (cream coloured powder) that is highly soluble in both hot and cold water due to the polyelectrolyte nature of the xanthan molecule. Xanthan solutions are highly viscous even at low concentrations and exhibit a high degree of pseudoplasticity or shear thinning behaviour in aqueous solutions even at low polymer concentration. Xanthan's viscosity depends on temperature, gum concentration, salt concentration, and pH (Garcia-Ochoa *et al*., 2000). Furthermore, xanthan may even exhibit gellify under certain conditions. These interesting properties of xanthan solutions have led to its widespread adoption by the food additive industry.

2.3.5.1 Influence of temperature on viscosity

Viscosity of xanthan solutions depend on both temperature and dissolution temperature (Garcia-Ochoa *et al*., 2000). Generally the viscosity decreases with the increase of measurement temperature. This behaviour is fully reversible between 10 and 80 °C. At low-dissolution temperature xanthan exists in a native ordered conformation (rigid double-strand helix), and the viscosity of the solution is relatively high due to the compact conformation of the molecule. This conformation undergoes a transition to an expanded conformation (random coiled) at high dissolution temperature and there is a progressive decrease of the rigidity. Although, the viscosity decreases as the dissolution temperature is increased up to 40 °C. Between 40 and 60 °C, the viscosity increases as the temperature is increased. At

temperatures above 60 °C, the viscosity decreases as the temperature is increased (Milas and Rinaudo, 1979; Garcia-Ochoa and Casas, 1994; Garcia-Ochoa *et al*., 2000).

Norton *et al*. (1984) studied the order-disorder transition of xanthan using optical rotation, differential scanning calorimetry, stopped-flow reaction kinetics and low-angle laser light scattering. The results demonstrated that the transition temperature is around 55 °C in distilled water and increases with the ionic strength (Norton *et al*., 1984).

2.3.5.2 Influence of polymer and salt concentration on viscosity

The viscosity increases significantly with an increase in xanthan concentration. This behavior is caused due to the polymer intermolecular interaction, leading to increases t effective macromolecule dimensions and molecular weight (Smith and Pace, 1982; Milas *et al*., 1985). Furthermore Xanthan viscosity is generally influenced by salt concentration. Although, Kang and Pettit (1992) reported that in salt concentrations more than 0.1% (w/v) viscosity of xanthan solutions is independent on salt levels. The addition of small amounts of salt to a low polymer concentration solution makes viscosity decrease slightly (Garcia-Ochoa *et al*., 2000). This can be related to the diminished intermolecular electrostatic forces that resulting in reduction of molecular dimensions (Smith and Pace, 1982).

2.3.5.3 Influence of pH on viscosity

Xanthan dissolves in most acids and bases. Solutions of xanthan gum are relatively unaffected by change in pH ranging from 2-11 for long periods of time. At pH 9 or higher the xanthan molecule loses its acetyl groups (de-acetylated) (Tako and Nakamura, 1985), and at pH 3 or lower the xanthan molecule loses pyruvic acid acetyl groups (depyruvylation). Either deacetylation or depyruvylation hardly affect on xanthan solution viscosity (Bradshaw *et al*., 1983).

2.3.5.4 Influence of acetal and acyl groups on viscosity

Most xanthan applications are based on its rheological properties. Cadmus *et al*. (1978 and 1979) reported that the pyruvic acid content of xanthan is influenced by the strain variants of genus *Xanthomonas*, medium composition and the incubation temperature. There was a suggestion that xanthan samples that were prepared under different fermentation conditions with different pyruvic acid acetal and o-acetal contents should not normally be used for assessing the contribution of these groups to solution viscosity.

Bradshaw *et al*. (1983) investigated the influence of acetal and acyl groups in determining the solution viscosity of xanthan. The viscosities at shear rates 8.8 – 88.3 /s of 0.3% w/v native, pyruvate-free and pyruvate/acetate-free xanthan solutions were similar in both distilled water and 1% KCl. In addition, the viscosity at low shear rate 10 /s of native and pyruvate-free xanthan solutions at concentrations range 0.2 - 1.5% were similar.

Tako and Nakamura (1985) studied the dynamic viscoelasticity of deacetylated xanthan in aqueous media at various concentrations. They found that the behaviour of deacetylated xanthan solutions at concentrations below 0.1% were pseudoplastic whereas at concentrations above 0.3% the flow behaviour was plastic.

The researchers suggested that the acetate groups, which are attached to the inner mannose residues of the side chains, stabilize the ordered conformation of xanthan by contributing in the intramolecular association with the backbone. Therefore, the side chains become more flexible after deacetylation, whereas the electrostatic repulsion of the pyruvate groups destabilizes the molecule (Dentini *et al*., 1984; Callet *et al*., 1987 and Kim *et al.,* 2006).

2.3.6 Compatibility with other polymers

Locust gum beans and guar gum are the most common galactomannans used industrially. Their backbones consist of mannose units linked to a monomolecular galactose unit. Galactose units are not uniformly distributed. The smooth regions of galactomannans, where there is no galactose linked to the mannose back bone, are the ones where xanthan gum preferentially interacts to form a strong thermo-reversible gel (Dea *et al.,* 1977). Each of the polysaccharides alone does not form a gel, but a mixture of a galactomannan and xanthan results in synergistic gelation. The maximum gel strength is obtained when xanthan is dissolved at 40 °C and galactomannan dissolved at 80 °C (Hui *et al*., 1964).

2.3.7 Xanthan gum production

Xanthan gum is used in a wide range of food and beverage applications with an annual worldwide production of 30,000 tons corresponding to a market of $408 million of which about 60 per cent is used in the food and pharmaceutical market (Kalogiannis *et al*., 2003). Xanthan is still one of the fastest growing hydrocolloids. Its versatility and, now its low price, make it a hydrocolloid of choice.

2.3.7.1 General process

Today xanthan gum is the most successful industrial polysaccharide. The industrial scale production of xanthan can be made by the aerobic fermentation with *X. campestris* NRRL B-1459 that is able to grow in both a complex and in completely defined medium (Garcia-Ochoa *et al.,* 2000). The production process and the product (xanthan gum) are influenced by the culture environment and the operational conditions (Cadmus *et al*., 1978; Zhang and Chen 2010).

X. campestris needs several nutrients for efficient production of xanthan gum including micronutrients and macronutrients, such as carbon and nitrogen sources. Garcia-Ochoa *et al*. (2000) reported that glucose and sucrose are the best carbon sources and that as much as 70% of the carbon source may be converted to polysaccharide. The production of xanthan gum has been studied widely since the early sixties covering both batch (Rogovin *et al*., 1961; Moraine and Rogovin 1971, 1973; Weiss and Ollis, 1980 ; Fiedler and Behrens, 1984; Pinches and Pallent 1986; Funahashi *et al.,* 1987; and Peters *et al.,* 1992) and continuous operations (Silman

and Rogovin, 1970, 1972). Industrial production of xanthan is most often carried out by a stirred-tank reactor. Although batch culture is commercially preferred having fewer parameters to be controlled and well understood, there are some problems in that throughout the process the environment for cell growth keeps changing, and could affect growth and product formation due to build-up of toxic products or exhaustion of nutrients. Whereas in continuous culture extreme conditions will not change as the growth medium is continuously supplied to the culture, and culture fluid continuously removed (Becker *et al*., 1998). Becker *et al*. (1998) have also pointed out that although there are reasonable conversions rates of substrate to polymer of 60 – 70% in continuous processes, other problems still exist, for example, maintaining sterility and the risks of fast-growing mutants that do not produce the desire product (Cadmus *et al*., 1976; Becker *et al*., 1998; Garcia-Ochoa *et al.*, 2000; and Sutherland, 2001).

2.3.7.2 Medium composition

An efficient conversion of a carbon source to xanthan gum requires a high carbon to nitrogen ratio (Souw and Demain, 1979). Nutritional studies on the composition of the production medium for xanthan were first carried in 1978 by Davidson in continuous culture, followed by Souw and Demain 1979 in batch cultures. Souw and Demain 1979 concluded that 4% w/v glucose or sucrose were the best carbon sources (Zhang and Chen, 2010). In contrast, certain amino acid such as glutamate and nitrate, as ammonium nitrate and sodium nitrate, are the best nitrogen sources for the production of xanthan. Moreover, they found that concentrations of these nitrogen sources higher than the optimal level (15 mM) inhibited the production of xanthan

while stimulating cell growth. In addition they showed that addition of organic acids such as succinic and citric acids led to enhanced xanthan production (Davidson, 1978).

Demain, (1979), Tait *et al.* (1986) and Garcia-Ochoa *et al*. (1992) described the optimal production medium composition of xanthan production in gram per litre as the following: sucrose (40), citric acid (2.1), NH_4NO_3 (1.144), KH_2PO_4 (2.866), $MgCl_2$ (0.507), Na_2SO_4 (0.089), H_3BO_3 (0.006), ZnO (0.006), $FeCl_3$ $6H_2O$ (0.020), $CaCO_3$ (0.020) and concentrated HCl (0.13); the pH should be adjusted to 7.0 by adding NaOH. The authors also showed that nitrogen, phosphorus and magnesium are nutrients have an influence on *X. campestris* growth, whereas nitrogen, phosphorus and sulphur are nutrients that have an influence on xanthan production. In addition, citric acid was used as a chelating agent to prevent the precipitation of salts during heat sterilisation. Jana and Ghosh 1995 reported on the role of citric acid under oxygen-limiting conditions. The addition of up to 2.6 g citric acid per litre improved cell viability as well as increasing xanthan yield.

2.3.7.3 Temperature

From the literature the optimal temperature of the growth was different from the optimal temperature of xanthan production, a range of temperatures from 25 to 34 °C was employed for xanthan production and the results were varied from one study to the other. Suh and Yang, (1990) studied the effect of temperatures ranging between 22 and 35 °C on cell growth and xanthan production. They showed that higher

fermentation temperatures of between 30 and 33 °C were best for higher xanthan yields, whereas optimal temperatures for cell growth lay between 24 and 27 °C. While Esgalhado *et al*. (1995) studied the interactive effects of pH and temperature on cell growth and polymer production and suggested that the optimal temperature for growth is 25 - 27 °C and for xanthan production the optimal temperature ranged between 25 and 30 °C. Earlier Moraine and Rogovin (1966) estimated the optimal production temperature at 28 °C. Suh and Yang (1990) concluded that the optimal temperature for xanthan production depended on the production medium used. In addition, the pyruvate content was influenced by the temperature of cultivation with a maximum of ~4.5% occurring between 27 and 30 °C.

2.3.7.4 pH

Most authors agree that the optimal pH for growth is around neutral. Rogovin *et al.* (1961) found that the optimum pH range for growth was 6.5 - 7.5, while a pH of 7 - 8 was most suitable for the xanthan production. Garcia-Ochoa *et al.* (1996) showed that pH control enhanced the bacterial growth, but did not affect the production of xanthan. The formation of organic acids during the production of xanthan leads the broth pH to decrease from neutral pH to values to close to 5.0. If the pH falls below 5 the formation of xanthan is drastically reduced. Thus it is necessary in the production process to maintain the pH close to the optimum pH by using buffers or addition of alkalis such as KOH, NaOH, or $(NH)_4OH$ in order to allow the process to continue until complete carbohydrate consumption has occurred.

2.3.8 Toxicity

Caloric availability and digestibility studies indicated that xanthan gum is not utilized by the human body (Booth *et al*., 1963). Booth *et al*. 1968 showed in a two year study that xanthan consumption by rats was not associated with any carcinogenic and toxic effects of the gum. Moreover, a reproductive study in rats demonstrated that xanthan did not inhibit growth. In addition, other studies on rats, rabbits, guinea-pigs, and dogs reported no toxic effects caused by consumption of xanthan in these species. In humans several studies indicated no adverse effects of ingestion at levels up to 10-13 grams daily (Eastwood *et al.*, 1986). On this basis the United States (FDA) approved xanthan for use as food additive without any specific quantity limitation (Kennedy and Bradshaw, 1984).

2.3.9 Industrial importance

The superior properties of xanthan gum have enabled it to compete with most of natural gums and also become the preferred product for many applications for a number of important reasons including its ability to impart a high viscosity solution, and high pseudoplasticity (Yoshida and Tanner, 1993). The high viscosity of solutions, water solubility of the polymer, emulsion stabilization, temperature stability up to 90 °C and pH (2 – 11) and compatibility with food ingredients have created important applications for xanthan in industrial food and non-food sectors as well as in oilrecovery (Lee, 1996; Sanderson 1981; Garcia-Ochoa *et al*., 2000; Rosalam and England, 2006). Table 2.1 lists some current uses of xanthan gum.

Table 2.1: Main industrial applications of xanthan gum (Garcia-Ochoa *et al.,* 2000).

Application	Functionality
Food industry	
Salad dressing	Emulsion stabilizer; suspending agent, dispersant
Dry mixes	Eases dispersion in hot or cold water
Syrups, topping, relishes, sauces	Thickener; heat stability and uniform viscosity
Beverages (Non-fat dry milk)	Stabilizer
Dairy products	Stabilizer, viscosity control of mix
Baked goods	Stabilizer, facilitates pumping
Frozen foods	Improve freeze-thaw stability
Pharmaceuticals	
Cream and suspensions	Emulsion stabiliser; uniformity in dosage formulation
Cosmetics	
Denture cleaners, shampoo, lotions	Thickener and stabilizer
Agriculture	
Additive in animal feed, pesticide formulations	Suspension stabilizer; improved spry ability, reduced drift, increased cling and permanence
Textile printing and dyeing	Control of rheological properties of paste, preventing dye migration
Ceramic glazes	Prevents agglomeration during grinding
Slurry explosives	Thickens formulation, improve heat stability (in combination with guar gum)
Petroleum production	Lubricant or friction reduction in drill-hole
Enhanced oil recovery	Reduces water mobility by increasing viscosity and decreasing permeability

As can be seen in Table 2.1, a small concentration of xanthan gum used in food products enables it to confer the required properties without affecting the taste of the final product. In the agricultural industry, the unique rheological properties of xanthan has been used to improve the suspension of the solid component increasing flow-ability, reducing drift and increasing cling and permanence in herbicides, and insecticides.

In order to meet the challenges of producing environmental friendly products, xanthan gum has been introduced in the formulation of new generations of thermo-setting coatings due to its ability to disperse and hydrate rapidly (Rosalam and England, 2006).

Approximately two barrels of oil remain in the ground for every one barrel produced (Rosalam and England, 2006). Because xanthan gum has excellent compatibility with salts, and resistance to thermal degradation, xanthan is useful as an additive in drilling fluids in the petroleum industry. In addition xanthan gum is used in oil drilling, fracturing, pipeline cleaning and in enhanced oil recovery (EOR). In EOR xanthan gum is used in tertiary oil recovery operations. The function of xanthan is to reduce the mobility of injected water by increasing its viscosity (Nasr *et al.*, 2007). The basic principle is to apply polymer-thickened brine to drive the slug of the surfactant through a porous reservoir rock to mobilise residual oil and improve the separation of water and oil, thereby increasing oil recovery (Byong, 1996; Marudova-Zsivanovits *et al.*, 2006).

The other applications of xanthan are removing rust, welding rods, wet slag, and cleaning other debris from gas pipelines. Many more application of xanthan gum can expected to be developed.

Chapter 3

Materials and Methods

3 Materials and Methods

This chapter presents the microorganism, culture techniques, and medium details in Section 3.1. The design, construction and operation of the Bioflo 3000 STR and oscillatory baffled reactor (OBR) is described in Section 3.2 as are the control and measurement procedures. The analytical techniques and methods used in this work are given in section 3.3. In section 3.4 a description of the modifications made to the OBR during the course of this research to fit it for effective production of xanthan gum are presented.

3.1 Culture Techniques

3.1.1 Microorganism

3.1.1.1 Resuscitation and preservation

Two strain of a wild type *Xanthomonas campestris* were selected to produce xanthan in this study ATCC 13951 and ATCC 33913 (*X. campestris*) were obtained from the American Type Culture Collection as a freeze dried culture in a double walled glass ampoule. The strain ATCC 13951 showed much better production than the strain ATCC 33913. Therefore, ATCC 13951 was chosen to be used in this study. The dried culture of the strain ATCC 13951 inside the ampoule was resuscitated by transferring aseptically 1.0 ml of sterile yeast malt (YM) medium then mixing gently. YM medium consists of (g per Litre): yeast extract, 4.0, malt extract, 10.0 and dextrose, 4.0. The medium pH was adjusted to pH 7.0 with 0.1 M NaOH. The above mentioned ingredients were obtained from the suppliers shown in table 3.1.

Table 3.1: Suppliers of medium components for the growth medium used for culture of *X. campestris* ATCC 13951 in the present study.

Product	Suppliers
Yeast extract	Oxoid (Basingstoke)
Malt extract	Sigma (Dorset)
Dextrose	Sigma (Dorset)
Agar	Sigma (Dorset)

After YM medium addition and mixing, the culture plus medium was allowed to stand for 10 min in order to facilitate rehydration. Several drops of this culture were transferred to sterile YM plates (solidified with 1.5% agar) and incubated at 30 °C for 24 hours. These stock culture plates were tested for purity visually and by microscopic inspection of Gram stains. The stock cultures were stored at 4 °C in the fridge, after which, several streak plates were then made in order to obtain a single colony of yellow-pigmented *X. campestris* ATCC 13951 that would be isolated, and used for freezing in glycerol at -70 °C.

A single isolate of *X. campestris* ATCC 13951was used to inoculate sterile 200 ml YM broth in a 500 ml flask and grown for 24 hours at 200 rpm at 30 °C. 0.5ml of a 20% v/v glycerol solution and 0.5 ml of an overnight culture of *X. campestris* ATCC 13951 were added to sterile freezing vials (Sigma). Cultures were then frozen at -70 °C. One vial containing frozen culture of *X. campestris* ATCC 13951 was opened every month and resuscitated as described previously. This culture was the source of the inoculum for each fermentation process during that month.

3.1.1.2 Inoculum preparation

One single growing colony of *X. campestris* ATCC 13951 from 24 hours old *X. campestris* ATCC 13951 plates was transferred to 200 ml of sterile YM broth in a 500 ml Erlenmeyer flask and incubated at 200 rpm and 30 °C for 24 hours, from which standardised inoculums was derived. An optical density of 1.60 (λ 600nm)

was found to be equivalent to approximately 2.2 x 10^7 cells/ml. A 10% v/v inoculum was used to seed the fermenter for the production of xanthan gum.

3.1.2 Production medium

A defined medium was used in this study to attempt to reduce process to process variability (Garcia-Ochoa *et al.,* 1992). The composition of this medium (in g per Litre) is: citric acid 2.1, NH_4NO_3 1.144, KH_2PO_4 2.866, $MgCl_2.6H_2O$ 0.507, Na_2SO_4 0.089 , H_3BO_3 0.006, ZnO 0.006, $FeCl_3.6H_2O$ 0.0024, $CaCO_3$ 0.020 and Extra-pure 37% HCl 0.13ml. The pH was adjusted to pH 7.0 with 1M NaOH, and the medium autoclaved for 15 min at 120 ºC. 400 ml of 20% w/v of glucose was autoclaved separately at 120°C for 15 minutes. The above mentioned ingredients were obtained from the suppliers shown in table 3.2.

Table 3.2: Suppliers of medium components for the synthetic medium used for culture of *X. campestris* ATCC 13951 in the present study.

Product	Suppliers	Product	Suppliers
Glucose	Sigma (Dorset)	Na_2SO_4	Sigma (Dorset)
Citric acid	BDH (Lutterworth)	H_3BO_3	BDH (Lutterworth)
NH_4NO_3	BDH (Lutterworth)	ZnO	BDH (Lutterworth)
KH_2PO_4	BDH (Lutterworth)	$FeCl_3.6H_2O$	BDH (Lutterworth)
$MgCl_2.6H_2O$	BDH (Lutterworth)	$CaCO_3$	Fisher (Loughborough)
HCl	BDH (Lutterworth)	NaOH	BDH (Lutterworth)

3.2 Equipment

3.2.1 Fermenters

Two fermenters of differing types were used in the course of the work.

3.2.1.1 Stirred Tank Reactor (STR)

The main fermenter used was a glass BioFlo-3000 (New Brunswick Scientific (UK) Ltd, St Albans, Hertfordshire, UK) which has a total volume of 3.3L and a working volume of 2L. The reactor consists of a glass vessel with stainless steel top plate with ports for pH and dissolved oxygen probes, air flow and temperature probes. Process related parameters such as dissolved oxygen, pH, temperature, and agitation speed were monitored and controlled via a digital control unit (DCU) with functions specially adapted to the automatic operation of the bioprocesses. The internal height to diameter ratio of the vessel is the standard 3:1, and the diameter of the vessel is 13 cm. A baffle basket with four baffles was used. The baffle width was 15 mm and the length 15 cm. Two six-bladed Rushton turbines of were attached to the agitator shaft, the diameter of each turbine was 6.5 cm.

The fermenter was connected to the main laboratory lines for air and water. The filtered sterile air was sparged into the vessel via a circular annular sparger fitted in the bottom of the vessel for even distribution of bubbles (Figure 3.1) Air was filtered through glass microfiber filter with polypropylene housing 50 mm diameter and 0.3 µm pore size (Whatman Ltd., Maidstone, UK). Process temperature was monitored

and controlled by a PID controller accurate to within ±0.2°C of the set-point. The pH of the culture broth was measured using a combined glass reference electrode (Mettler Toledo Ltd., Leicester, UK). The pH probe was calibrated before sterilisation using two buffer solutions, pH 7.0 and pH 4.0. The pH was not controlled during the process. Dissolved oxygen tension (DOT) was monitored by a pO_2 electrode (Mettler Toledo Ltd., Leicester, UK). The DO probe was calibrated after sterilisation and cooling to the fermentation temperature at the prevailing agitation speed before inoculation by introduction of oxygen free nitrogen (OFN) to set 0% followed by air to set 100%. 1 ml of polypropylene glycol 1950 g/mol (BDH) was added to the medium before sterilisation as an antifoam agent. The fermenter containing the medium (except the glucose) was autoclaved at 120 ºC for 15 min with pH and DO probe in place. The general appearance and layout of the fermenter is shown in figure 3.2.

Figure 3.1: The agitation and aeration systems within the New Brunswick Bioflo 3000 STR fermenter, two six-bladed Rushton turbines and annular sparger.

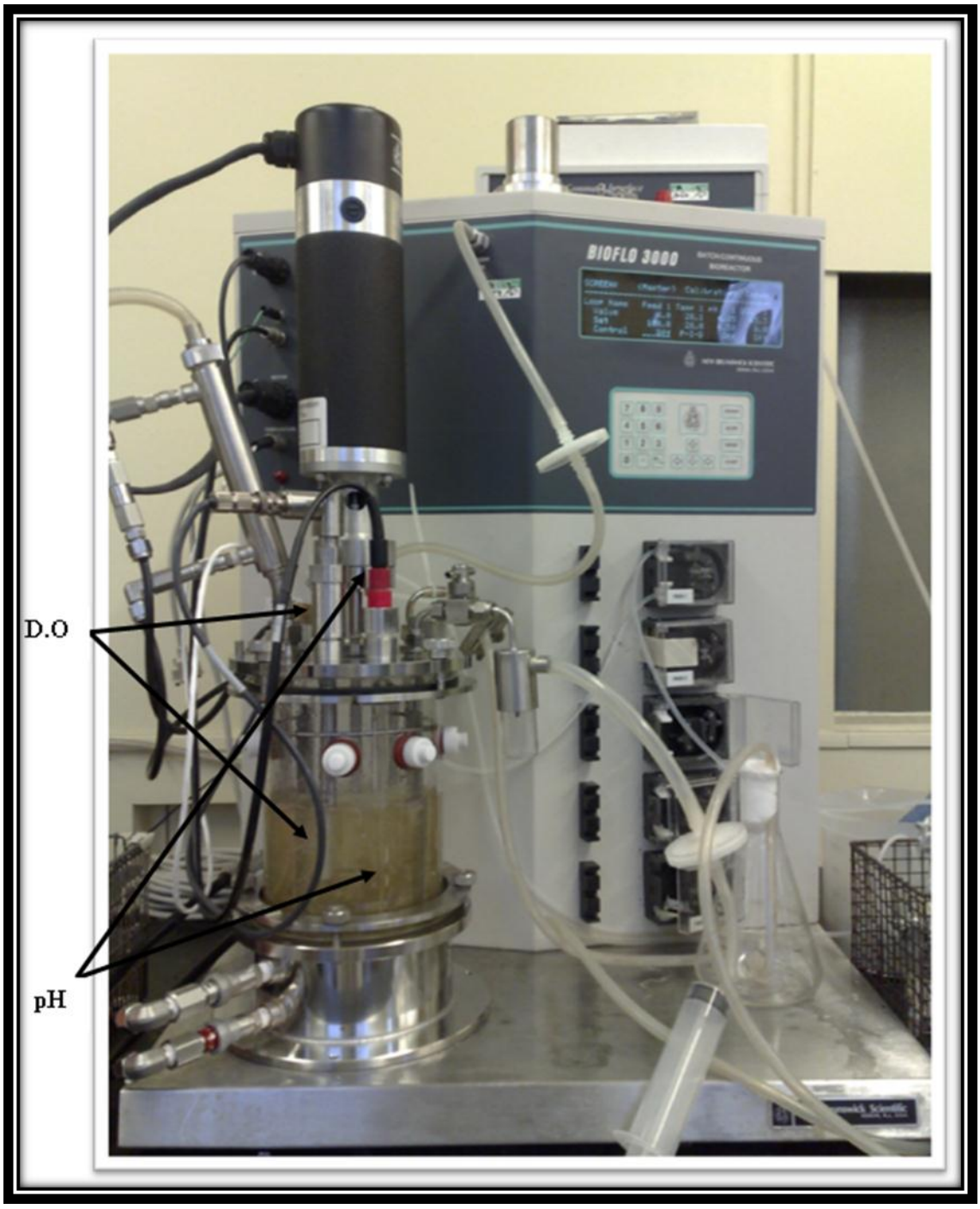

Figure 3.2: Operational configuration of the New Bruswick BioFlo 3000 STR during batch fermentation of *X. campestris* ATCC 13951.

3.2.1.2 Oscillatory Baffled Reactor (OBR)

A novel fermenter was used in this study, and was compared to the STR which was used as a benchmark. The OBR used in this study was supplied by Heriot Watt University in Edinburgh and consisted of a stainless steel column of 100 mm internal diameter and 420 mm in height, with a total volume of 3.3L and a working volume of 2L. Two side ports of 12 mm internal diameter were provided for housing a dissolved oxygen probe and a pH probe. In addition there is a port of 4 mm diameter for a temperature probe as shown in figure 3.3. Dissolved oxygen, pH and temperature were monitored via a digital control unit (Electrolab) (FerMac 240 Module Electrolab Ltd, Tewkesbury, Glos, UK) which was connected to a PC via (Electrolab) Interface box (Pico ADC-11 Data logger) and the process was monitored via a special program called PICO. The pH of the culture broth was measured using a combined glass reference electrode (Mettler Toledo Ltd., Leicester, UK). The pH probe was calibrated before sterilisation using two buffers pH 7.0 and pH 4.0. The pH was not controlled during the process due to lack of addition ports. The pH probe was sterilised separately in water, and then inserted aseptically into the vessel before adding the medium. This was challenging in microbiological terms. Dissolved oxygen tension (DOT) was monitored by a pO_2 electrode (Mettler Toledo Ltd., Leicester, UK). The DO probe was calibrated after sterilisation but before inoculation at the fermentation temperature, amplitude and frequency by introduction of oxygen free nitrogen (OFN) to set 0% and air to set 100%. The DO probe was sterilised separately in water and then inserted to the vessel before adding the medium to the vessel. The vessel was heated via a heat jacket, and the temperature

was controlled using an Electrolab temperature probe, the controller and heating belt. The temperature probe was sterilised chemically by immersing the probe in sodium hypochlorite 2% v/v (Fisher Scientific) for 2 hours before the run, and then aseptically inserted into the vessel before addition of the medium to the vessel. 1 ml of polypropylene glycol 1950 g/mol (BDH) was added to the medium before sterilisation as an antifoam agent. The fermenter was connected to the main laboratory lines for air and water. Air entered the vessel after being filtered through a glass microfiber filter within a polypropylene housing measuring 50 mm diameter and with a 0.3 µm pore size (Whatman). For the purpose of sampling, three 5 mm diameter sample lines were fitted to column at different heights, but due to the large volume of the sample needed only the middle port was used for sampling. The large sample volume was caused by the significant dead volume in these lines. A set of 3 stainless steel annular baffles of 3 mm thickness were used to enhance bulk mixing and gas dispersion. The baffles were equally spaced 150 mm apart and supported by two 6.35 mm diameter stainless steel rods. The orifice diameter was 46 mm. For agitation, the baffle set was connected to the shaft of a piston which entered through a supporting plate. An inverter attached to an external electrical motor drove this piston with a reciprocal action (Figure 3.4).

The oscillation frequency used in these studies ranged from 0.2 up to 10 Hz, and this was controlled using a speed controller. Oscillation amplitudes of 5 up to 30 mm (centre-to-peak) were generated by adjusting the preset distance between the linkage and the flying arm (Figure 3.5). The vessel was sterilised empty with ports and lines

sealed and taped, and the medium was autoclaved separately and then fed aseptically into the vessel.

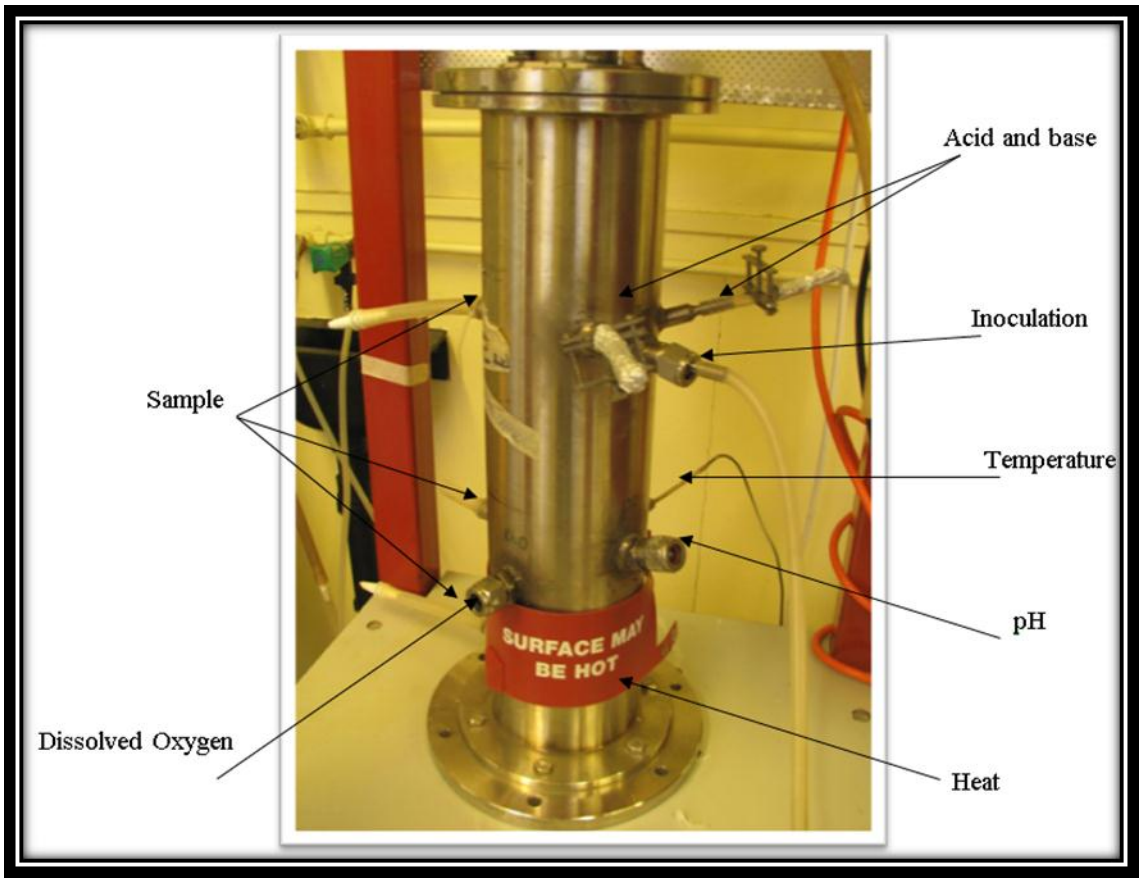

Figure 3.3: The OBR vessel and associated ports.

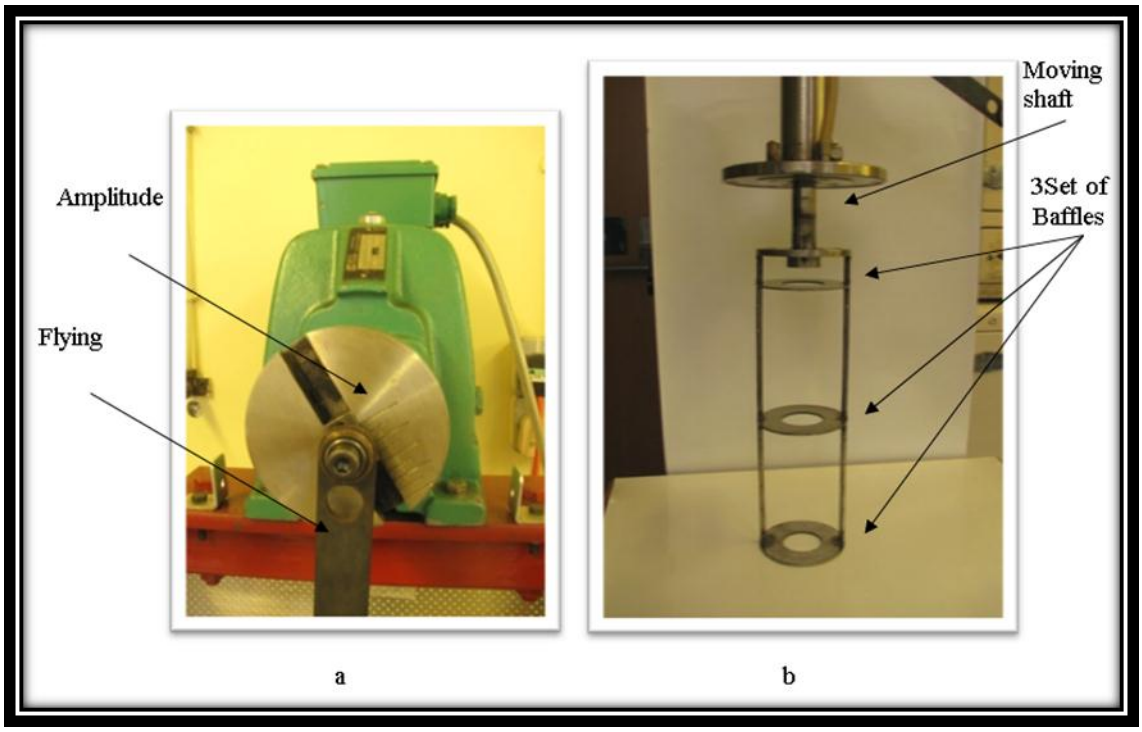

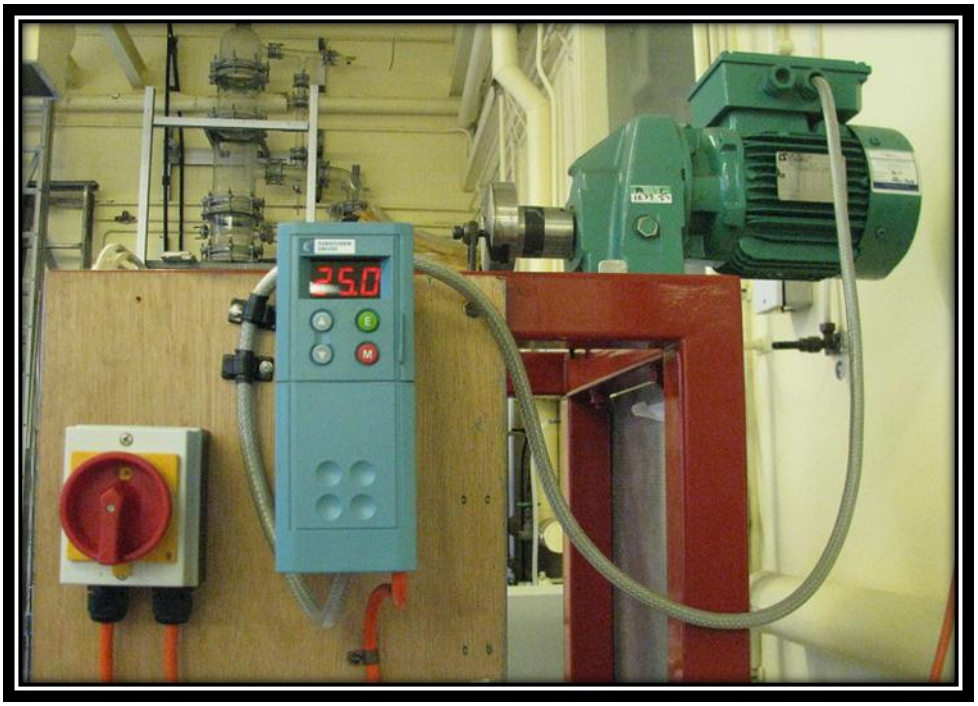

c

Figure 3.4: The OBR agitation and motor arrangement (a) Motor and amplitude scale (b) A set of 3 stainless steel annular baffles (c) Switch and the digital frequency controller.

Figure 3.5: The operational configuration of the OBR during batch fermentation of *X. campestris* ATCC 13951.

3.2.2 Incubator

Cultivations in 500 ml Erlenmeyer flasks were carried out in a rotary shaker (New Brunswick Scientific, Edison, USA) at a temperature of 30 °C and rotational speed of 200 rpm for 120 hours.

3.2.3 Spectrophotometer

A dual-light path UV-Vis spectrophotometer with thermostatted rotary 7-cell changer in sample position (BioMate 5, Thermo Scientific, Hemel Hempstead, Hertfordshire, UK) was used to measure the optical density of the inoculums.

3.2.4 Gas analysis

The exit gas composition was measured using a digital gas analyser TANDEM PRO (Applikon Biotechnology Ltd, Tewkesbury, Gloucestershire, UK). Two gases were used for calibration Oxygen 19.0% (v/v) and 1.75% CO_2.

3.3 Analytical methods

3.3.1 Biomass Estimation

Biomass was measured as dry cell weight. The fermentation broth was diluted up to 5 times according to the viscosity and centrifuged at 10,000 rpm for 30 min to separate the cells in a refrigerated multifunction centrifuge (Jouan BR4i, Thermo Electron Corporation, East Grindstead, West Sussex, UK). The maximal spin rate was 14000 rpm (18407×g). The supernatant after centrifugation was used for the estimation of glucose and xanthan gum. The cell pellet was re-suspended in 20 ml distilled water to remove any remaining xanthan gum and centrifuged at 10,000 rpm for 15 min twice. The pellet was then transferred to a pre-weighted Eppendroff tube dried at 80 °C for 24 h and centrifuged for 5 min at 10,000 rpm in a bench top microcentrifuge (Eppendorf Microcentrifuge 5415D, Eppendorf AG, Hamburg, Germany). The maximal spin rate was 13200 rpm (16110×g) to remove the excess water, after which the Eppendorf with the cell pellet was dried in an oven at 80 °C for 24 h then was weighed after cooling in desiccator for 2 h.

3.3.2 Xanthan gum estimation

The biopolymer (xanthan gum) was precipitated by adding 5 volumes of iso-propanol to 3 ml of cell free fermentation broth; this was then left to stand for 1h in the fridge. The precipitate was then filtered through a pre-dried pre-weighed glass microfibers filter paper disk range MF200 47mm diameter (Fisher Scientific). The

precipitated biopolymer and filter disc was then dried in a microwave for 25 min at thaw setting. Followed by oven drying at 80 °C for 30 min, then cooled in the desiccator and weighed.

3.3.3 Residual glucose determination

D-glucose was determined using an enzymatic ultra violet (UV) determination assay kit (R-Biopharm). The test involved two steps: an enzymatically catalysed reaction in which D-glucose was phosphorylated eventually yielding D-gluconate-6-phosphate (G-6-P) and ADP in the presence of ATP. This reaction was catalyzed by the enzyme Hexokinase (HK). G-6-P was then oxidised by NADP yielding D-gluconate-6-phosphate and NADPH the reaction was catalysed by the enzyme glucose-6-phosphate dehydrogenase (G6P-DH). The amount of NADPH formed is stoichiometric to the amount of D-glucose present in each sample. The concentration of glucose in each sample was assayed using the automated COBAS MIRA (Roche Diagnostics Ltd., Burgess Hill, West Sussex, UK) or by the biochemistry auto-analyser YSI 2700 SELECT (YSI Ltd, Fleet, Hampshire, UK).

.

3.3.4 Residual citrate determination

Citric acid was determined using an enzymatic/ UV determination assay kit (R-Biopharm). The test involved a two step enzymatically catalysed reaction in which citrate was converted first into oxaloacetate and acetate in a reaction catalyzed by the enzyme citrate lyase (CL). Oxaloacetate and its decarboxylation product pyruvate were then reduced to L-Malate and L-Lactate respectively by reduced (NADH) in a

reaction catalyzed by the enzyme L-Malate dehydrogenase (L-MDH) and L-Lactate dehydrogenase (L-LDH) respectively. The amount of (NADH) formed is stoichiometric to the amount of citrate present in each sample. The concentration of citrate in each sample was assayed using the automated COBAS MIRA (Roche Diagnostics Ltd., Burgess Hill, West Sussex, UK).

3.3.5 Residual acetate

Free acetic acid was determined via an enzymatic/ UV determination kit (R-Biopharm). The test involved a three step enzymatic reaction in which acetate is converted to acetyl-CoA by the enzyme Acetyl-CoA synthase in the presence of Adenosine 5 Triphosphate (ATP) and Coenzyme A. Acetyl CoA then reacts with oxaloacetate in the presence of citrate synthase to form citrate. Oxaloacetate was formed from L-malate and NAD, hence reduction of NAD to NADH in the presence of L-malate dehydrogenase. The amount of NADH formed is proportional to the amount of acetate present and was measured spectrophotometrically at a wave length of λ340nm. 50 µl of sample was used to make up a volume of 2 ml kit reagent, which consisted of L-malic acid, ATP and NAD and the first absorbance read. Solution (5 µl) containing L-malate dehydrogenase and citrate synthase was then added to the mixture and the absorbance (A_1) read after three minutes. Acetyl-CoA synthase (10 µl) was then added and the final absorbance (A_2) read after 15 minutes, after which the acetic acid could be calculated. Acetate estimation was carried out in a dual-light path UV-Vis spectrophotometer (BioMate 5, Thermo Scientific, Hertfordshire, UK).

3.3.6 Molecular weight determination

For molecular weight determination the samples were sent to the Malvern Instruments Company, Malvern, UK where the samples were subjected to size exclusion chromatography (SEC) analysis using the Triple Detection GPC method. The samples were sent to the company as a fine dried powder in polyethylene vials and kept in room temperature.

3.3.6.1 Sample preparation

The samples provided were dissolved in phosphate buffered saline (PBS) solvent for 60 h. Then they were filtered with a 1.0 μm PTFE filter prior to injection into the SEC system.

3.3.6.2 Chromatographic condition

Table 3.3: Chromatography condition for the molecular weight estimation in the gel permeation chromatography (GPC).

Solvent	phosphate buffered saline (PBS)
Flow rate	0.7 ml/min
Injection volume	100 μl
Column/ Detector temperature	40 °C
Columns	ViscoGEL A7000 VsicoGEL A6000M x 2 ViscoGEL A3000
Detector	TDA305

3.3.7 Rheological determination

Rheological measurements were carried on all whole broth samples taken from the fermenter using RM180 Rheomat viscometer (Model RM180, Rheometric Scientific, Inc., NJ, USA). The apparent viscosity (μ_a) of the fluid was measured at system number 22, which includes the measuring bob 1 (φ = 30 mm, 1 = 45mm) and the measuring tube 1 (φ = 32.54 mm) at 30 ± 0.5 ^{o}C. Samples were subjected to different shear rates (from 100-1000 /s). The torque readings were used as an indication of the accuracy/stability of each system. The limitation in the rheometer RM180 is that at lower shear rates (100 – 200 /s) in initial samples where xanthan gum in low concentration the following error message kept appearing: *M too low* (<0.25 mN.m), reducing the number of data points obtained per sample.

3.4 Modification

This section presents the technical modifications that have been applied to the OBR in order to overcome some problems that have been encountered in the production of xanthan gum. It is divided into three broadly areas: sterilisation, sparging and mechanical alignment. These modifications were proposed by the author in consultation with supervisors.

3.4.1 Sterilisation

In the previous tests, the pH and DO probes (Figure 3.6) were made of plastic hence were difficult to sterilise as chemical methods had to be used. This was followed by an aseptic transfer to the vessel.

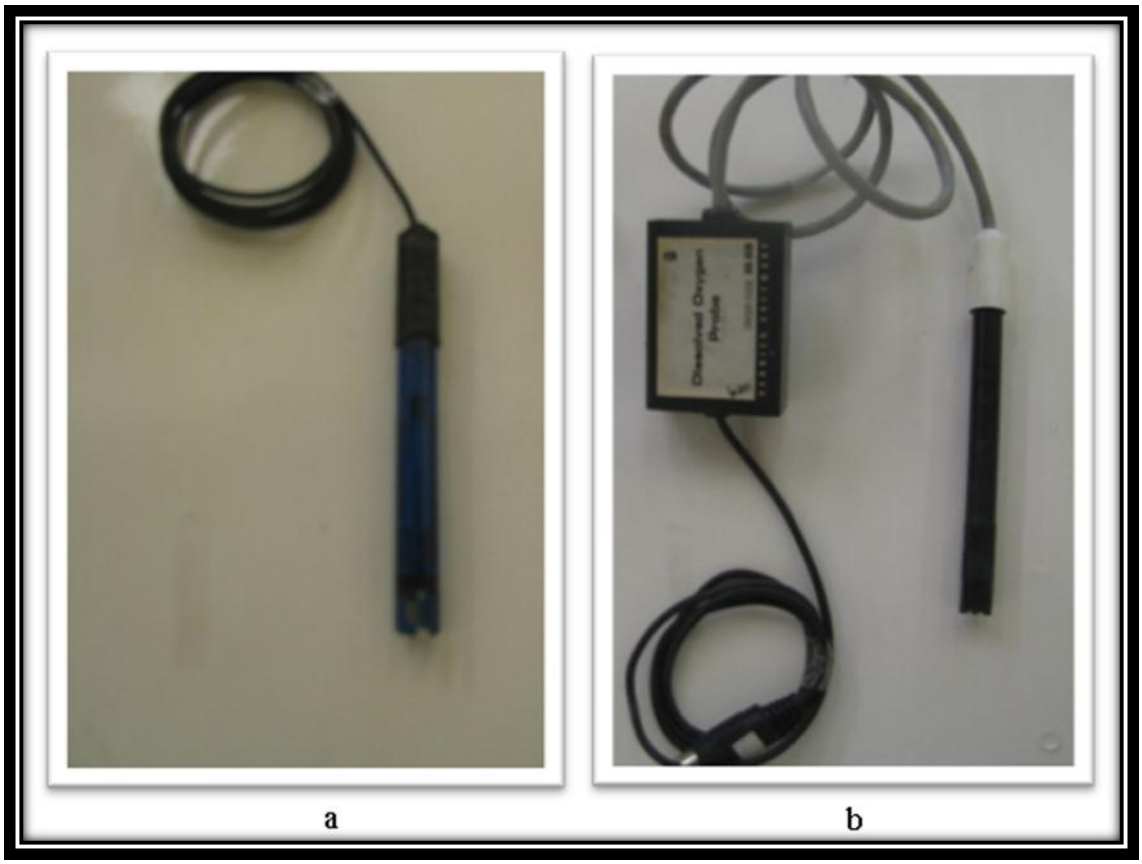

Figure 3.6: (a) A plastic Anglicon pH probe. (b) A plastic Vernier DO probe.

To remedy this shortening, an autoclaveable and detachable glass pH probe (Mettler Toledo Ltd., Leicester, UK) and stainless steel DO probe (Mettler Toledo Ltd., Leicester, UK) were used as shown in figure 3.7.

Figure 3.7: a) An Autoclaveable detachable glass pH probe (Mettler Toledo Ltd., Leicester, UK (b) An autoclaveble detachable stainless steel DO probe (Mettler Toledo Ltd., Leicester, UK).

In the previous tests, the Temperature sensor used was a Biolab Biostat control system, with a sensing element located inside the fermenter and a heating coil wound outside the fermenter column. Due to the difficulty in attaching the heating coil and removing it for autoclaving and to communicate with the new interface the

temperature system was replaced with heat jacket, and the temperature was controlled using an Electrolab temperature probe (Figure 3.8). This allowed much improved temperature control.

The OBR vessel was routinely sterilised lying horizontally, sealed and empty. The 2 L medium was sterilised separately in a 5 L Erlenmeyer conical flask. The pH and dissolved Oxygen probes were immersed in reagent bottles half full with distilled water sealed with cotton and covered with aluminium foil, whereas the temperature sensor was chemically sterilised using sodium hypochlorite 2% v/v (Fisher Scientific) for 2 hours before the run, as can be seen in figure 3.9 and 3.10.

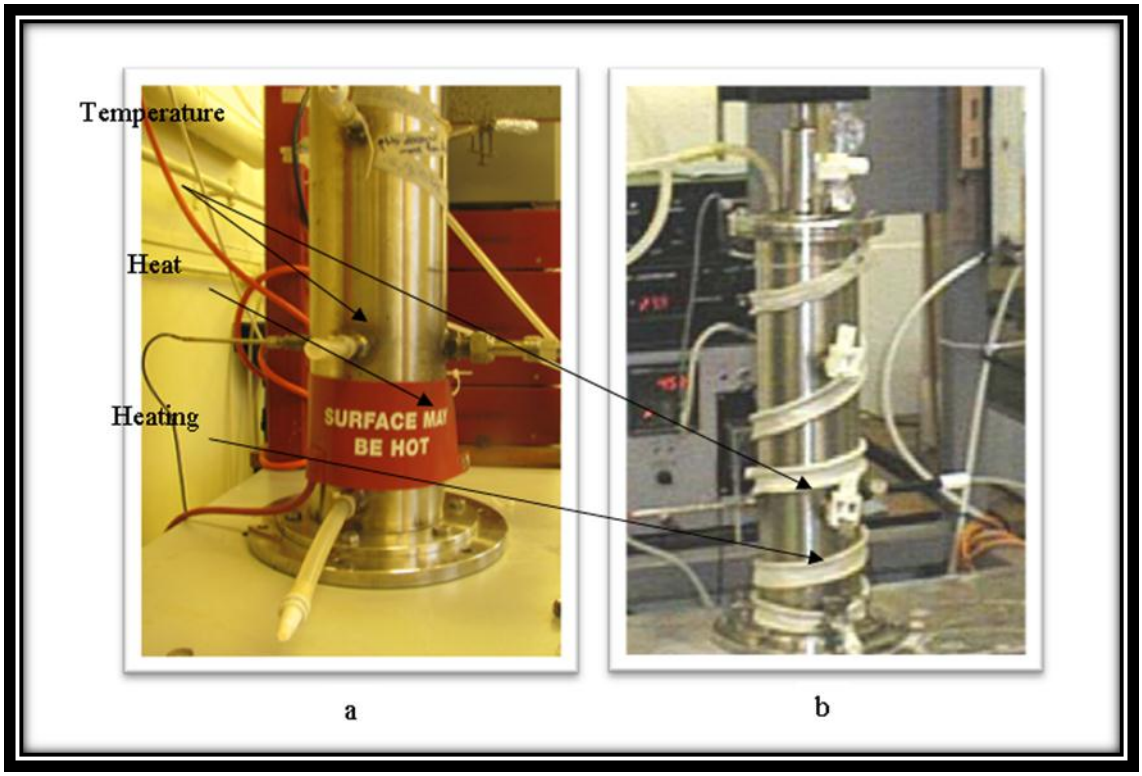

Figure 3.8: (a) Current temperature controller heating jacket and temperature sensor (b) Old temperature controller heating coil and temperature sensor.

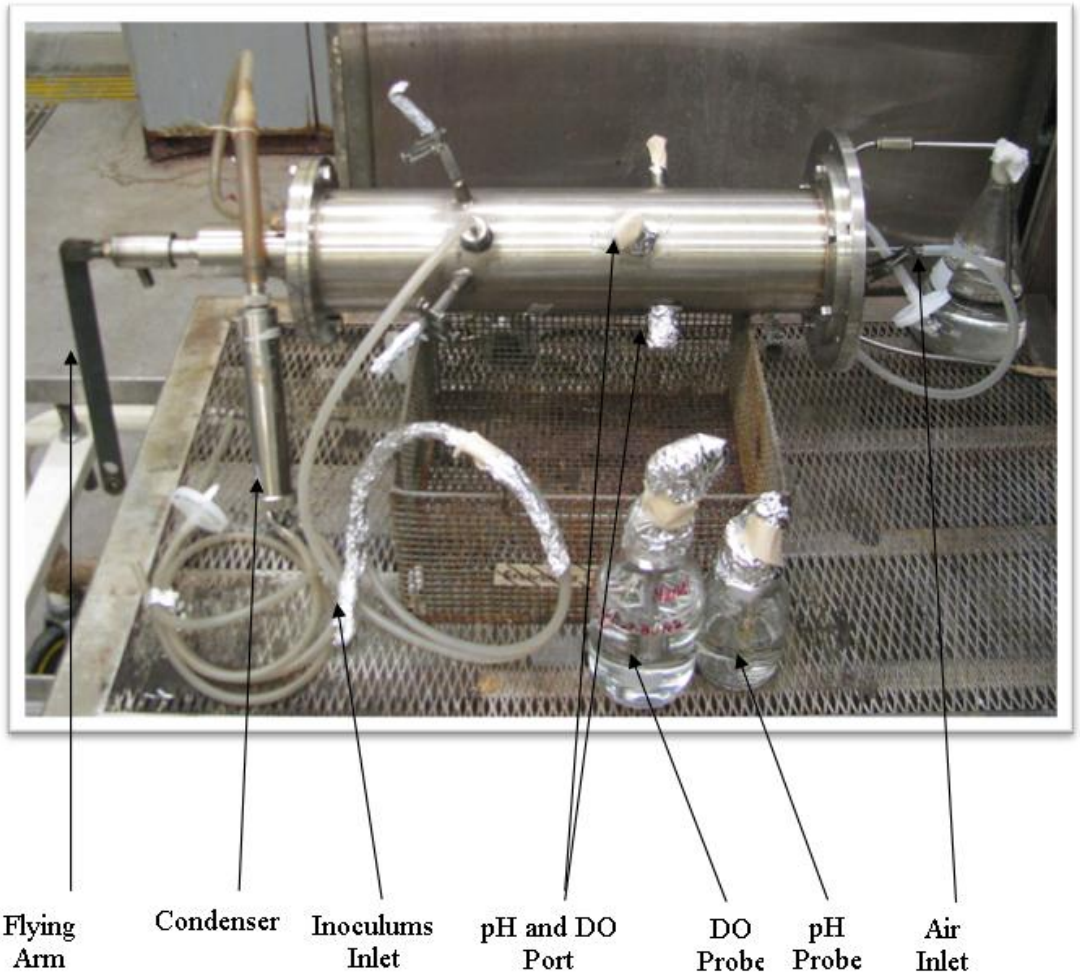

Figure 3.9: Operational Configuration of the OBR for sterilisation by autoclaving.

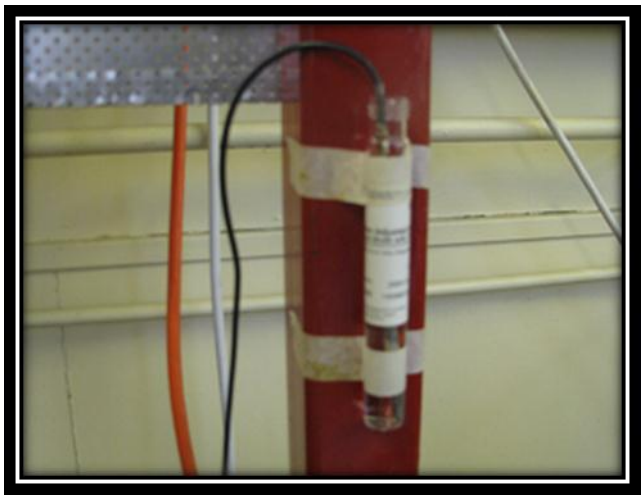

Figure 3.10: Temperature sensor chemically sterilisation.

3.4.2 Sparger

Due to the viscous medium, the direction of air sparging within the vessel was considered to have an effect on the yield. Previously, the holes in the sparger faced down towards the bottom of the vessel as shown in figure 3.11. In the modified version the orientation of the sparging holes was reversed so that they were upward pointing.

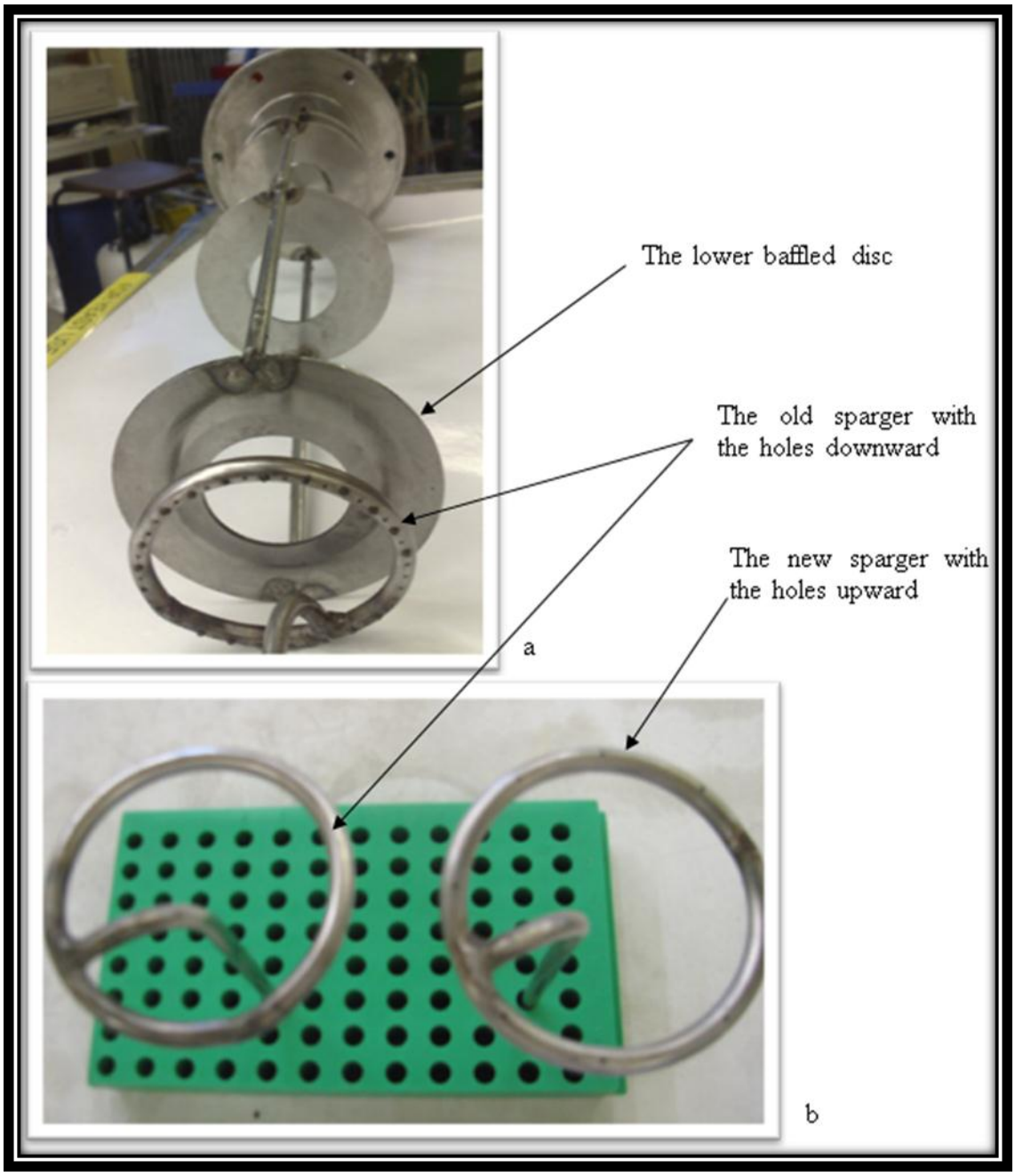

Figure 3.11: (a) The sparger placed under the lower baffled disc. (b) The old and the new spargers.

3.4.3 Alignment

The OBR was fabricated at Heriot Watt University lab, but initially the precision in the piston was not very high. This caused miss-alignment between the piston and the moving arm during tests. The outcome from this was the unexpectedly high friction, leading to unusual amounts of heat being generated. The friction in the seals very quickly wore down the seals (less than a day) and as the seals disintegrated allowed to black carbon powder getting into the medium causing contamination. In addition the heat caused jerky movement of a moving arm, which sometimes stuck (Figure 3.12).

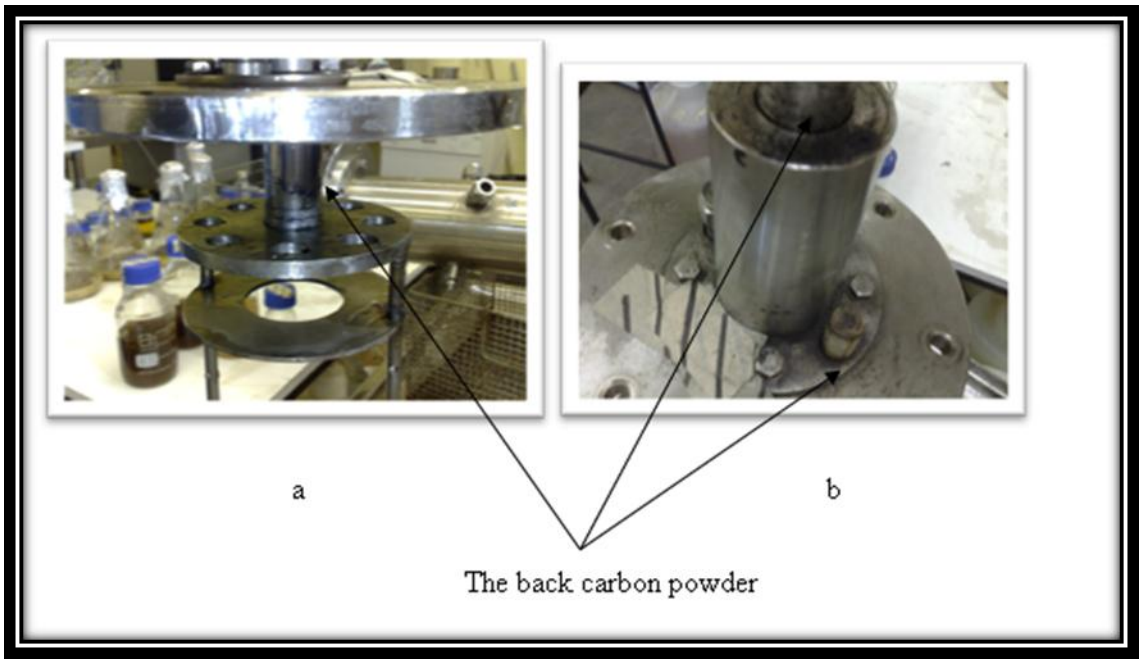

Figure 3.12: The back carbon powder (a) Outside view in the top plate of the plate and around the piston and the shaft (b) Inside view around the piston and in the top of the baffled disc support.

The actions to rectify the problem involved cleaning the piston before autoclaving and a white silicone grease lubricant was applied around the outer part of the piston as shown in figure 3.13 after autoclaving.

To overcome the jerky movement of the piston a couple of nuts and screw (As shown in figure 3.14 were used to better secure the elements of the agitator system.

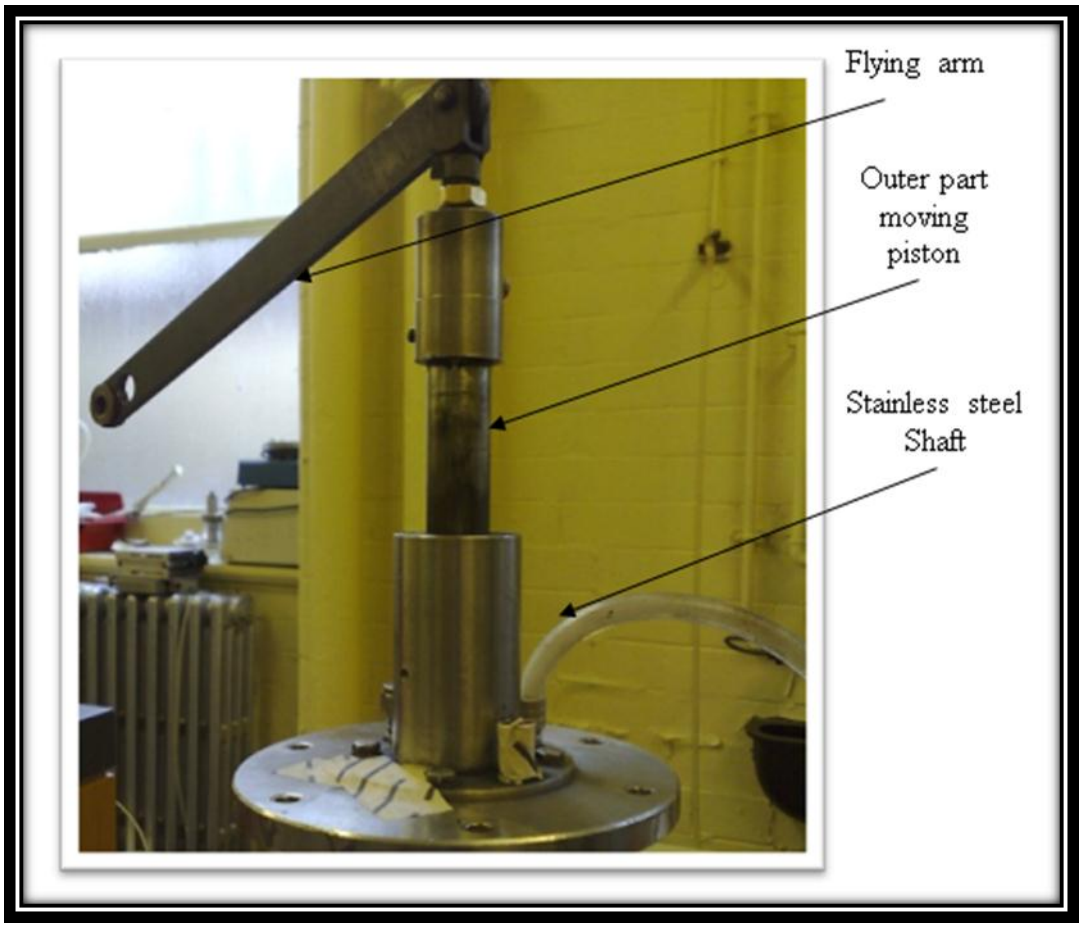

Figure 3.13: The upper part of the fermenter.

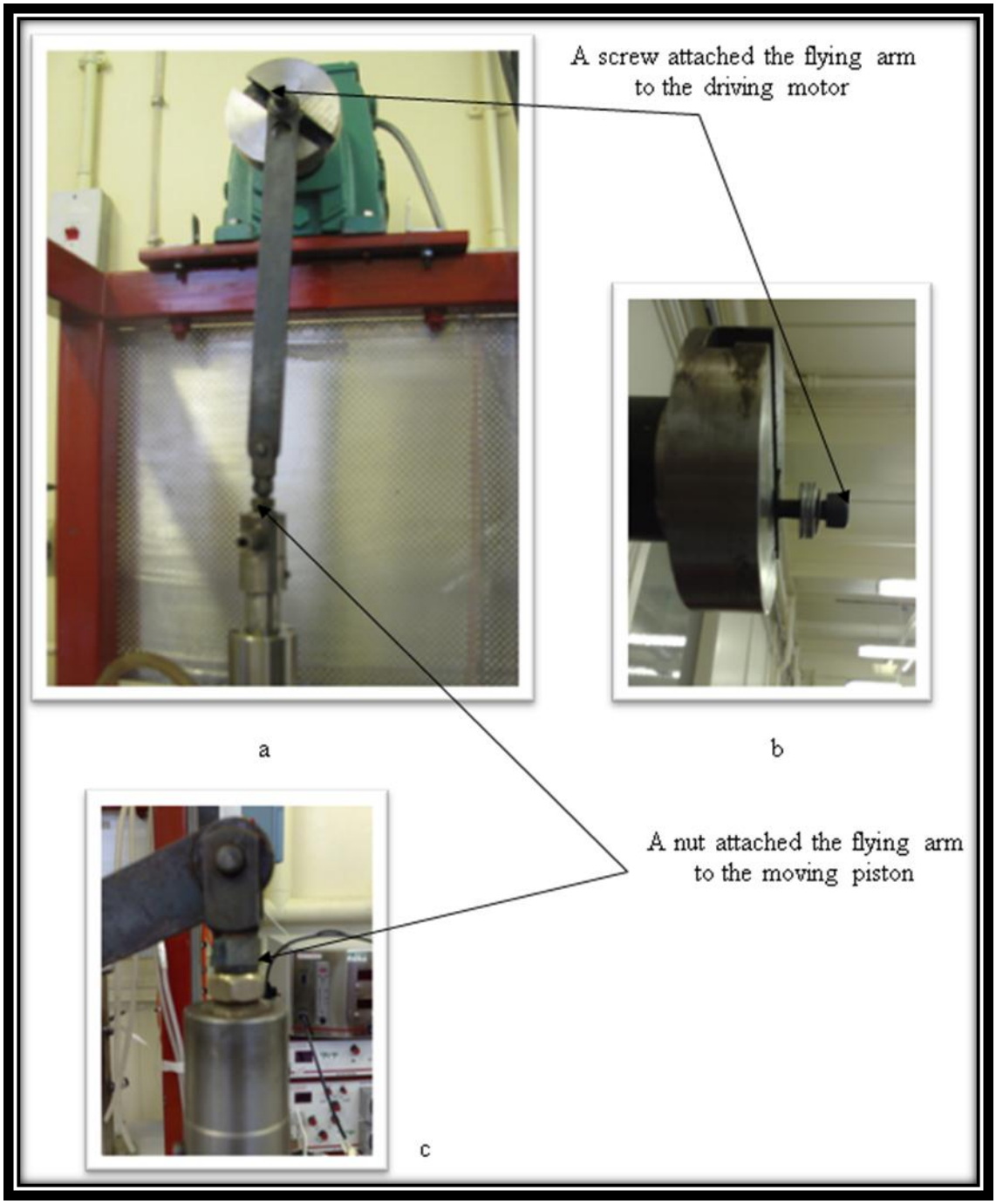

Figure 3.14: (a) The flying arm attached to the driving motor and to the moving piston. (b) Side profile for the driving motor plate with the new 15 mm length screw (c) the new 8 mm thickness jam nut.

Chapter 4

Results

4 Results

Chapter 4 presents the results that were obtained from the fermentation of *X. campestris* ATCC 13951 for the production of xanthan gum. The chapter is divided into five sections. The production of xanthan gum in shake flasks is given in Section 4.1. The production of xanthan gum in the STR is discussed in Section 4.2, and the production of xanthan gum in the OBR is detailed in Section 4.3. Note that in both sections 4.2 and 4.3 the process state is generally discussed in relation to five main indicators; change in culture pH, dissolved oxygen, total biomass, xanthan concentration, and glucose consumption. The production of acetic acid is presented in Section 4.4. In addition, in Section 4.5 the molecular weight results for xanthan are presented. Finally, a comparison of the power consumptions of the OBR, and the conventional industry workhorse, STR are given in Section 4.6.

4.1 The production of xanthan gum in shake flasks

This section focuses on the production of xanthan gum in shake flask batch cultures of *X. campestris* ATCC 13951. Three processing factors are investigated: section 4.1.1 deals with the effect of glucose source concentration in the growth medium YM, while section 4.1.2 examines the effect of citric acid concentration in a defined production medium and section 4.1.3 examines the effect of agitation rate.

4.1.1 The effect of initial glucose concentration

As mentioned in the literature review (Chapter 2), the production of xanthan gum is dependent on the carbon nitrogen ratio (C/N) in the medium, therefore, in order to investigate the effect of such variations of C/N ratio on microbial growth and xanthan gum production in the growth medium YM, experiments were carried out where yeast extract (Nitrogen source) was fixed to 4 g/l and glucose concentration (Carbon source) was varied from 2 - 8 g/l in 400 ml growth medium in 1l flasks, at a shaking speed of 200 rpm and fixed temperature of 30 C throughout the duration of the fermentation, which was typically 120 hours. A total of 4 fermentation experiments carried out, covering initial glucose concentrations of 2, 4, 6 and 8 g/l. All the experiments were repeated in triplicate for the purpose of assessing reproducibility, and the replicate data are shown with error bars in all figures in this section.

4.1.1.1 The effect of initial glucose concentration on growth (as total biomass)

The effect of initial glucose concentration on the microbial growth as dry cell weight (DCW) is presented in figure 4.1. It can be seen that generally an increase in initial concentrations of glucose led to faster increased in biomass accumulation in the first 24 hours. The highest biomass concentration of 1.60 g/L was obtained at 24 hours with an initial glucose concentration of 8 g/L compared to 1.18 g/L biomass obtained at an initial glucose concentration of 2 g/L, although the malt and yeast extract concentrations remained the same throughout 10 g/L at the same time. Examining the microbial growth profiles more closely, it can be seen in all fermentations that the growth of the bacterium *X. campestris* exhibits a growth phase which is usually completed by 24 hours, followed by a sharp decline in cell mass, before the cultures enter what appears to be a stationary phase which generally prevails until the end of the experimental period (Figure 4.1). The corresponding measurements of xanthan gum concentration and the residual glucose concentration are given in figure 4.2 and figure 4.3, respectively.

4.1.1.2 The effect of initial glucose concentration on xanthan gum production

Figure 4.2 shows the effect of initial glucose concentration upon production of xanthan gum with respect to the process time. It is clear that in the initial phase (exponential phase) the production of xanthan gum occurs at almost at similar rates regardless of the initial glucose concentration in the medium. After 48 hours of

cultivation, the rate of xanthan production still increased at different rates, although the glucose was totally consumed at initial glucose concentrations of 2 and 4 g/l however xanthan continued to be produced until the end of the fermentation time, with the highest production occurring at an initial glucose concentrations of 8 g/l.

4.1.1.3 The effect of initial glucose concentration on glucose consumption

The patterns of glucose consumption in shake flask cultures at different initial glucose levels are shown in figure 4.3. Overall patterns of glucose consumption have broad similarities. For example, the most rapid glucose consumption rates occur before 24 hours with different consumption rates respectively to the initial glucose concentration. For the two lowest initial glucose concentrations (2 and 4 g/l) maximum consumption rates are 0.06 g/l/h and 0.102 g/l/h respectively, and most glucose was consumed by 48 hours. Whereas in the process with the higher glucose concentrations (6 and 8 g/l) maximal glucose consumption rates of 0.11 g/l/h and 0.13 g/l/h respectively are achieved early in the process, but after this glucose consumption continues at a lower rates toward the end of the fermentation time.

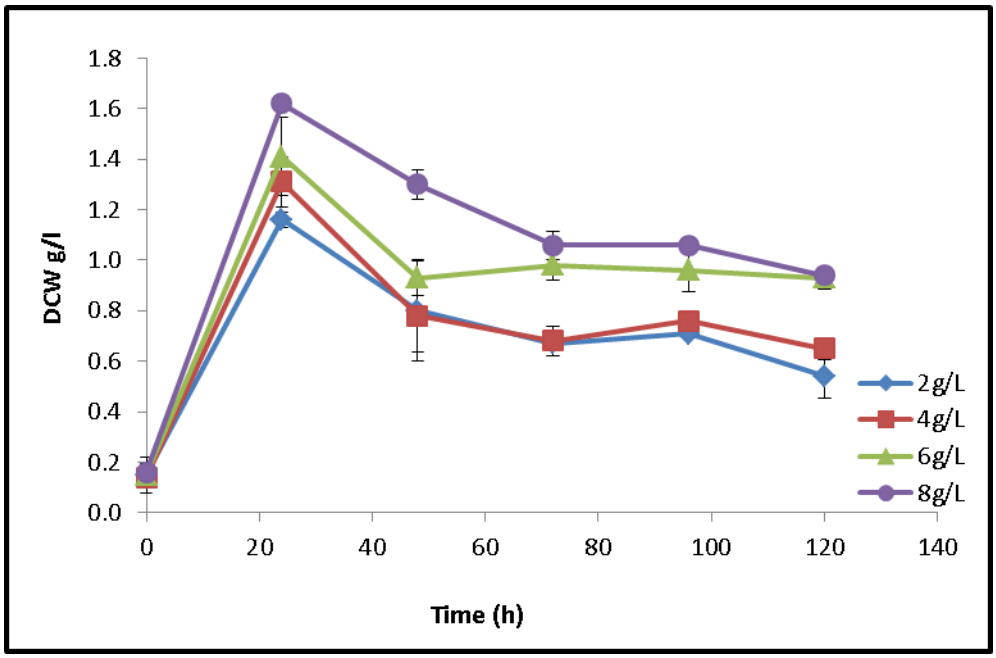

Figure 4.1: The effect of initial glucose concentration on total biomass production in batch cultures of *X. campestris* ATCC 13951 in YM medium in shake flask fermentations carried out at 200 rpm and 30 °C.

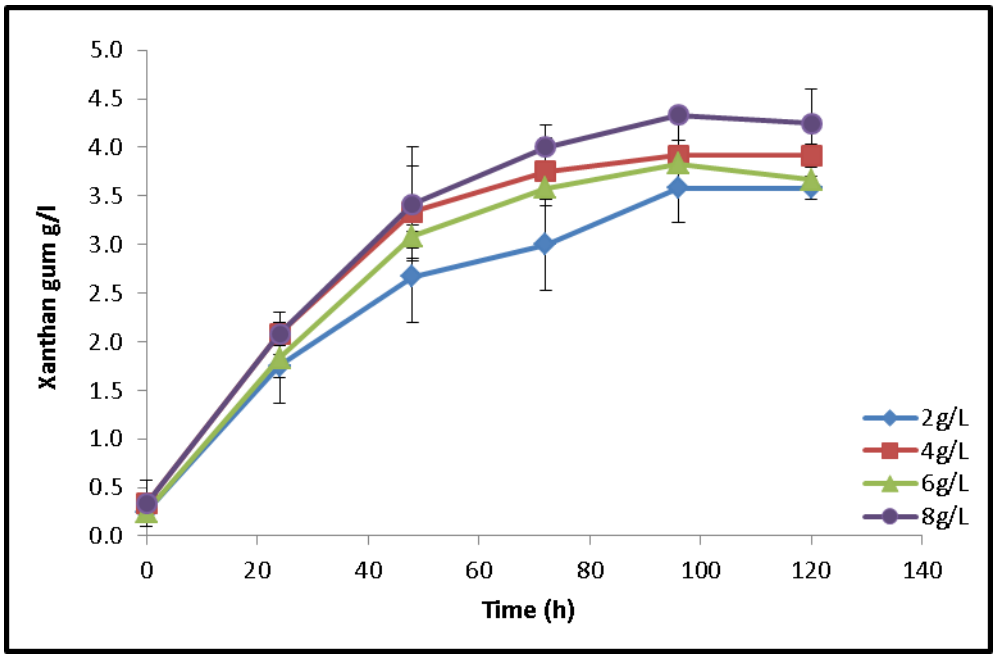

Figure 4.2: The effect of initial glucose concentration on the production of xanthan gum in batch cultures of *X. campestris* ATCC 13951 in YM medium in shake flask fermentations carried out at 200 rpm and 30 °C.

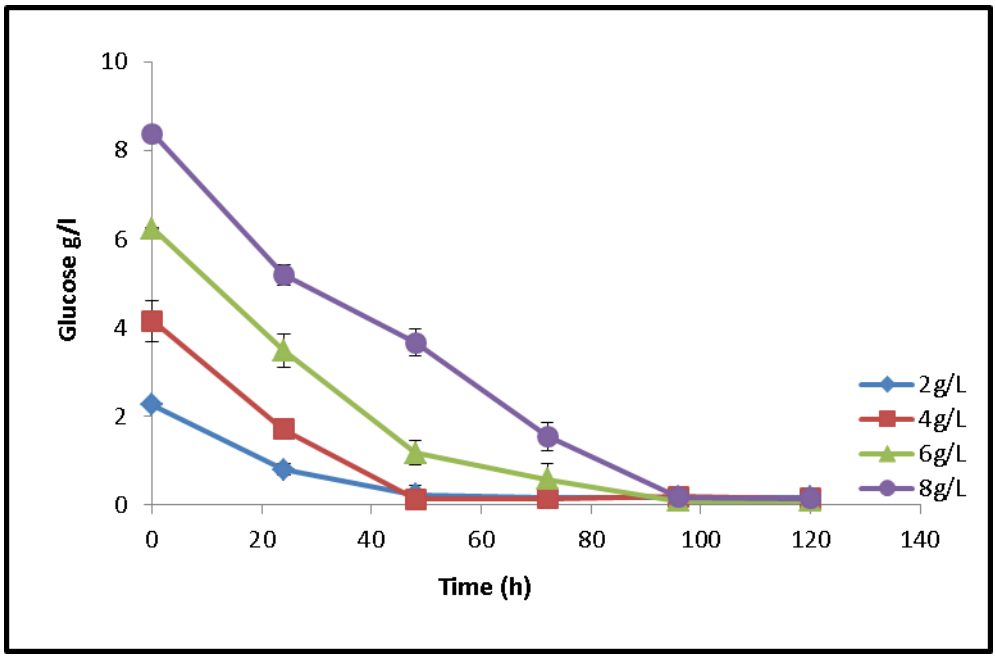

Figure 4.3: The effect of initial glucose concentration on the glucose consumption in batch cultures of *X. campestris* ATCC 13951 in YM medium in shake flask fermentations carried out at 200 rpm and 30 °C.

4.1.2 The effect of citric acid supplementation on the process

For production of xanthan using synthetic media, citric acid is often used as a chelating agent to prevent the precipitation of salts during heat sterilisation. In addition, it is reported to reduce foam formation

In the present study, the role of citric acid supplementation of the medium was studied in terms of microbial growth and xanthan gum production. The experiments were carried out with citric acid concentrations from 0-4 g/l in 400 ml synthetic medium in 1L flasks, all other conditions are the same as described in section 4.1.1. There were a total of 5 fermentation experiments carried out, covering citric acid concentration of 0, 0.5, 1.0, 2.0 and 4.0 g/l. All the experiments were repeated for the purpose of assessing reproducibility, and the duplicate data are shown with error bars in all figures in this section. Figure 4.4a and b show the effects of citrate supplementation upon appearance of the medium post-autoclaving (Figure 4.4 a) and after 96 hours fermentation time (Figure 4.4 b).

4.1.2.1 The effect of citric acid supplementation on growth as total biomass

Figure 4.5 shows the effect of different citric acid concentrations on the growth of *X. campestris* ATCC 13951 in a synthetic medium containing 20 g/l glucose in shake flask. It can be seen from the figure that supplementation with citrate at any level led

to an extended growth phase and elevated biomass levels relative to the control where no citrate was present. In the citrate supplemented batch there was little evidence of an actual stationary phase, instead the growth phase was followed very closely by sharp biomass decline phase. In general the increase in citric acid concentration seems to enhance the biomass concentration.

4.1.2.2 The effect of the citric acid supplementation on xanthan gum production

The effects of citric acid supplementation on xanthan gum production in shake flask culture experiments at different citric acid concentrations (0.0 g/l - 4.0 g/l) are shown in figure 4.6. The results clearly indicate that with an increase in citric acid concentration xanthan gum production increased. The amount of polysaccharide formation was at maximum (9.0 g/l) with 4.0 g/l citrate added. By contrast, at the control where no citrate was added, xanthan concentration was only 3.0 g/l at the end of the process (96 hours) and was the lowest production recorded in this study.

4.1.2.3 The effect of citric acid supplementation on glucose consumption

The effect of citric acid addition to the culture medium on glucose concentrations are shown in figure 4.7. In a medium without any citrate present, glucose consumption rate over the first 24 hr was 0.54 g/l/h whereas at 2.0 g/l citrate glucose consumption rate was 0.24 g/l/h and in the highest citric acid concentration of 4.0 g/l, the average glucose consumption rate was 0.38 g/l/h. Note that glucose was not entirely

exhausted after 96 hours in the control process (0 g/l citrate). Overall, this is consistent with the rapid uptake of citrate and its use as a carbon and energy source fuelling both growth and end energy metabolism.

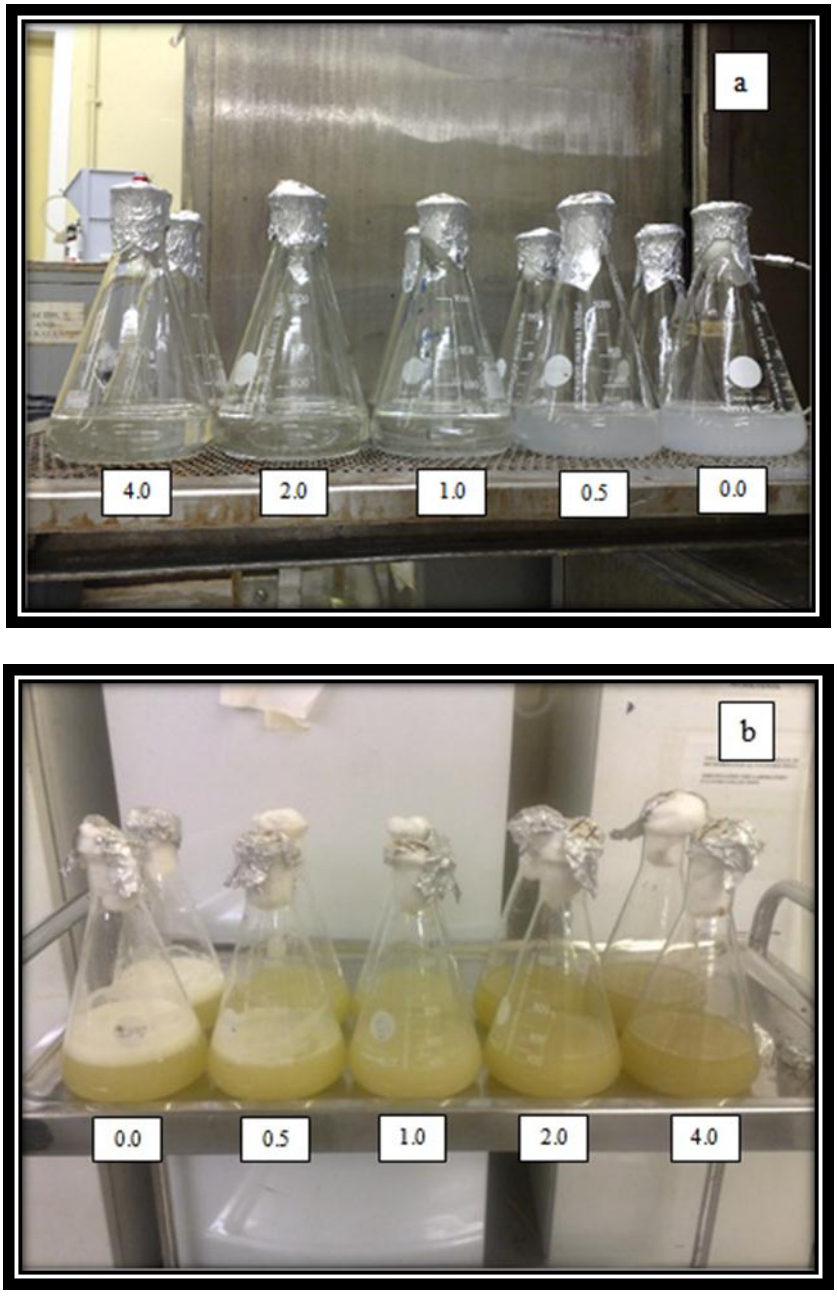

Figure 4.4: The effect of citric acid concentration on the production of xanthan gum by *X. campestris* ATCC 13951 in a synthetic medium in shake flask fermentations. (a) The effect of varying citric acid concentrations (0 – 4 g/l) upon medium clarity and general appearance following autoclaving (b) The effect of varying citric concentrations (0 – 4 g/l) upon foaming in the flasks after 96 hours fermentation time.

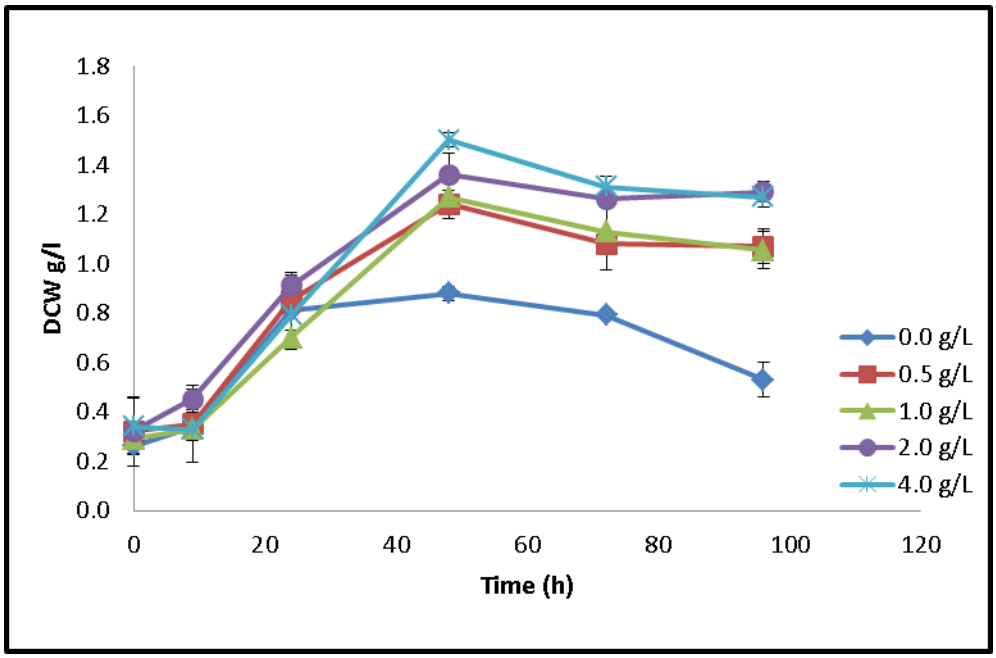

Figure 4.5: The effect of citric acid supplementation on total biomass production in batch cultures of *X. campestris* ATCC 13951 in a synthetic medium in shake flask fermentations carried out at 200 rpm and 30 °C.

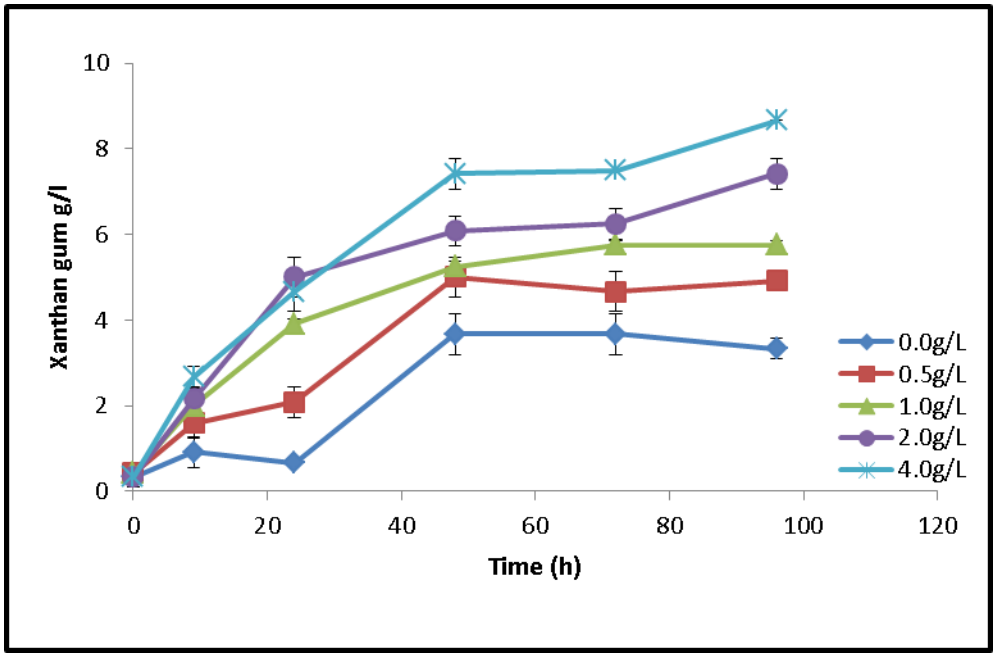

Figure 4.6: The effect of citric acid supplementation on the production of xanthan gum in batch cultures of *X. campestris* ATCC 13951 in a synthetic medium in shake flask fermentations carried out at 200 rpm and 30 °C.

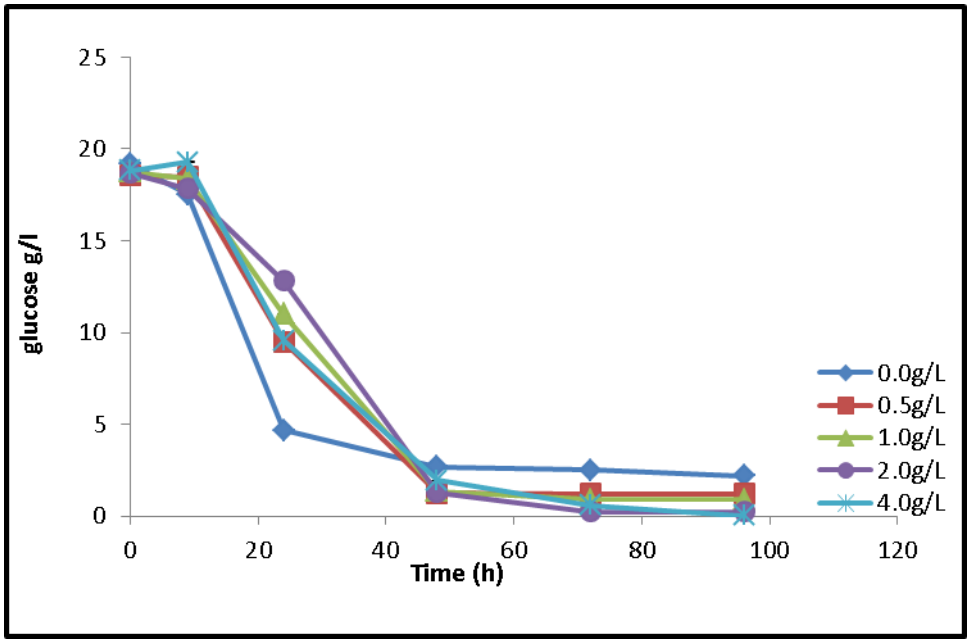

Figure 4.7: The effect of citric acid supplementation on glucose consumption in batch cultures of *X. campestris* ATCC 13951 in a synthetic medium in shake flask fermentations carried out at 200 rpm and 30 °C.

4.1.3 The effect of agitation rate

The kinetics of growth and xanthan production by *X. campestris* ATCC 13951 were studied in shake flasks. Fermentations were carried out over a range of rotational speeds. The experiment was carried out in 400 ml synthetic production medium with 20% w/v glucose and 2.1 g/l citric acid in 1l flask at 30 °C. A total of 3 fermentation experiments were carried out, covering rotational speeds of 100, 200 and 300 rpm. All the experiments were repeated for the purposes of assessing reproducibility and the duplicate data are shown with error bars in all figures in this section.

4.1.3.1 The effect of agitation speed on growth as total biomass

Figure 4.8 shows the cell dry weights over time at 100, 200, and 300 rpm. Growth rate (r_x) increased with the increase in rotational speed, but broadly speaking the growth curves at different agitation rates had similar trends. The maximum biomass by the end of the fermentation was (1.38 g/l) at the highest speed 300 rpm. At low rotational speed biomass reached only 1.12 g/l and at the moderate rotational speed the cell growth was slightly higher (1.20 g/l) by the end of fermentation time (96 hours).

4.1.3.2 The effect of agitation speed on xanthan gum production

Figure 4.9 shows that xanthan gum production was low and similar to the lower speed of 100 rpm and 200 rpm with xanthan production of 3.94 g/l and 4.50 g/l respectively in the first 24 hours. While xanthan production appeared slightly higher in the high rotational speed of 300 rpm at the same time with xanthan production of

6.6 g/l. The maximum xanthan production rate at the lower rotational speed 100 rpm was only 6.4 g/l by the end of the fermentation. It was noticed that the production levels increased as a result of an increase in the rotational speed, the maximum xanthan production for the higher rotational speed 200 rpm and 300 rpm were 9.17 g/l and 10.49 g/l respectively.

4.1.3.3 The effect of agitation speed on the glucose consumption

The glucose consumption was also affected by the rotational speed (Figure 4.10). In the first 24 hours the glucose consumption rate was almost the same in both the lower rotational speed of 100 and 200 rpm with glucose consumption rate of 0.15 g/l/h and 0.17 g/l/h respectively, while at the highest rotational speed of 300 rpm the glucose consumption rate was the highest with glucose consumption rate of 0.25 g/l/h. Almost 50% of the original amount of glucose still remained by the end of the fermentation time at the lowest rotational speed of 100 rpm and 28 % of the original amount of glucose remained by the end of the fermentation time at the moderate rotational speed of 200 rpm, while at the highest rotational speed of 300 rpm the remaining glucose was 25% by the end of the experiment (96 hours).

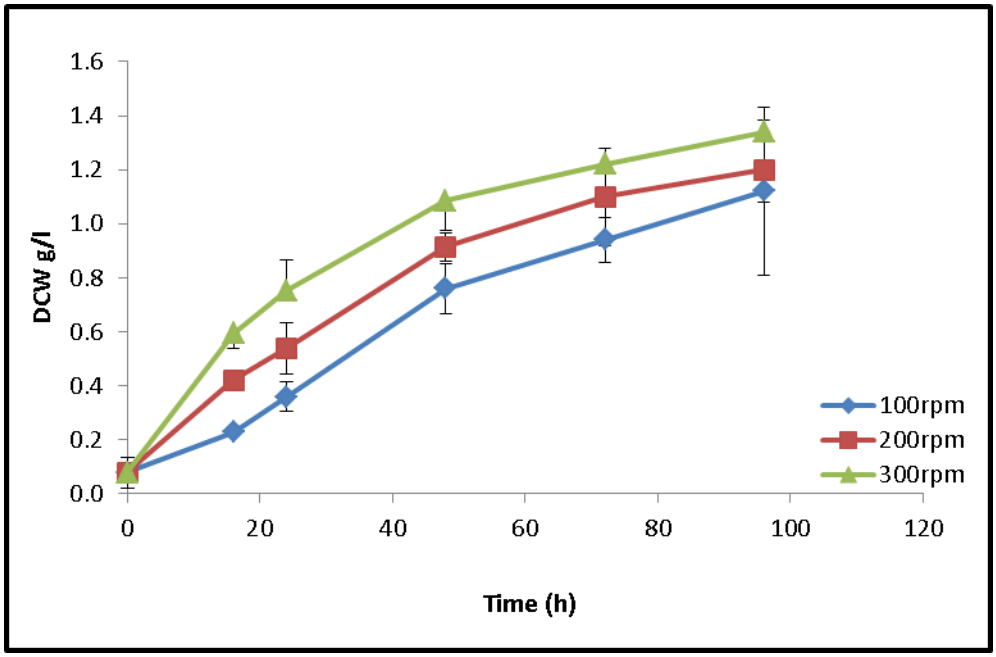

Figure 4.8: The effect of agitation speed on total biomass production in batch cultures of *X. campestris* ATCC 13951 in a synthetic medium in shake flask fermentations carried out at 30 °C.

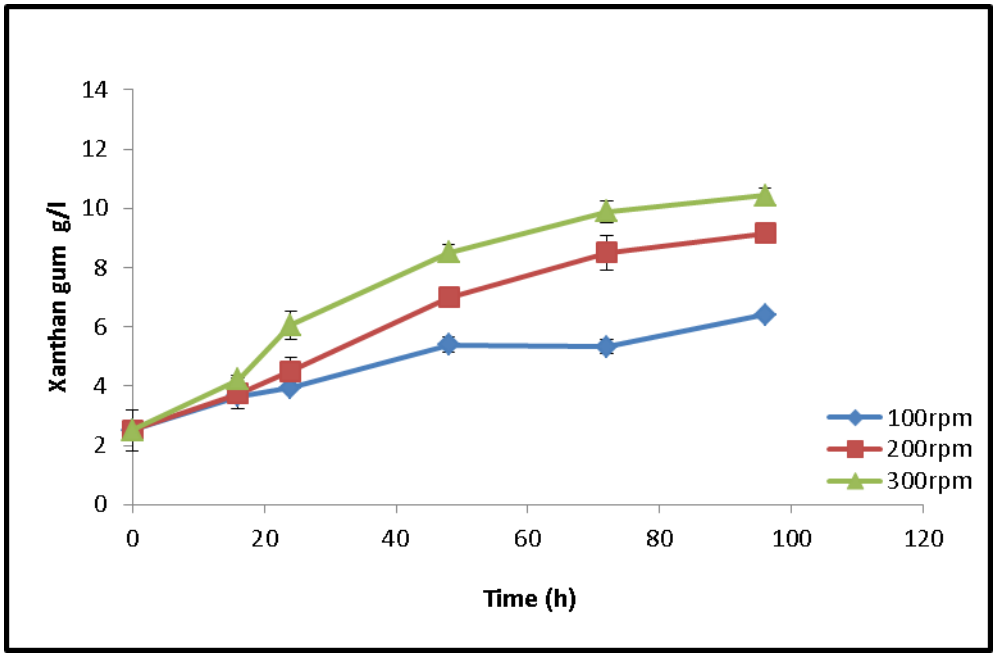

Figure 4.9: The effect of agitation speed on xanthan gum production in batch cultures of *X. campestris* ATCC 13951 in a synthetic medium in shake flask fermentations carried out at 30 °C.

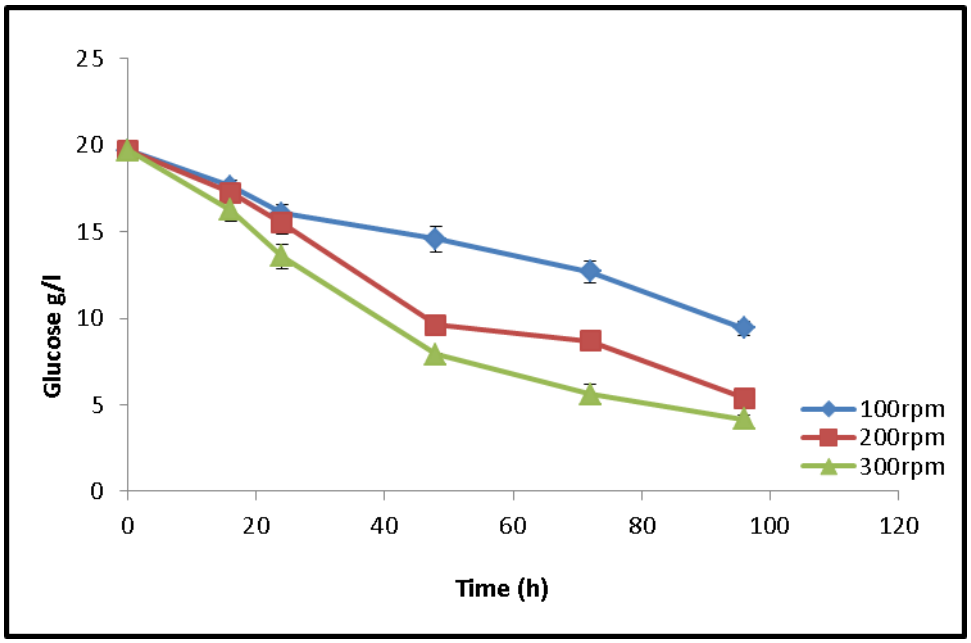

Figure 4.10: The effect of agitation speed on glucose consumption in batch cultures of *X. campestris* ATCC 13951 in a synthetic medium in shake flask fermentations carried out at 30 °C.

4.2 The production of xanthan gum in the Stirred Tank Reactor (STR)

Both aeration and agitation are important for the production of xanthan gum, as they affect both the mixing and the mass transfer rate. This section presents the results that were obtained from the fermentation of *X. campestris* ATCC 13951 in the Stirred Tank Reactor (STR) batch cultures at varying agitation speeds and with two different aeration rates.

The pH of these cultures was allowed to evolve naturally, that is, the pH was not controlled throughout the time course of the fermentations.

A 2 L BIOFLO 3000 Glass-Stainless Stirred Tank Reactor (STR) was used (see Materials and Methods, Chapter 3). The fermenter was steam sterilised by steaming continuously for 30 minutes and contained production medium, anti-foam, pH probe and dissolved oxygen probe. The carbon source (glucose), which was sterilised separately, was aseptically added to the sterile fermenter vessel before inoculation.

4.2.1 The effect of agitation speed

This section will present the results for the effect of different agitation speeds on the production of xanthan gum. The experiments were carried out with different agitation rates varied from 100-500 rpm in 2l production medium inoculated with 10% (v/v) *X. campestris* ATCC 13951culture, aeration was 1vvm, uncontrolled pH and temperature was maintained at 30 °C. A total of 4 fermentation experiments were carried out, covering agitation speeds of 100 rpm, 200 rpm, 300 rpm and 500 rpm. All the experiments were repeated for the purpose of assessing reproducibility and the replicate data are shown with error bars in all figures in this section.

4.2.1.1 The effect of agitation speed on dissolved oxygen

Oxygen was supplied to the cultures in the form of air, at an initial concentration of 100% air containing 21% oxygen and at a gassing rate equal to 1vvm. As can be seen in figure 4.11, the dissolved oxygen reached limiting levels much faster at lower agitation speeds. At an impeller speed of 100 rpm dissolved oxygen reached 0% within 7 hours and stayed at this level to the end of the fermentation time. At 200 rpm and 300 rpm, dissolved oxygen reached 0% at 17 hours and 24 hours respectively. At 200 rpm the D.O remained for 31 hours at 0%, before it rose again in the broth at 48 hours, while at 300 rpm it remained for a longer time at 0% (46 hours) before it increased at 70 hours. On the other hand, at 500 rpm there was no oxygen limitation during the fermentation time course, but D.O fell to 50% by 43 hours. At 43 hours there was a turning point when dissolved oxygen increased in the medium again up to 80 % by the end of the fermentation time.

4.2.1.2 The effect of agitation speed on pH

Figure 4.12 shows the changes in the medium pH with respect to the time of fermentations where it was allowed to evolve naturally. As can be seen, the initial pH of the culture medium is neutral (pH = 7.0) in all processes. It is clear that, at the early stages of uncontrolled pH fermentation, pH values increased slightly for the first 24 hours followed by an obvious decrease for up to 40 hours with all processes broadly following the same trend. The corresponding final pH values in the low agitation rate processes (200 rpm and 300 rpm) were slightly acidic (pH < 7.0) while in the highest agitation speed process the final pH value was slightly alkaline (pH > 7.0).

4.2.1.3 The effect of agitation speed on growth as total biomass

As can be seen in figure 4.13 a and b, the biomass concentration increased steadily for all agitation speeds during the first 24 hours. At agitation 500 rpm, however, cell growth increased rapidly at a mean rate of (0.041 g/l/h) during the first 24 hours to a concentration of 1.01 g/l. Generally, growth rate increased in these cultures with increased impeller speed. Upon comparison of all four processes, the highest biomass production was observed at 500 rpm (1.41 g/l at 96 hours). Increasing the agitation from 200 rpm to 300 rpm showed no differences in the cell mass. At agitation rates 200 rpm and 300 rpm biomass production was followed the same trend, started at the similar growth rate of (0.024 g/l/h and 0.025 g/l/h) respectively, followed by superior growth rate at 200 rpm than that at 300 rpm. By the end of the fermentation run growth rate was almost (0.0 g/l/h) at all agitation rates.

4.2.1.4 The effect of agitation speed on xanthan gum production

As can be seen in figure 4.14 the processes started with similar xanthan gum concentrations of about 2.2 g/l that came from the carryover from the inoculum. Production of xanthan gum was growth related in most processes. The maximal concentration of xanthan gum was 15.3 g/l and this was obtained at 96 hours for the process at 500 rpm. However, formation of xanthan gum in the first 18 hours is almost similar in all lower agitation rate processes. The process of the highest agitation rate 500 rpm produced double the xanthan of any slower agitation rate processes. Although growth rate started to decline after 24 hours the microbe continued to produce xanthan gum. By the end of the fermentation time, the production of the different agitation rates 100, 200, and 300 rpm were 8.13, 9.56 and 9.85 g/l respectively.

4.2.1.5 The effect of agitation speed on glucose consumption

The initial concentration of glucose used in the medium was 20 g/l. As can be seen in figure 4.15 the microorganism *X. campestris* ATCC 13951 consumed around 25% of the carbon source within 24 hours in all these processes. Overall, the glucose was fully utilised only in the process operated at 500 rpm, in this process glucose reached near limiting levels by 48 hours where at the same time when the oxygen was at the lowest point, later the glucose was exhausted by around 72 hours. Although, almost 50% of glucose was consumed by 48 hours at the processes of the lower agitation speed, the utilisation of glucose was incomplete by the end of the fermentation, with around 25% of glucose remaining.

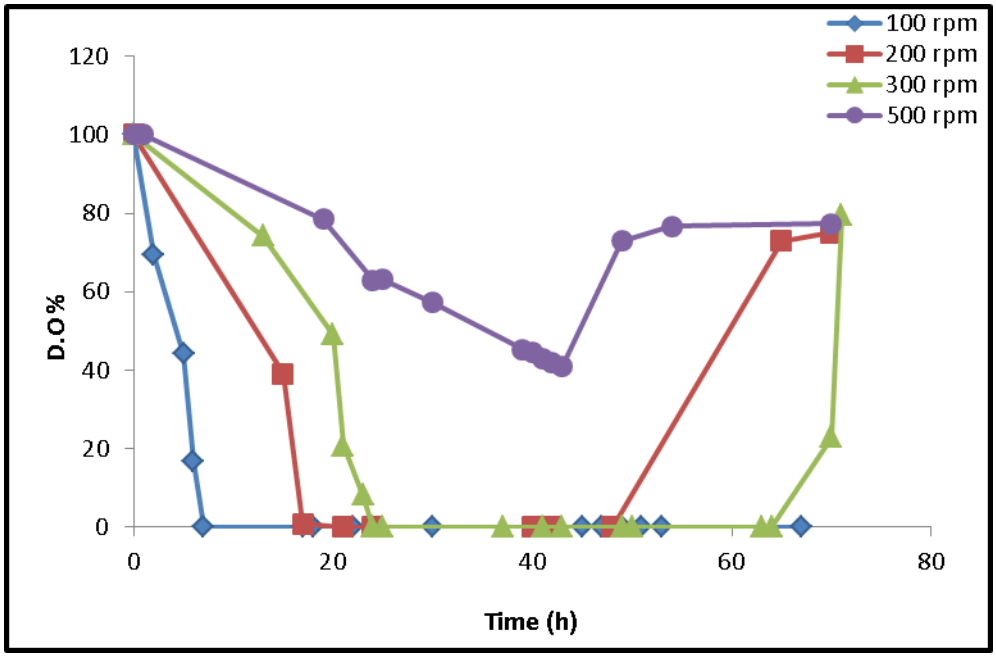

Figure 4.11: The effect of agitation speed on dissolved oxygen in batch cultures of *X. campestris* ATCC 13951 in a Stirred Tank Reactor (STR) fermentations carried out at 30 °C.

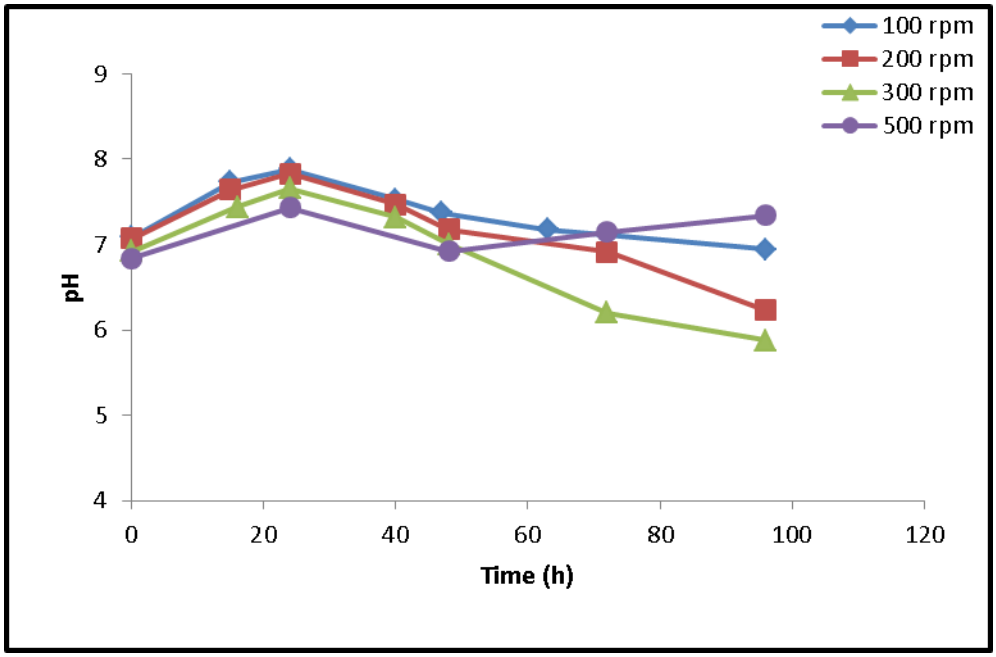

Figure 4.12: The effect of agitation speed on pH profile in batch cultures of *X. campestris* ATCC 13951 in a Stirred Tank Reactor (STR) fermentations carried out at 30 °C.

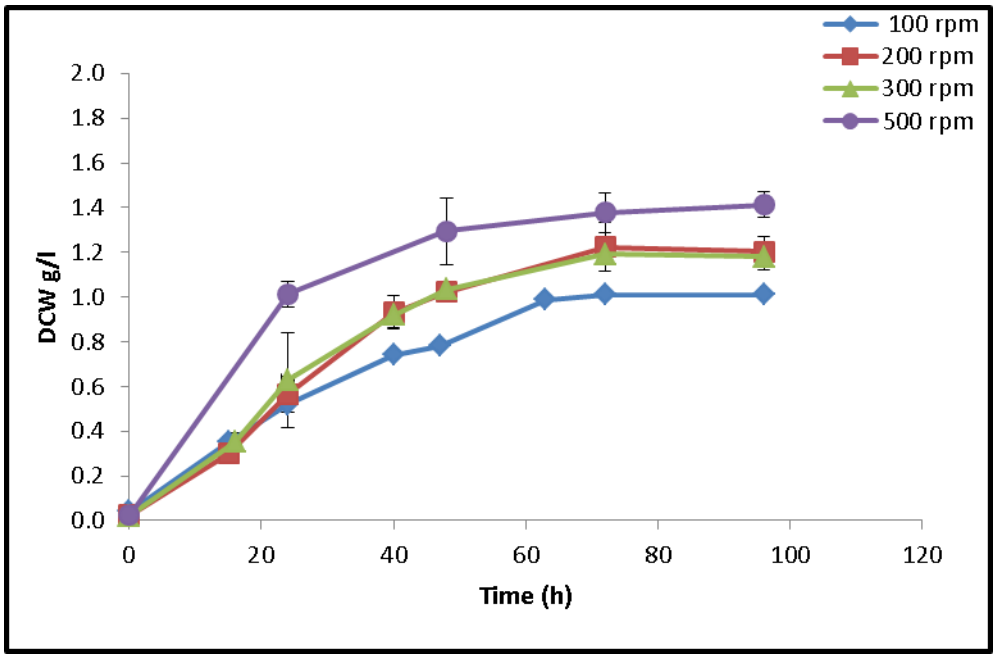

a

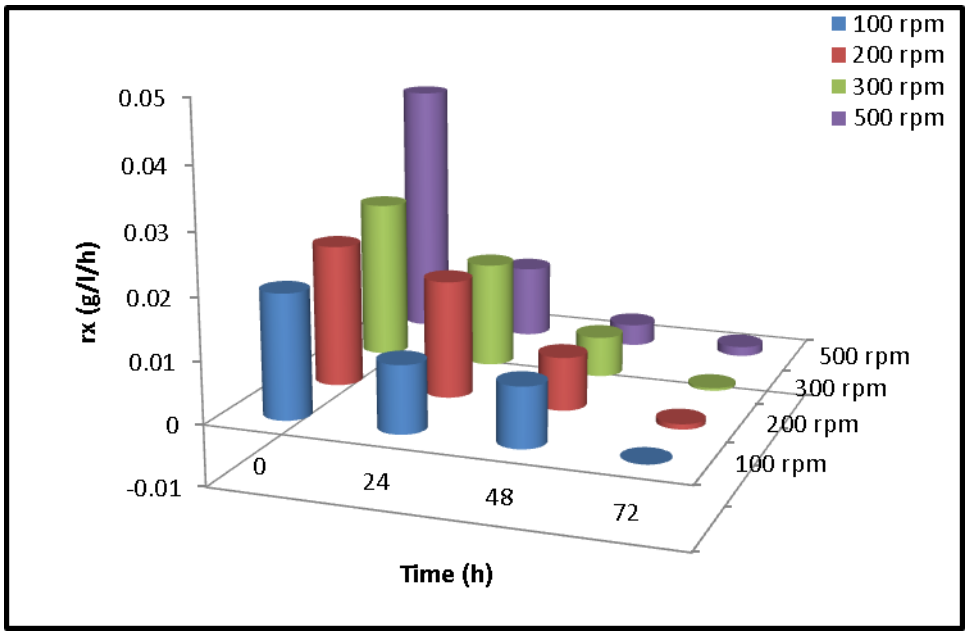

b

Figure 4.13: The effect of agitation speed on (a) total biomass production and growth rate (r_x) (b) in batch cultures of *X. campestris* ATCC 13951 in Stirred Tank Reactor (STR) fermentations carried out at 30 °C.

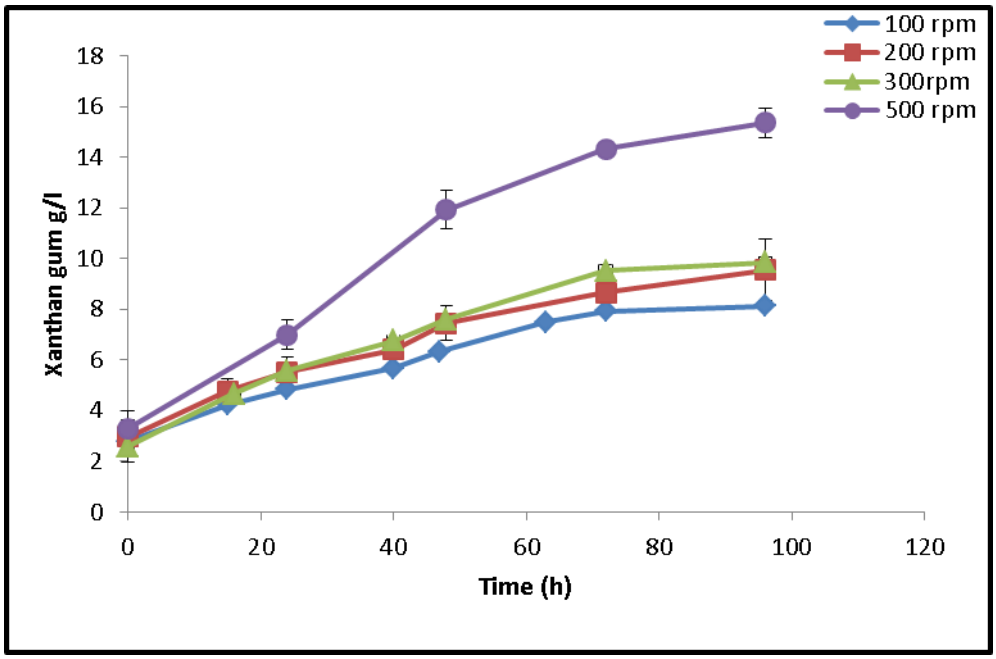

Figure 4.14: The effect of agitation speed on xanthan gum production in batch cultures of *X. campestris* ATCC 13951 in Stirred Tank Reactor (STR) fermentations carried out at 30 °C.

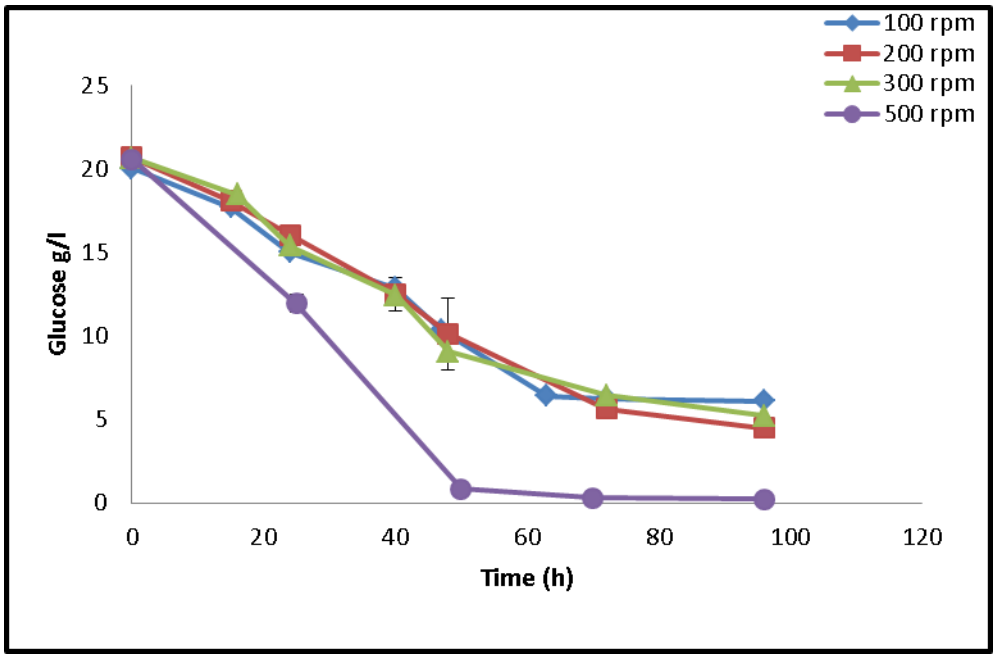

Figure 4.15: The effect of agitation speed on glucose consumption in batch cultures of *X. campestris* ATCC 13951 in Stirred Tank Reactor (STR) fermentations carried out at 30 °C.

4.2.2 The effect of aeration

As mentioned in the literature review (Chapter 2), *X. campestris* ATCC 13951 requires aerobic conditions for the production of xanthan gum. Since supply of oxygen to these cultures is so critical to the success of these processes, it was important to examine the effect of aeration rate upon the process. This section presents the data on the effect of two different aeration rates (1vvm and 2vvm) at two different agitation speeds of 200 rpm and 500 rpm. The experiment was carried out in 2l production medium inoculated with 10% (v/v) *X. campestris* ATCC 13951 culture, uncontrolled pH and temperature was maintained at 30 °C. A total of 4 fermentation experiments were carried out.

4.2.2.1 The effect of agitation and aeration on dissolved oxygen

As can be seen in figure 4.16 in both processes at 200 rpm, 1vvm and 2vvm, the D.O fell rapidly to 0% within 17 hours and 24 hours at 30 °C respectively and stayed at that oxygen limited level for a period of time before rising again after 48 hours. At 200 rpm 1vvm D.O rose to 75% at 72 hours, whereas it rose to only 32% in the process 200 rpm 2vvm at that time. In contrast, at the higher agitation speed in both processes, 1vvm and 2vvm there was no oxygen limitation during the fermentation time. Instead in the 500 rpm 1vvm process D.O fell to around 43% by 43 hours, and in the 500 rpm 2vvm process D.O dropped to 22% by 24 hours and stayed at that level for 24 hours before it rose to 71% at 72 hours.

4.2.2.2 The effect of agitation and aeration on pH

This section focuses on the effect of two different aeration rates within batch culture of *X. campestris* ATCC 13951 upon culture pH evolution in the conventional STR. As mentioned in section 4.2.1.2, the experiments were carried out in uncontrolled pH, while the temperature of the medium was fixed at 30ºC. Figure 4.17 shows the changes in the medium pH with respect to the time when it was allowed to evolve naturally. As can be seen, the initial pH of the culture medium is neutral (pH = 7.0) in all processes. It is clear that, in the early stages of all uncontrolled pH fermentations, the pH values increased in the first 24 hours followed by an obvious drop, therefore in all processes. The corresponding final pH values at the lower agitation speed of 200 rpm 1vvm and 2vvm were slightly acidic (pH < 7.0), while in the higher agitation speeds of 500 rpm 1vvm and 2vvm the final pH value was slightly alkali (pH > 7.0).

4.2.2.3 The effect of aeration speed on the bacterial growth as total biomass

As can be seen in figure 4.18a and b, the biomass concentration increased steadily in all these processes during the first 24 hours. The highest value of 1.01 g/l being achieved in the 500 rpm 1vvm process with growth rate (rx) of 0.041 g/l/h. In contrast, the lowest cell mass 0.6 g/l and growth rate (rx) of 0.024 g/l/h occurred in the process at 200 rpm and 1vvm at the same time. The processes 200 rpm 2vvm gave cell mass of 0.78 g/l in 24 hours but the culture continued to grow to reach 1.09 g/l at 48 hours. On the other hand, after 24 hours in the processes at agitation speed

of 500 rpm the aeration affected the growth rate where the process at 500 rpm 1vvm was higher than at the process at 500 rpm 2vvm and was continued to the end of the run at the same trend with maximum cell mass of 1.4 g/l.

4.2.2.4 The effect of agitation and aeration on xanthan gum production

As mentioned before all processes started with some xanthan gum g/l present that came from the inoculum. Production of xanthan gum initially followed a very similar trend in all these processes with the exception of the 200 rpm 1vvm process.

The maximal concentration of xanthan gum from the STR in this study was 15.8 g/l at 96 hours in the process operated at 500 rpm and 2vvm. Formation of xanthan gum was found to be similar in two different conditions of aeration and agitation, that is, 200 rpm and 2vvm (low agitation with high aeration) and 500 rpm and 1vvm (high agitation with low aeration), where the maximum xanthan in these two processes was 14.25 g/ l and 15.08 g/l respectively. At 200 rpm and 1vvm (low agitation with low aeration) the maximum production was only 9.56 g/l by the end of fermentation at 96 hours (Figure 4.19).

4.2.2.5 The effect of agitation and aeration on glucose consumption

As mentioned in the Materials and Methods (Chapter 3), the initial concentration of glucose used in the medium was 20 g/l. Figure 4.20 shows the glucose consumption profile of the fermentation, as can be seen, during the first 24 hours, the glucose consumption rate of the lower agitation rate processes 200 rpm 1vvm and 2vvm was

0.081 g/l/h and 0.083 g/l/h respectively, while in the process operated at 500 rpm and 2vvm the glucose consumption in the same period was far higher (0.247 g/l/h). After 48 hour the bacterium *X. campestris* ATCC 13951 had consumed around 98% of the initial glucose in the condition of 500 rpm 1vvm process and 90% in the condition of 500 rpm 2vvm process. By contrast, only 50% and 60% of the glucose was consumed by this time in the processes at low stirrer speed (200 rpm, 1 and 2vvm respectively. By the end of the fermentation time, the glucose was almost completely consumed in the high agitation rate processes, while in the lower agitation speed there was around 10–15% of the glucose still remaining at process end.

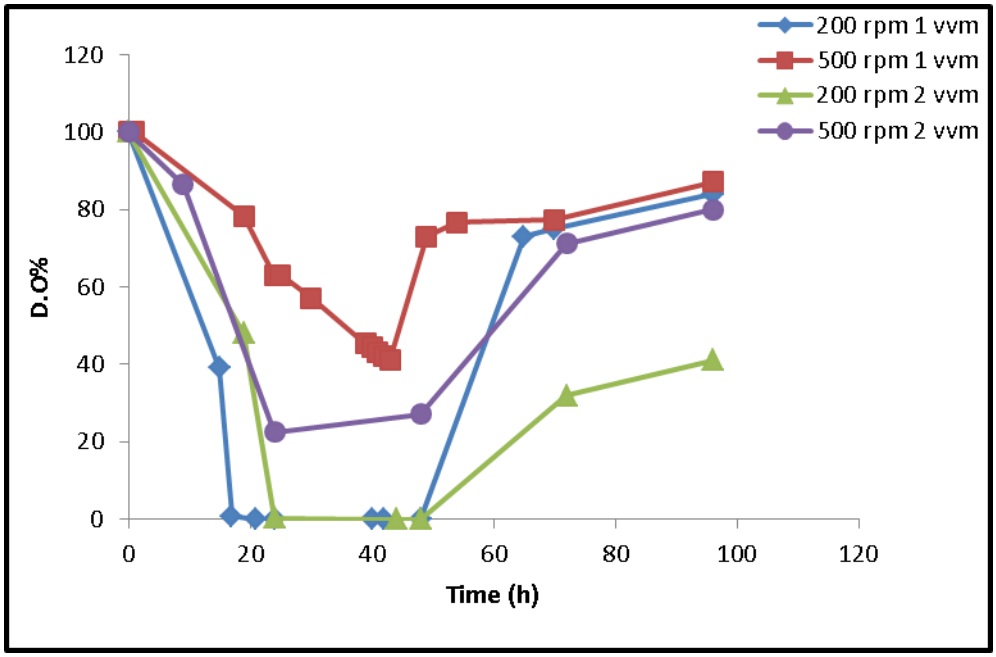

Figure 4.16: The effect of aeration and agitation on dissolved oxygen in batch cultures of *X. campestris* ATCC 13951 in Stirred Tank Reactor (STR) fermentations carried out at 30 °C.

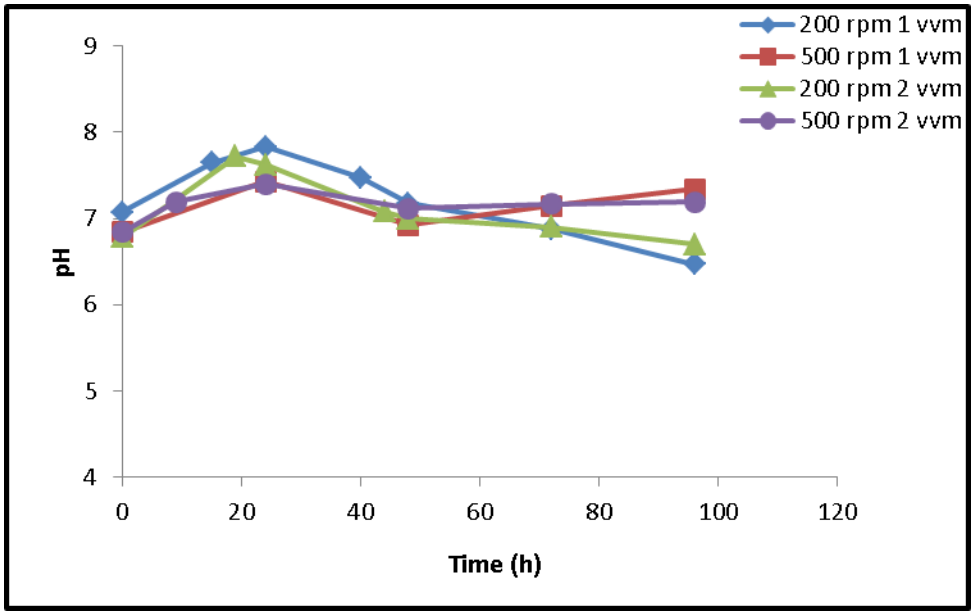

Figure 4.17: The effect of aeration and agitation speed on pH profile in batch cultures of *X. campestris* ATCC 13951 in Stirred Tank Reactor (STR) fermentations carried out at 30 °C.

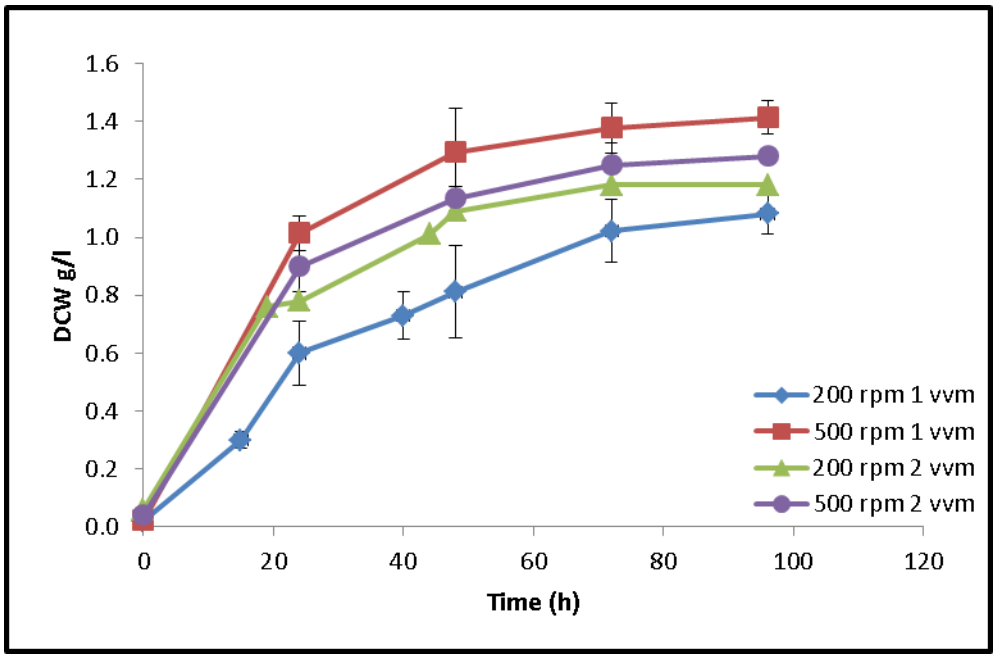

a

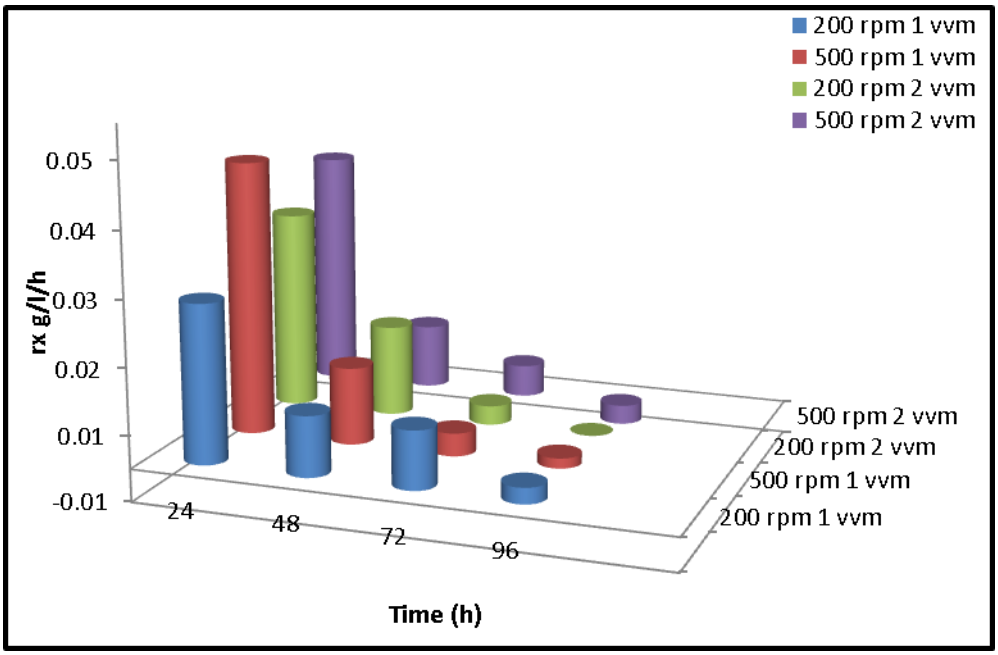

b

Figure 4.18: The effect of aeration and agitation on (a) total biomass production and (b) growth rate (r_x) in batch cultures of *X. campestris* ATCC 13951 in Stirred Tank Reactor (STR) fermentations carried out at 30 °C.

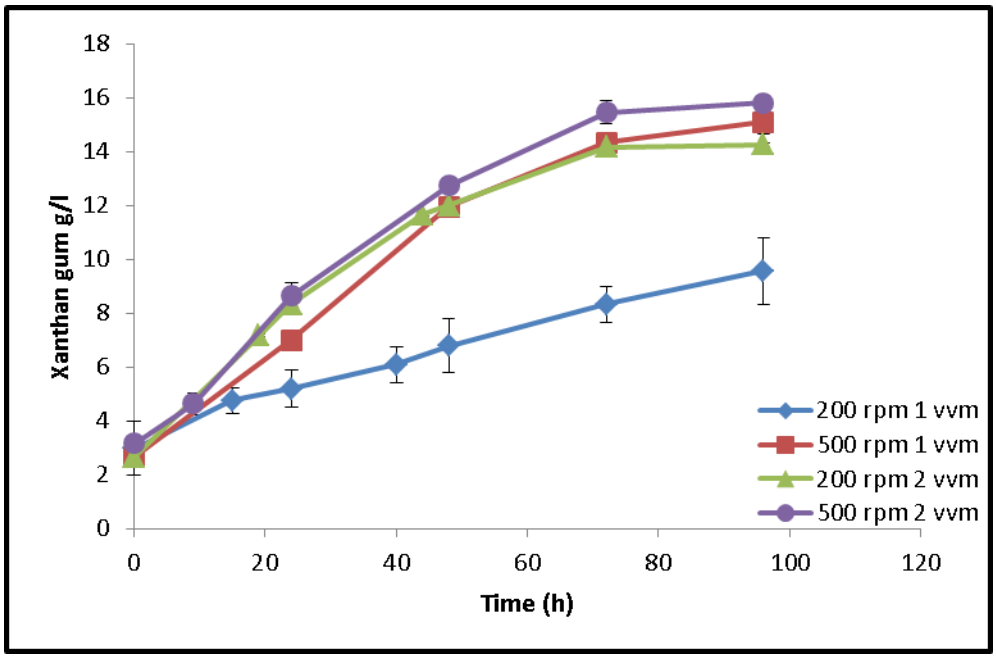

Figure 4.19: The effect of aeration and agitation speed on xanthan gum production in batch cultures of *X. campestris* ATCC 13951 in Stirred Tank Reactor (STR) fermentations carried out at 30 °C.

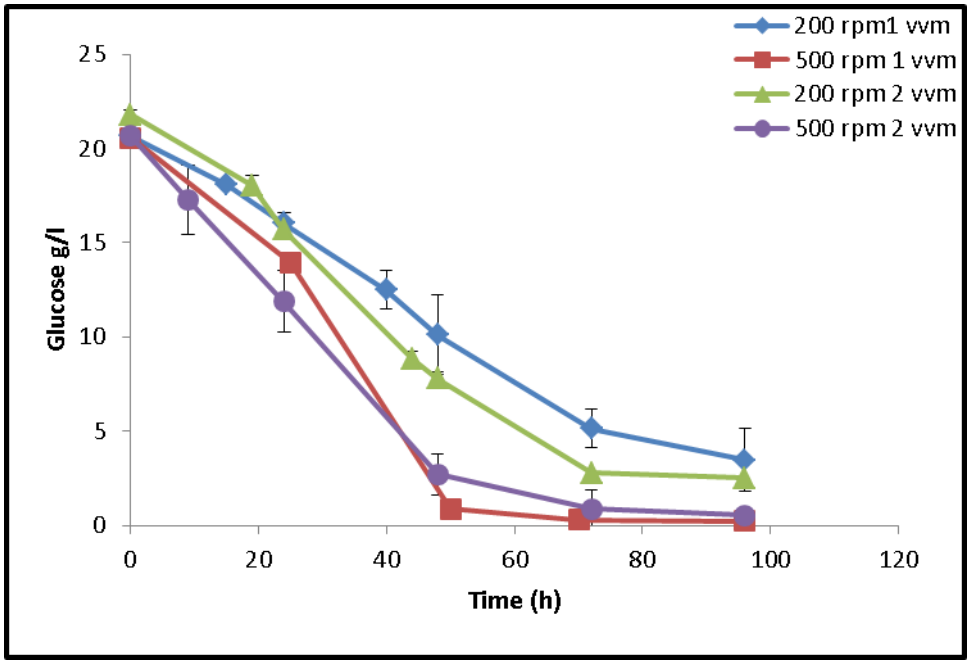

Figure 4.20: The effect of aeration and agitation speed on Glucose consumption in batch cultures of *X. campestris* ATCC 13951 in Stirred Tank Reactor (STR) fermentations carried out at 30 °C.

4.3 The production of xanthan gum in the Oscillatory Baffled Reactor (OBR)

This section will present the experimental results of the fermentation of *X. campestris* ATCC 13951 in the OBR, and is divided into three sub-sections. The effect of the sparged air direction on *X. campestris* fermentation is given in section 4.3.1, including two different aeration rates. The effect of oscillation conditions of *X. campestris* fermentation process is discussed in section 4.3.2 where oscillation frequency and amplitude are varied. Finally, section 4.3.3 details the effect of the aeration rate on the xanthan production process.

2l Stainless OBR was used (see Materials and Methods, Chapter 3). The experiment was carried out with different frequencies (2, 3 and 5 Hz) and amplitudes were varied from (5, 15 and 25 mm) in 2l production medium inoculated with 10% (v/v) *X. campestris* ATCC 13951 culture, at aeration rates of 1 and 2vvm, uncontrolled pH and temperature maintained at 30 °C. All the experiments were repeated for the purpose of assessing reproducibility, and the replicate data are presented with error bars in all figures in this section.

4.3.1 The effect of sparger attitude

This section will present the data results for the effect of different sparger attitudes, which are different orientations of the sparger, leading to altered directions of gas flow (aeration) in the OBR vessel on the growth of the *X. campestris* ATCC 13951 culture and production of xanthan gum. The OBR was supplied with its original sparger where the direction of the air was downwards towards the bottom of the vessel (see Materials and Methods section 3). Two experiments were carried out in the original sparger at 2 Hz frequency and 25 mm amplitude at two different aeration rates of 1vvm and 2vvm in 2L production medium; otherwise conditions were as described above. There were a total of four fermentations and the results were compared to the new upward sparger results. All the experiments were repeated for the purpose of assessing reproducibility and the replicate data are shown with error bars in all figures in this section.

4.3.1.1 The effect of sparged air direction on dissolved oxygen

As can be seen in figure 4.21, when the downward sparger was used the dissolved oxygen did not reach limiting levels in these processes, whereas by contrast oxygen limitation did occur using the upward sparger. In both processes with both spargers (downward and upward), dissolved oxygen declined rapidly in the first 24 hours, while in the process with the downward sparger direction at both aeration rates 2 and 1vvm the dissolved oxygen was declined only to 25 and 20% respectively, then increased gradually. By contrast, when the air was sparged upwards in both

processes (2 and 1vvm) D.O fell to 0% in 24 hours and the processes remained oxygen limited state for 48 and 24 hours respectively D.O started to rise again. It is therefore very clear that the sparger attitude, which determines gas flow direction, had a profound effect upon the D.O profile in these processes.

4.3.1.2 The effect of sparged air direction on pH

The effect of sparger attitude upon process pH of batch culture of *X. campestris* ATCC 13951 in the OBR is presented in this section. Figure 4.22 shows the changes in the medium pH with respect to the time when it was allowed to evolve naturally. As can be seen, the initial pH of the culture medium is neutral (pH = 7.0) in all processes. It is clear that the pH profile of uncontrolled pH fermentations of the batch culture of bacterium *X. campestris* ATCC 13951 all showed a slight increase in the first 24 hours; after that, the pH fell at different rates.

Although the pH trends were different following the initial pH rise, overall the final pH's in these processes were broadly similar by the process end, e.g. with the downward sparger end pH was 5.2 and 5.4 (2 and 1vvm) respectively, and for the upward sparger end pH was 5.3 and 5.2.

4.3.1.3 The effect of sparged air direction on growth as total biomass

As can be seen in figure 4.23, the biomass concentration increased steadily for all processes during the first 24 hours giving a highest value of 1.19 g/l and a maximum growth rate (r_x) of 0.043 g/l/h in the process using the upward sparger direction amplitude 25 mm frequency 2 Hz and gas rate of 2vvm. The lowest values (0.44 g/l

and growth rate (r_x) of 0.017 g/l/h) were obtained using the downwards sparger direction at 25 mm 2 Hz 1vvm downward The processes using the upward sparger at 25 mm 2 Hz 1vvm and downwards sparger at 25 mm 2 Hz 2vvm gave similar biomass (1.01 g/l and 0.97) in the first 24 hours and comparable growth rates (r_x) of 0.40 g/l/h and 0.39 g/l/h respectively.

Maximal biomass levels in the processes using the upwards oriented sparger gave higher maximal biomass levels of 1.62 g/l, compared to only 1.50 g/l for the downwards sparger at high gas rate(2vvm) and only 0.84 g/l the same sparger at low gas rate(1vvm). Once again this shows the strong influence of design changes in the vessel to the biomass accumulation in the OBR.

4.3.1.4 The effect of sparged air direction on xanthan gum production

The effects of sparger attitude on xanthan gum production can be seen in figure 4.24. Both processes operated with the upward and downward, upwards oriented sparger design, as proposed by the author, outperformed the processes using the original downwards oriented sparger in terms of maximum xanthan gum produced. Highest xanthan gum levels of 15.3 g/l were achieved using the upward sparger design at high gas flow rate (2vvm), and this process exhibited an extended xanthan production phase compared to others. By contrast, the original sparger design at low gas flow rate (1vvm) gave the lowest xanthan gum levels recorded in this experimental series of only 9.08 g/l.

4.3.1.5 The effect of sparged air direction on glucose consumption

As might be expected from the data shown above for biomass, xanthan and D.O the glucose consumption pattern of this cultures were influenced by sparger attitude. In xanthan production phase the consumption of glucose was higher in the processes using the novel design of sparger (upwards), while the glucose consumption rate was lowest in the process operated at low gas flow rate using the original (downwards) oriented sparger. Consumption rate in the process using high gas flow and the originals sparger was close that in the processes using the novel design. In all processes residual glucose at process end ranged from around 5 to 8 g/l (Figure 4.25).

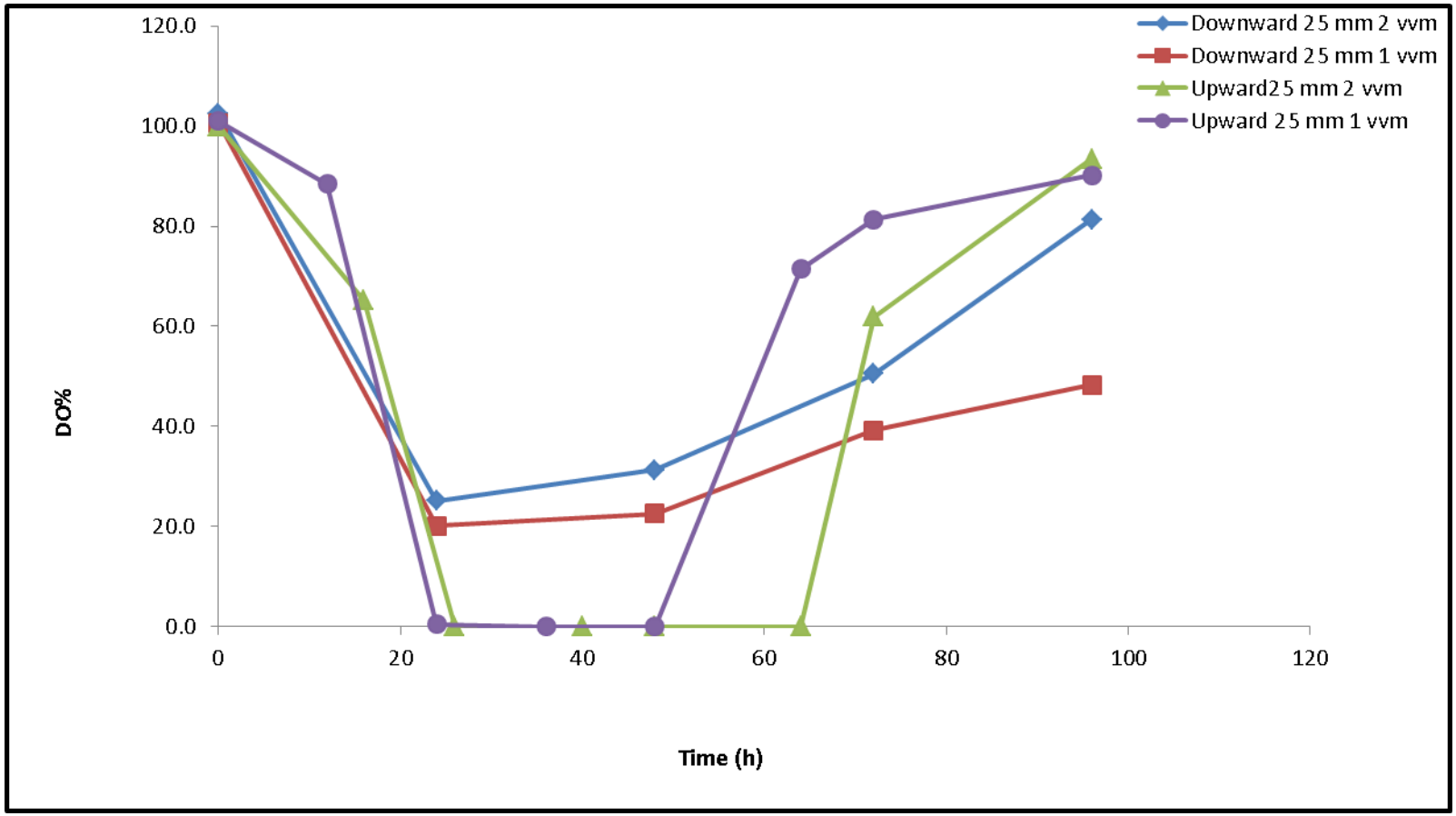

Figure 4.21: The effect sparged air direction on dissolved oxygen in batch cultures of *X. campestris* ATCC 13951 in OBR carried out with two spargers the downward one and the upward one at 25 mm amplitude and 2Hz oscillation frequency with aeration of 1vvm and 2vvm at 30 °C.

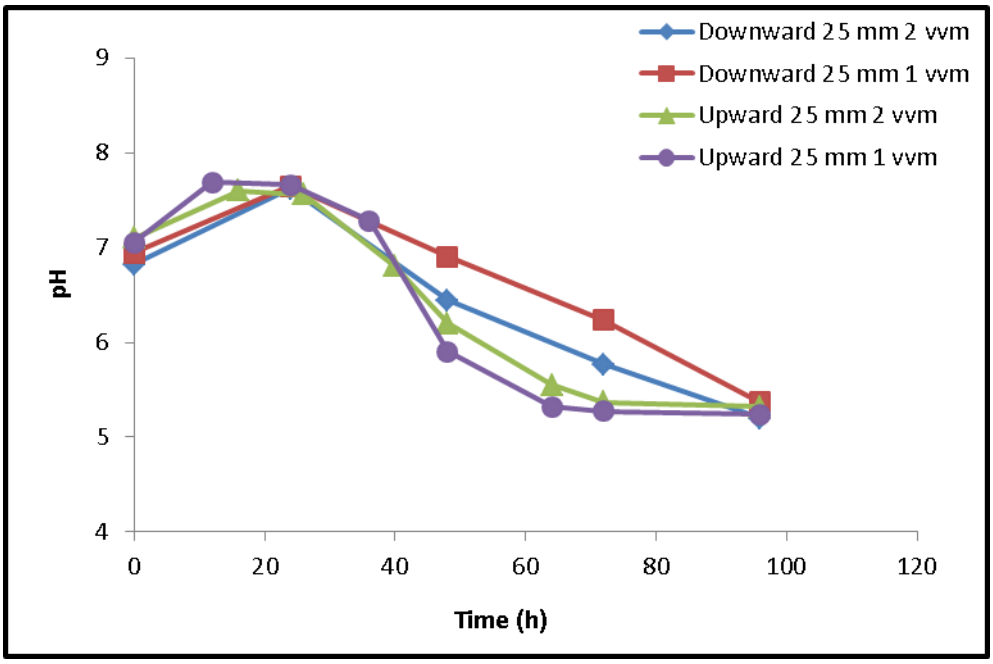

Figure 4.22: The effect of sparged air direction on pH in batch cultures of *X. campestris* ATCC 13951 in OBR carried out with two spargers, the downward one and the upward one, at 25 mm amplitude and 2Hz oscillation frequency with aeration of 1vvm and 2vvm at 30 °C.

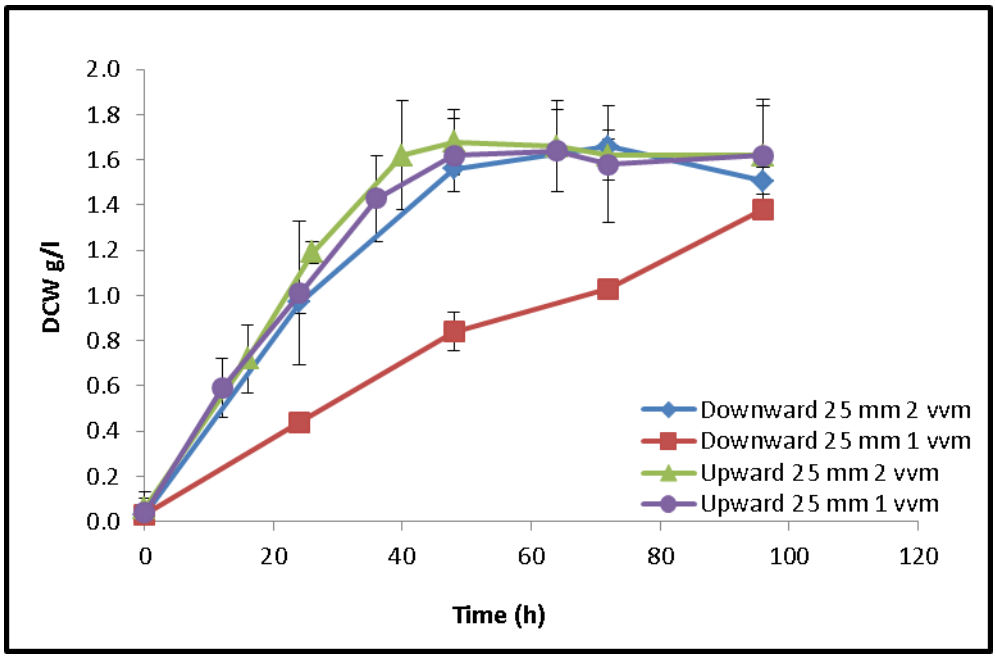

Figure 4.23: The effect of sparged air direction on total biomass production in batch cultures of *X. campestris* ATCC 13951 in OBR carried out with two spargers, the downward one and the upward one at 25 mm amplitude and 2Hz oscillation frequency, with aeration of 1vvm and 2vvm at 30 °C.

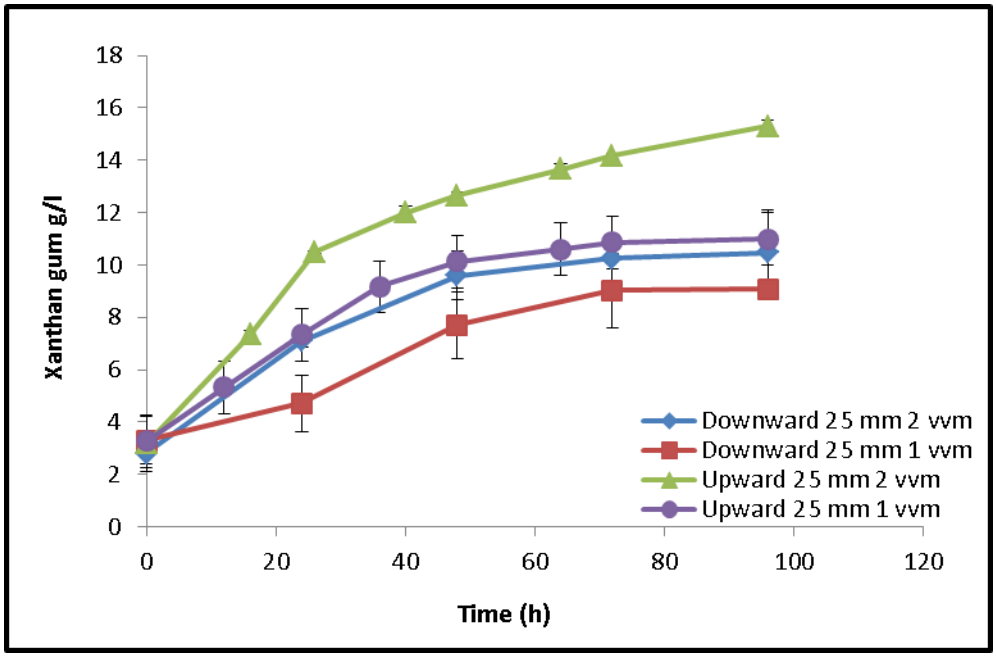

Figure 4.24: The effect of sparged air direction on xanthan gum production in batch cultures of *X. campestris* ATCC 13951 in OBR carried out with two spargers the downward one and the upward one at 25 mm amplitude and 2Hz oscillation frequency with aeration of 1vvm and 2vvm at 30 °C.

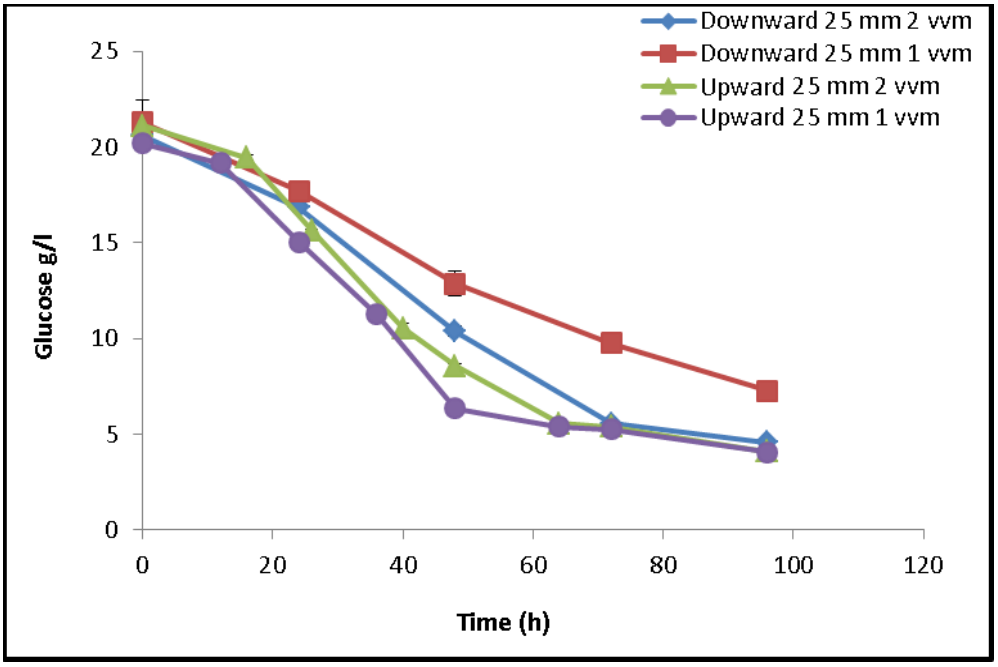

Figure 4.25: The effect of sparged air direction on glucose consumption in batch cultures of *X. campestris* ATCC 13951 in OBR carried out with two spargers the downward one and the upward one, at 25 mm amplitude and 2Hz oscillation frequency with aeration of 1vvm and 2vvm at 30 °C.

4.3.2 The interaction between aeration, frequency and amplitude in the xanthan production process in the OBR

This section will present the results of a study on the interactions between aeration rate, oscillation frequency and amplitude on the production of xanthan gum by the bacterium *X. campestris* ATCC 13951 in the OBR with the upward direction sparger.

Two amplitudes were examined, 25 mm and 15 mm at fixed frequency 2 Hz, at two aeration rates (1vvm and 2vvm). One experiment was done in at frequency 3 Hz at amplitude 25 mm but the results were not shown due to the technical fault that occurred in the OBR as mentioned in the materials and methods chapter 3. The operating temperature was 30^{o}C throughout the duration of the fermentation, which is typically 96 hours. The pH of the medium was uncontrolled. A total of four fermentation experiments were carried out.

4.3.2.1 The effect of aeration and high amplitude low frequency

4.3.2.1.1 The effect of aeration and high amplitude low frequency on dissolved oxygen

As can be seen in figure 4.26, in both processes operated at amplitude 15 mm (2 and 1vvm) D.O dropped rapidly to limiting levels in only 16 hours and 18 hours respectively. The process at amplitude 15 mm 1vvm had the shortest duration at D.O equal to zero for all the processes in this experimental series, as the D.O rose again

after only 6 hours. By contrast, in the process with the same amplitude but at 2vvm D.O reached zero at 16 hours and stayed constant for 56 hours thereafter. Both processes at amplitude 25 mm (2 and 1vvm) D.O limitation was reached later than in the equivalent process at lower amplitude, demonstrating a clear impact of amplitude upon dissolved oxygen levels in these processes.

4.3.2.1.2 The effect of aeration and high amplitude low frequency on pH

The effect amplitude on the pH in batch cultures of the bacterium *X. campestris* ATCC 13951 in the OBR is shown in this section. Figure 4.27 shows the changes in the medium pH with respect to the time. As can be seen, the starting pH value of the culture medium was around 7.0 in all processes, and rose in the early stage of all these fermentations. Low amplitude processes (15mm, 2 and 1vvm) tended to show a gradual decline after the peak rise in the pH, achieving a pH at process end around 6.5. In contrast, high amplitude processes (25mm, 2 and 1vvm) showed a much more pronounced drop in the culture pH than the low amplitude equivalents, ending the process at around pH 5.4.

4.3.2.1.3 The effect of aeration and high amplitude low frequency on growth as total biomass

Figure 4.28 shows the effect of amplitude on the growth of the bacterium X. campestris ATCC 13951 in the OBR. Both high amplitude processes (25mm, 2 and 1vvm) followed similar trends and reached their respective biomass maximum earlier than the equivalent low amplitude processes. The low amplitude low gassing rate

process took longest to achieve the biomass maximum and the lowest value (1.37 g/l).

4.3.2.1.4 The effect of aeration and high amplitude low frequency on xanthan gum production

The effects of amplitude upon xanthan gum formation are shown in figure 4.29. In general, the fermentations carried out at high gassing rate (2vvm, and 25 and 15 mm amplitude) considerably outperformed those carried out at lower gassing rate (1vvm, 25 and 15 mm). So, in terms of xanthan production although amplitude clearly had an influence, this was complicated by the dominant effect of gassing rate upon xanthan synthesis.

4.3.2.1.5 The effects of aeration and high amplitude low frequency on glucose consumption

The effects of amplitude on glucose consumption are shown in figure 4.30. In both the high amplitude processes (25mm, 2 and 1vvm) glucose consumption patterns were broadly similar and the culture ceased to utilise glucose earlier at high amplitude than low amplitude processes did. In all processes glucose consumption ceased while there still remained significant levels of residual sugar. The process operated at 15mm (low amplitude) and 2vvm (high gassing rate) gave the highest xanthan concentration in this series of experiments, was associated with prolonged consumption of glucose long after other cultures had ceased to take up glucose.

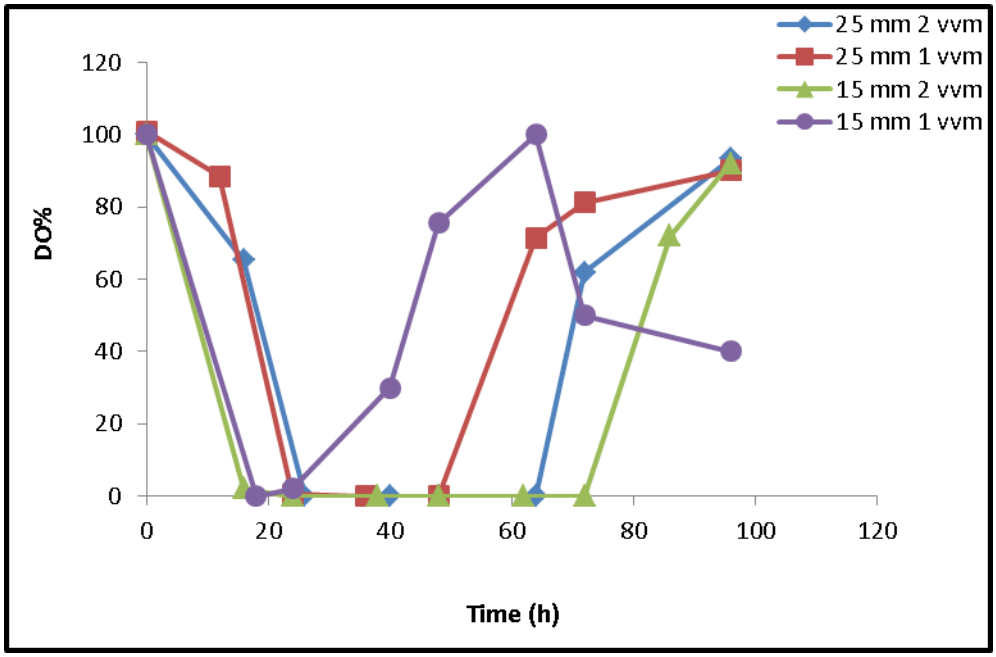

Figure 4.26: The effect of the interaction between aeration, frequency and amplitude on dissolved oxygen in batch cultures of *X. campestris* ATCC 13951 in OBR at 25 mm and 15 mm amplitude and 2Hz oscillation frequency with aeration of 1vvm and 2vvm at 30 °C.

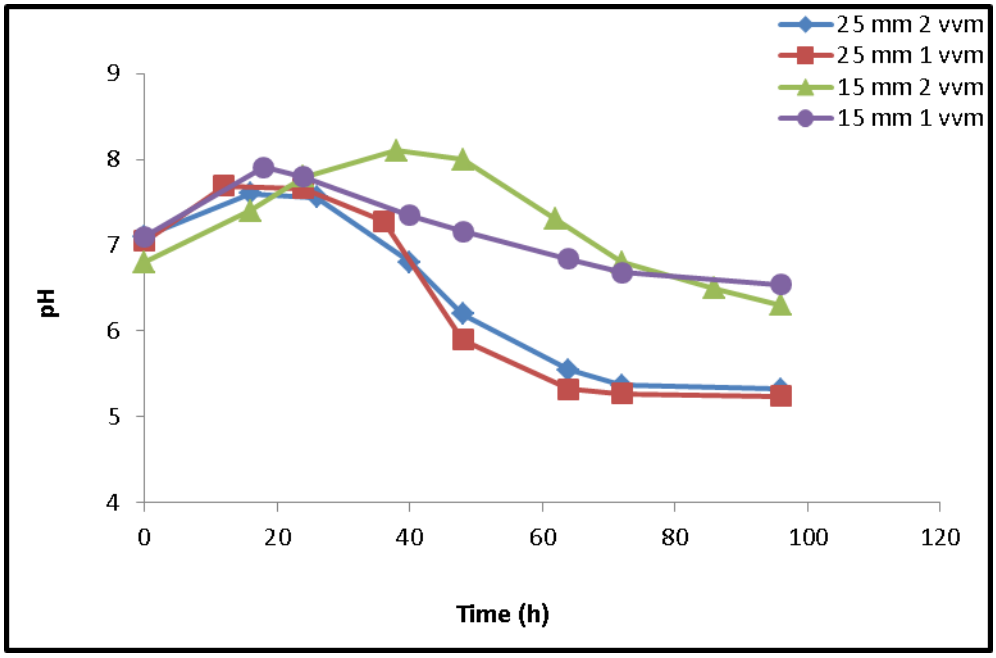

Figure 4.27: The effect of the interaction between aeration, frequency and amplitude on pH in batch cultures of *X. campestris* ATCC 13951 in OBR at 25 mm and 15 mm amplitude and 2Hz oscillation frequency with aeration of 1vvm and 2vvm at 30 °C.

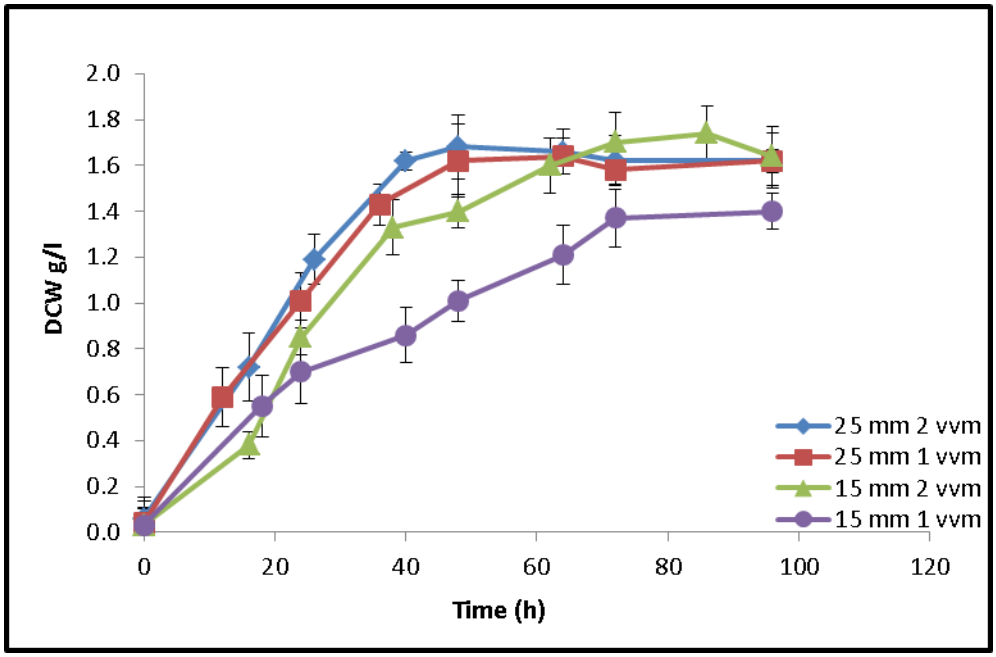

Figure 4.28: The effect of the interaction between aeration, frequency and amplitude on total biomass production rate in batch cultures of *X. campestris* ATCC 13951 in OBR at 25 mm and 15 mm amplitude and 2Hz oscillation frequency with aeration of 1vvm and 2vvm at 30 °C.

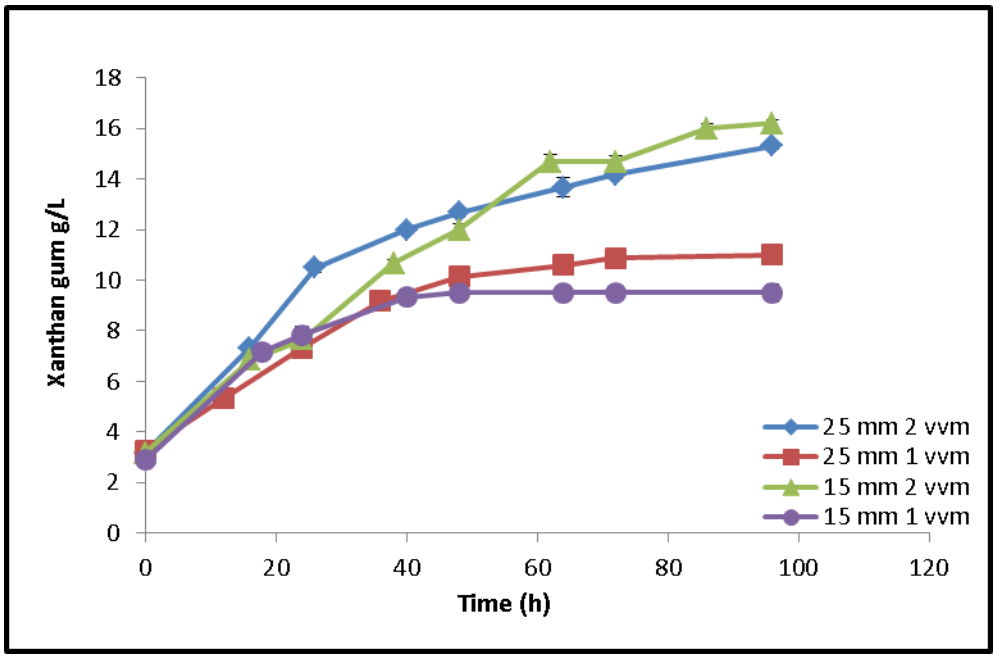

Figure 4.29: The effect of the interaction between aeration, frequency and amplitude on xanthan gum production in batch cultures of *X. campestris* ATCC 13951 in OBR at 25 mm and 15 mm amplitude and 2Hz oscillation frequency with aeration of 1vvm and 2vvm at 30 °C.

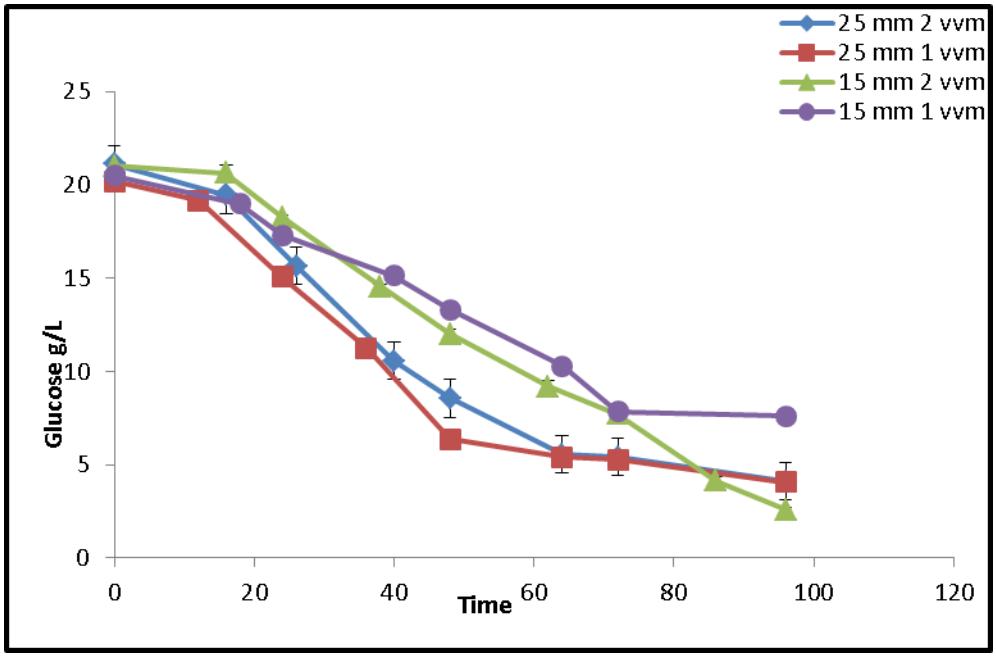

Figure 4.30: The effect of the interaction between aeration, frequency and amplitude on glucose consumption in batch cultures of *X. campestris* ATCC 13951 in OBR at 25 mm and 15 mm amplitude and 2Hz oscillation frequency with aeration of 1vvm and 2vvm at 30 °C.

4.3.2.2 The effects of aeration and low amplitude high frequency

This section presents the results of a study into the effects of operating the reactor at differing aeration rates (2 and 1vvm) and different eddies speed and size at high frequency 5Hz and low amplitude (5mm) on the production of xanthan gum by *X. campestris* ATCC 13951 in the OBR vessel.

4.3.2.2.1 The effect of aeration and low amplitude high frequency on dissolved oxygen

Figure 4.31 shows the effect of differing aeration rates upon D.O under high frequency and low amplitude operational conditions in the OBR. Although in both processes D.O fell rapidly in the first 24 hours following inoculation, D.O did not reach limiting levels in either process. In the 1vvm process the D.O minimum of around 10% was maintained for a lengthy period relative to the process aerated at the higher gassing rate. In both processes a period of relatively low and stable D.O was then followed by a sharp rise in D.O.

4.3.2.2.2 The effect of aeration and low amplitude high frequency on pH

In this section, the effect of aeration rate on the pH in batch culture of *X. campestris* ATCC 13951 in the OBR operated at high frequency and low amplitude was studied. From a starting pH around 7.0 both processes showed the usual rise in the pH during the first 16 hours up to the pH (7.5 and 7.4) respectively, and then a fall in the pH after 24 hours At 48 hours, the process at high gas rate process (2vvm) became more acidic with a pH 6.46; then the pH increased slightly to the end of the fermentation to finish at pH 6.61 at 96 hours. The process low gas rate process (1vvm) showed a

steady fall in culture pH to 5.9 by the end of the fermentation at 96 hours (Figure 4.32).

4.3.2.2.3 The effect of aeration and low amplitude high frequency on growth as total biomass

Figure 4.33 shows the effect of aeration rate on the growth of the bacterium X. campestris ATCC 13951 in the OBR under operational conditions of high frequency and low amplitude. Under these operating conditions, a higher maximum biomass of 1.61 g/l was reached much earlier in the process with a higher gassing rate, though 1.54 g/l was achieved by only 48 hours. By contrast, the lower aeration rate process had much lower biomass maximum and this was reached much more slowly and followed by biomass decline.

4.3.2.2.4 The effect of aeration and low amplitude high frequency on xanthan gum production

The results for the effect of aeration upon xanthan production under these operating conditions in the OBR are shown in figure 4.34. From the figure it can be seen that broadly speaking the pattern of xanthan production was not influenced by aeration rate within the first 72 hours of the fermentation. After this point, at high aeration rate, xanthan synthesis continued to the process end with a significantly higher xanthan yield (14.4 g/l) than in the lower aeration rate process (12.3 g/l). In the latter process some decrease in xanthan may have occurred late in the process.

4.3.2.2.5 The effect of aeration and low amplitude high frequency on glucose consumption

Figure 4.35 shows the effects of aeration upon glucose consumption under these operating conditions. Despite differences in growth and xanthan production patterns associated with differing aeration rates, under these operational conditions glucose consumption patterns were basically similar in the first 24 hours. In both processes glucose was still being utilised by the process end, but the higher aeration rate process had much less residual glucose left at the process end compared to the low aeration rate process.

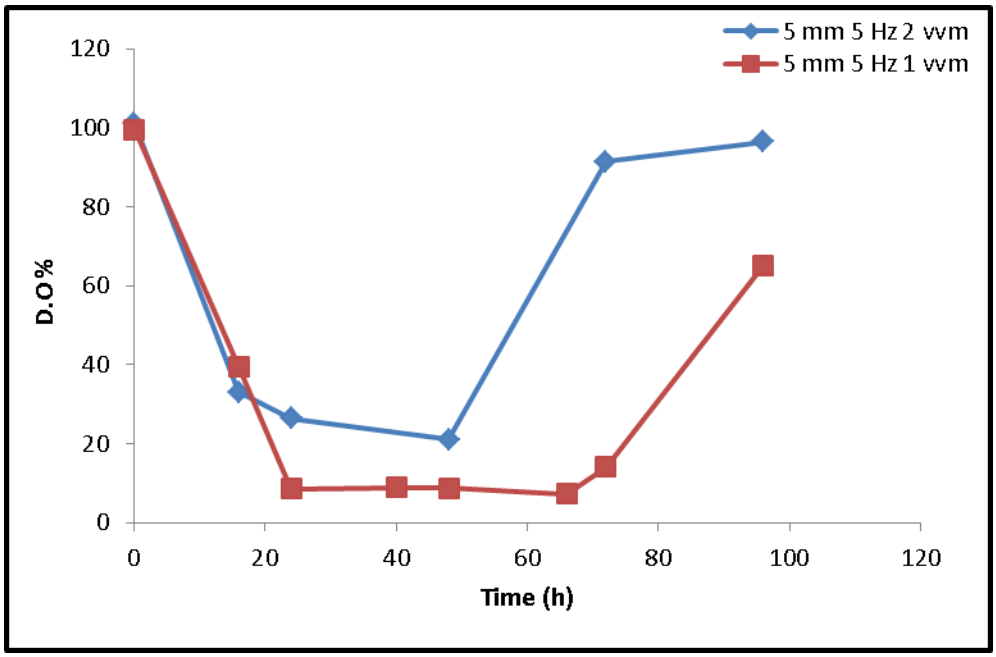

Figure 4.31: The effects of aeration on dissolved oxygen in processes operated at high frequency and low amplitude in batch cultures of *X. campestris* ATCC 13951 in OBR at 5 mm amplitude and 5 Hz oscillation frequency with aeration of 1vvm and 2vvm at 30 °C.

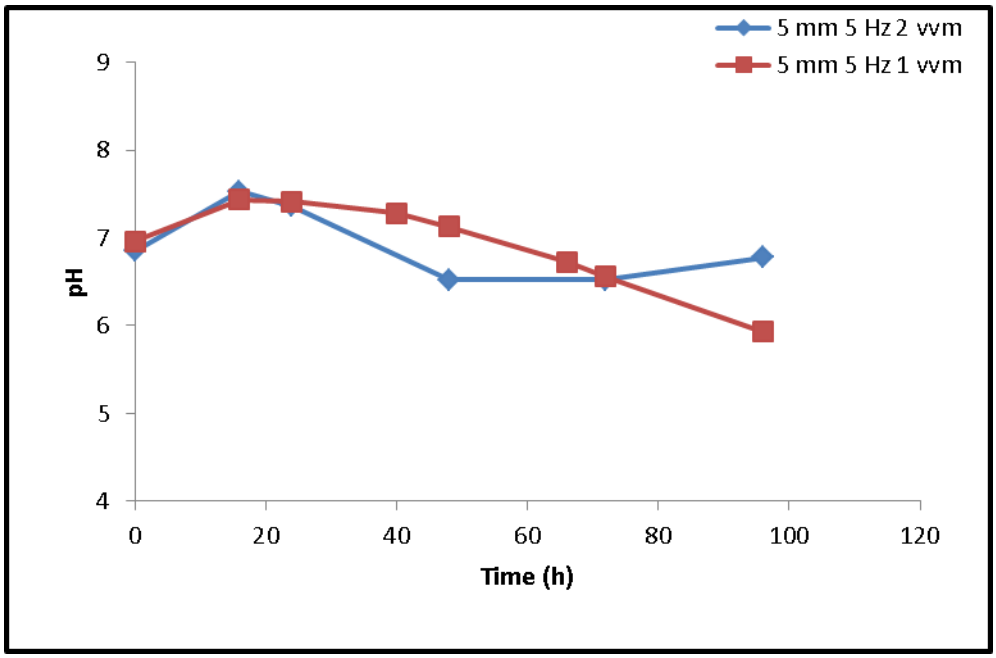

Figure 4.32: The effect of aeration in processes with high frequency and low amplitude on pH in batch cultures of *X. campestris* ATCC 13951 in OBR at 5 mm amplitude and 5 Hz oscillation frequency with aeration of 1vvm and 2vvm at 30 °C.

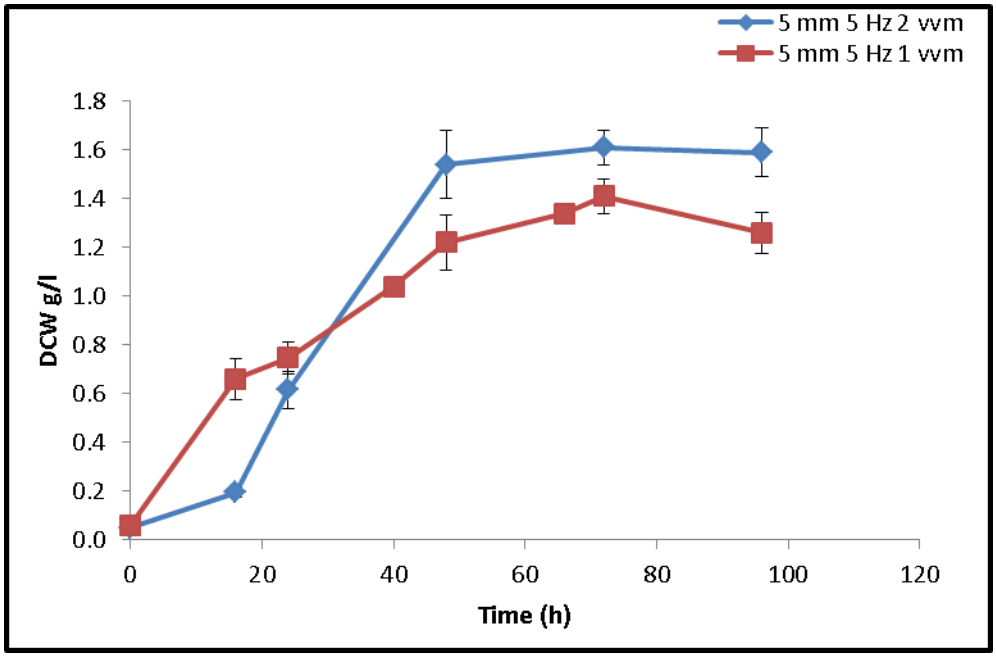

Figure 4.33: The effect of aeration with high frequency and low amplitude on total biomass production rate in batch cultures of *X. campestris* ATCC 13951 in OBR at 5 mm amplitude and 5 Hz oscillation frequency with aeration of 1vvm and 2vvm at 30 °C.

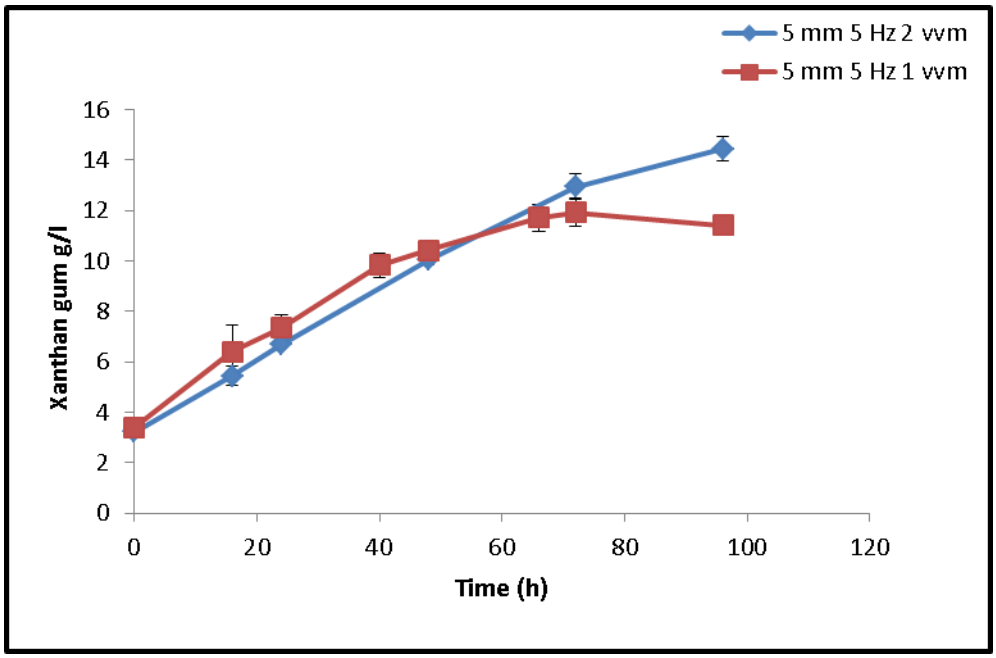

Figure 4.34: The effect of aeration in processes with high frequency and low amplitude on xanthan gum production in batch cultures of *X. campestris* ATCC 13951 in OBR at 5 mm amplitude and 5 Hz oscillation frequency with aeration of 1vvm and 2vvm at 30 °C.

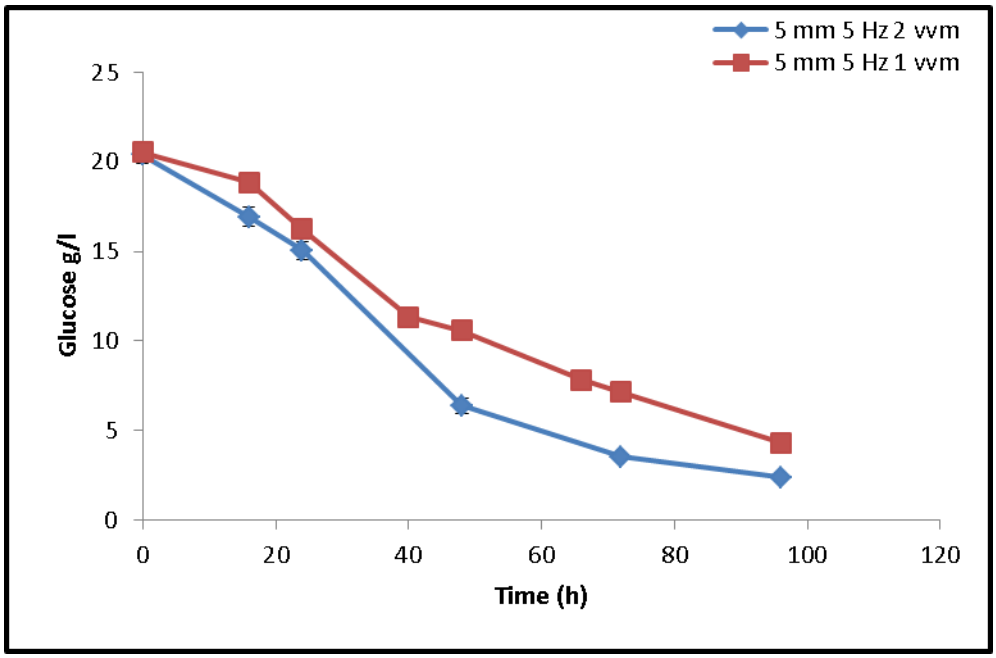

Figure 4.35: The effect of aeration in processes with high frequency and low amplitude on glucose consumption in batch cultures of *X. campestris* ATCC 13951 in OBR at 25 mm and 15 mm amplitude and 2Hz oscillation frequency at different aeration rates of 1vvm and 2vvm at 30 °C.

4.4 The production of acetic acid

All the experiments were done in an uncontrolled pH conditions. The pH profiles were monitored throughout the fermentation time and it was noticed that there was a decrease in the pH after 24 hour in all experiments accompanied with a strong odour of acetic acid during the sampling. Therefore, the author studied the production of acetic acid throughout the fermentation time under two different conditions; the production of acetic acid in the OBR at 25 mm 2 Hz 1vvm and the production of acetic acid in the STR at 200 rpm 1vvmn where the concentration of acetic acid was detectable. Figure 4.36 shows the pH profile for both conditions where the starting broth pH medium is neutral, followed by a increases in the first 24 hours to slightly basic medium after that point the pH decreases dramatically. Figure 4.37 shows the production of acetic acid under both conditions, where acetic acid production went up as pH decreased.

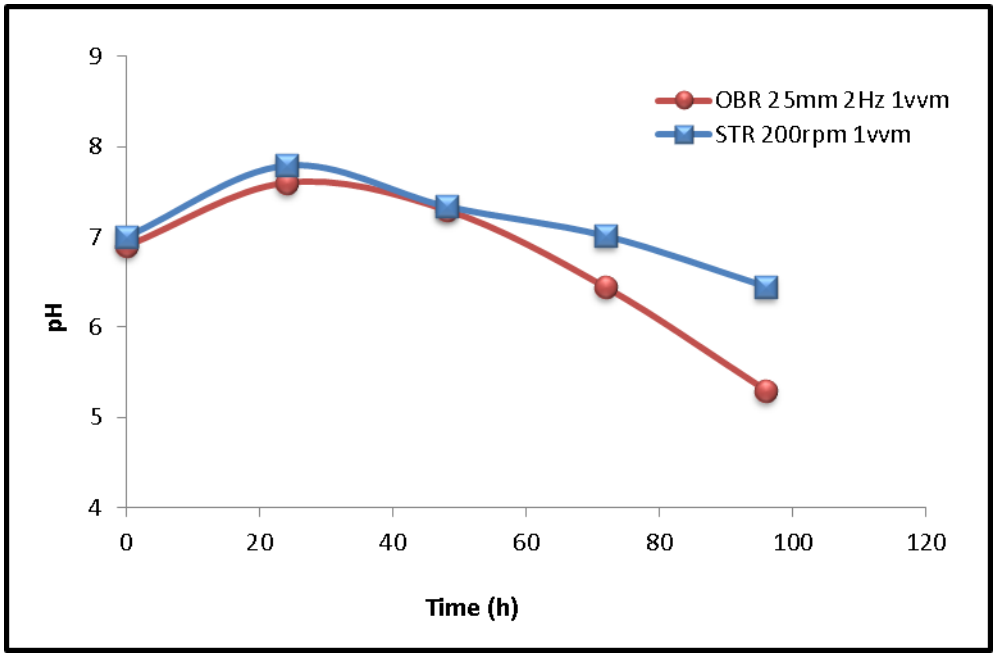

Figure 4.36: pH profile for the OBR at 25 mm 2 Hz 1vvm and the STR at 200 rpm 1vvm.

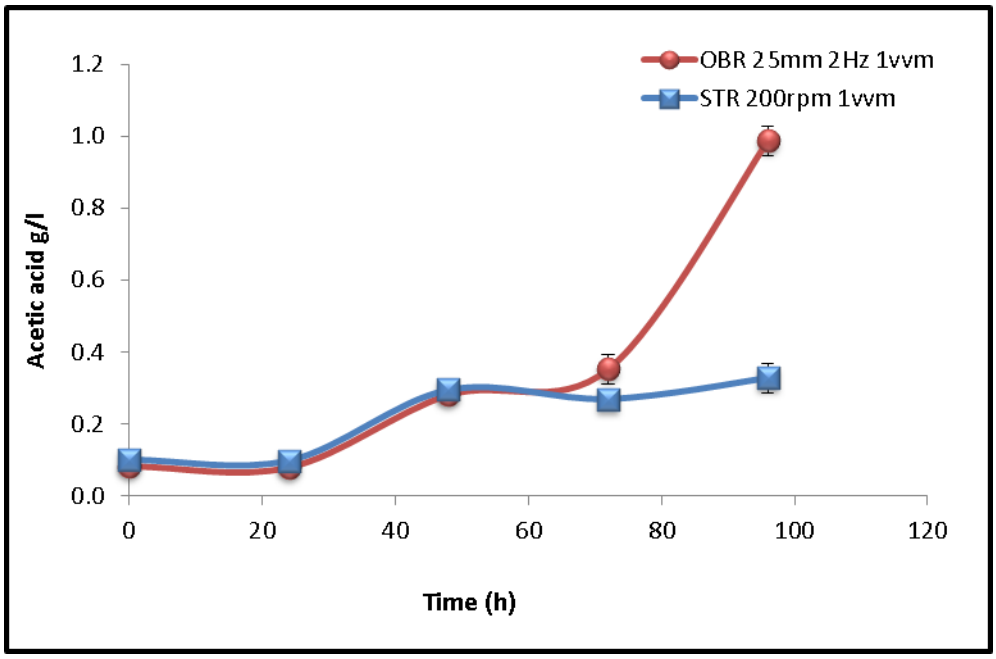

Figure 4.37: Acetic acid production profile for the OBR at 25 mm 2 Hz 1vvm and the STR at 200 rpm 1vvm.

4.5 Molecular weight

For molecular weight determination, the samples were subjected to size exclusion chromatography analysis (SEC) using the triple detection (GPC) method (see Materials and Methods, Chapter 3). Six samples were analysed for molecular weight estimation: Three samples of xanthan gum were extracted from a 72 hour old culture in the STR operated at different agitation rates: 500 rpm at 2 vv m, 200 rpm at 2vvm and 100 rpm at 1vvm. Three different samples of xanthan gum were extracted from a 72 hour old culture in the OBR at 25 mm amplitude 2 Hz frequency 2vvm, 25 mm amplitude 2 Hz frequency 1vvm, and 5 mm amplitude 5 Hz frequency 2vvm. All samples showed some slight column retention effects varying from 55.81- 54.31 %; the duplicates showed excellent agreement in molecular weight, size and intrinsic viscosity and was chromatographed well under the conditions used. The calculated results for duplicate sample injections are shown in Table 4.1. The molecular weight of the xanthan gum produced from STR 100 rpm at 1vvm has the lowest value of 2940 kDa, with lowest intrinsic viscosity of 6.14 dl/g, but xanthan gum produced from STR at 200 rpm 2vvm has the highest 5470 kDa with mild intrinsic viscosity of 8.44 dl/g, whereas xanthan gum produced from STR at 500 rpm 2vvm was in between with 3890 kDa and had the highest intrinsic viscosity of 9.78 dl/g.

Table 4.1: Quantitative analysis results of 6 samples of xanthan gum: 3 samples produced by STR and 3 samples produced by OBR using triple detection method and size exclusion chromatography at 40 °C and dn/dc =0.145 ml/g.

Samples	Mw	Mn	Mw/Mn	IV	Rh	Recovery%	Yield after 96 hour g/l
STR 500 rpm 2vvm	3870	3590	1.08	9.78	83.15	55.26	15.80
	3910	3620	1.08	9.77	83.62	55.01	
STR 200 rpm 2vvm	5500	4740	1.16	8.45	88.84	54.66	14.25
	5440	4850	1.12	8.42	87.90	54.78	
STR 100 rpm 1vvm	2940	2450	1.20	6.15	64.20	55.70	8.13
	2940	2420	1.22	6.13	63.66	55.56	
OBR 25 mm 2vvm	4370	4050	1.08	8.62	83.65	54.31	15.30
	4400	4060	1.08	8.69	83.98	54.55	
OBR 25 mm 1vvm	4340	2940	1.48	7.28	75.40	54.48	11.00
	4320	3200	1.35	7.27	74.51	54.57	
OBR 5 mm 2vvm	3100	2580	1.20	7.01	68.15	54.80	14.45
	3120	2650	1.18	6.92	68.48	55.81	

Mw: Weight average molecular weight (kDa) Mn: Number average molecular weight (kDa) Mw/Mn Polydispersity
IV: Intrinsic viscosity (dl/g) Rh: Hydrodynamic radius (nm).

On the other hand, there were no significant differences in molecular weight of xanthan gum produced from OBR at 25 mm 2 Hz in both aeration rates (1vvm and 2vvm), but there were a slightly higher intrinsic viscosity and hydrodynamic radius in the higher aeration rate. The results showed the lowest molecular weight of 3110 kDa and lowest intrinsic viscosity of 6.96 dl/g in the xanthan gum produced from OBR at 5 mm amplitude 5 Hz frequency 2vvm.

4.6 Power consumption

Power is required for mixing and mass transfer in fermentation systems. The turbulent dynamic forces improve macro scale mixing and therefore mass transfer by causing bubble breakup (Vant Riet and Tramper, 1991). In order to compare the power density measurements between the two reactor systems, the operating conditions applied in the experiments for both the STR and the OBR reactors are shown in Table 4.2. Power density was calculated for the conditions of STR and OBR fermentation runs in this study.

For the estimation of the power density in the STR an equation of the form below was used (Rushton *et al.*, 1950).

$$P/V = \frac{P_0 \rho N^3 D_s^5}{V_v} \qquad \left(W/m^3\right) \tag{4.1}$$

where

P_0 = Number power of the impeller (Gimbun *et al*., 1993) = 4.5

ρ = Density of the fluid (kg/m^3)

N = Rotational speed of the impeller (rpm)

D_s = Diameter of impeller (m)

V_v = Volume (m^3)

For the estimation of the power density in the OBR a quasi-steady flow model equation form was used (Ni and Mackley, 1993).

$$P/V = \frac{2\rho N_b}{3\pi C_D^2} \frac{1-\alpha^2}{\alpha^2} x_o^3 (2\pi f)^3 \qquad \left(W/m^3\right) \qquad (4.2)$$

where

$f =$ Frequency (Hz)

$x_o =$ Amplitude (m)

$\alpha =$ Ratio of effective baffle area to tube area (Ni and Goa, 1995) = 0.212

$\rho =$ Density of the fluid (kg/m^3)

$C_D =$ Discharge coefficient (Ni and Goa, 1995) = 0.7

$N_b =$ Number of baffles per unit length

Table 4.2: Operating parameters for both the STR and the OBR reactors for batch cultures of *X. campestris* ATCC 13951.

	2-litre STR fermenter	2-litre OBR fermenter
Total volume (l)	3.3 l	3.3 l
Operating volume (l)	2.0 l	2.0 l
Working volume (l)	1.3 l	1.3 l
Total height (mm)	248 mm	420 mm
Liquid height (mm)	98 mm	165 mm
Diameter of the vessel (mm)	130 mm	100 mm
Number of baffles	4	3
Width/diameter of baffle (mm)	Width 15 mm	Orifice diameter 46 mm
Sparger type	Ring sparger	Ring sparger (upward)
Aeration rate (vvm)	1vvm and 2vvm	1vvm and 2vvm
Agitation type	Two six-bladed Rushton turbines	Three stainless steel annular baffles
Agitation speed	500 rpm, 300 rpm, 200 rpm and 100 rpm	25 mm 2 Hz, 15 mm 2 Hz and 5 mm 5 Hz
pH	Uncontrolled	Uncontrolled
Temperature (°C)	30 °C	30 °C

Figure 4.38 shows the power density of different agitation rates used in this study of STR vs. the yield after 96 hours. At 500 rpm, the highest power density of 2.321 kW/m^3 was achieved. An overall trend is apparent in the STR, in that as power density increases so does xanthan yield in most cases. This is most apparent at low gassing rate 1vvm, but the effect is still clear at high aeration rate 2vvm though not quite so pronounced. Figure 4.39 shows the power density under different operational conditions used in this study of OBR vs. the yield after 96 hours. A clear effect of aeration rate is apparent in these figures. At high aeration rates, yield rises significantly with power density up to 0.761 kW/m^3 and then falls somewhat at higher energy density. By contrast at low gas rate, thus effect is less apparent. All OBR yield vs. power consumption in different condition was compared to the STR yield vs. power consumption in different condition in figure 4.40, that shows the maximum power consumption of all the fermentation was shown in the OBR 25 mm. Figure 4.41shows a comparison of maximum yield between OBR 15 mm 2 Hz and STR 500 rpm at the high aeration rates 2vvm vs. power consumption.

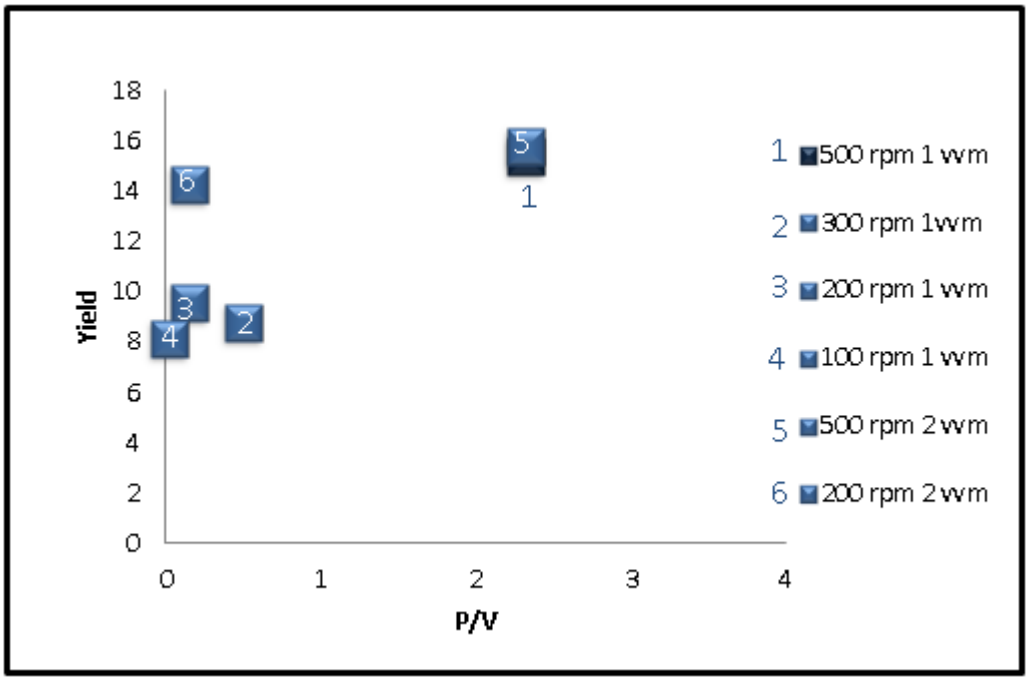

Figure 4.38: Power density vs. yield of xanthan gum in (STR) in different agitation and aeration rates.

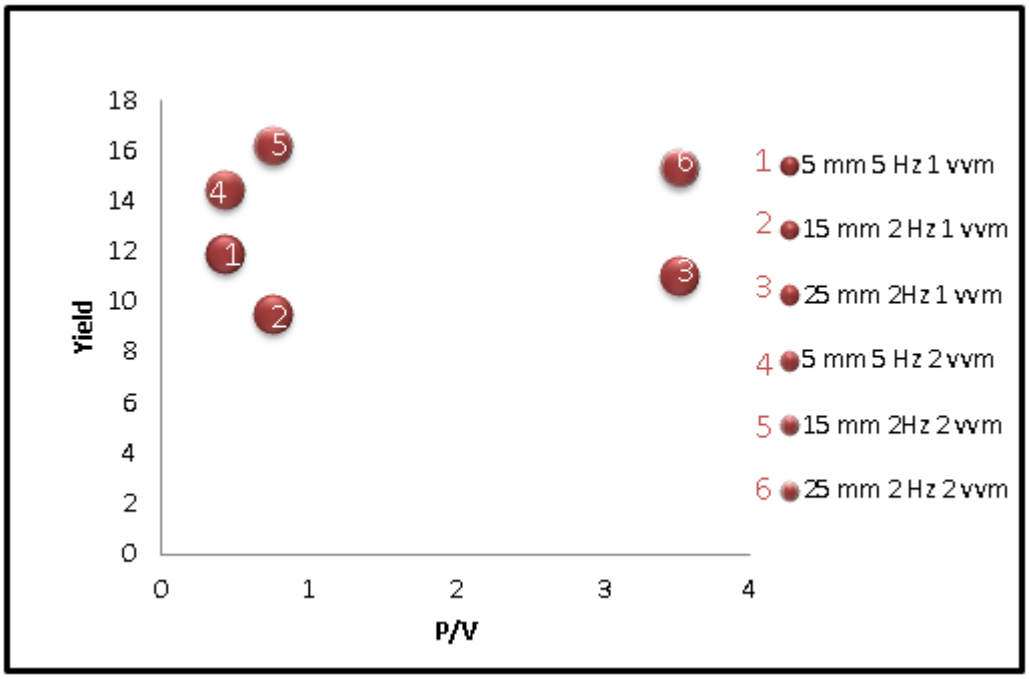

Figure 4.39: Power density vs. yield of xanthan gum in the OBR in different conditions of frequency, amplitude and aeration.

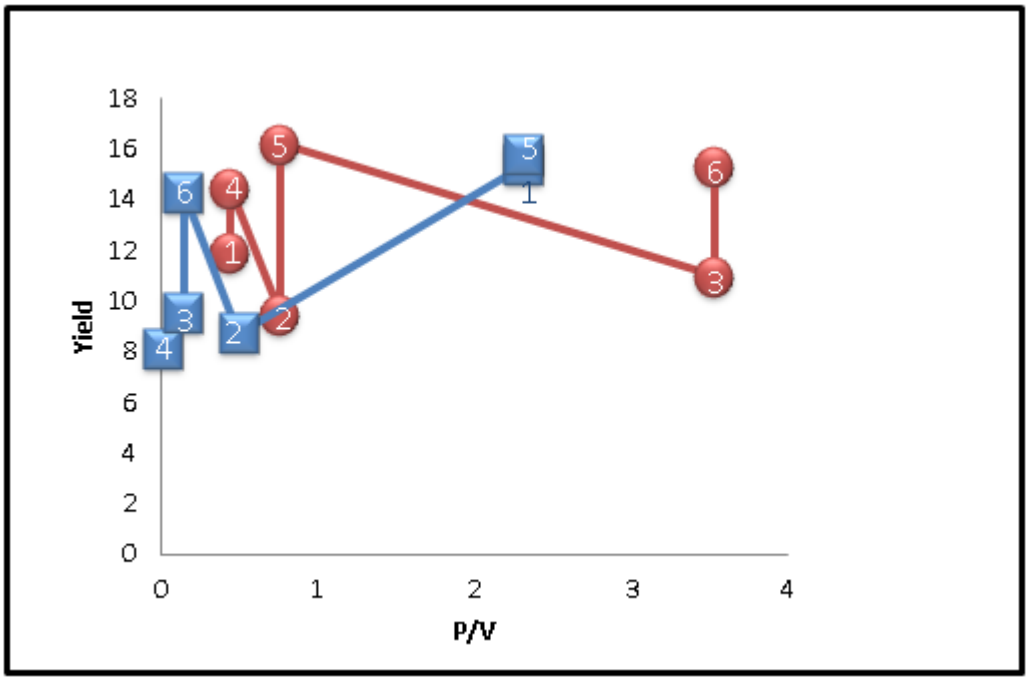

Figure 4.40: Power density vs. yield of xanthan gum in the OBR in different conditions of frequency, amplitude and aeration vs. (STR) in different agitation rates and aeration rates.

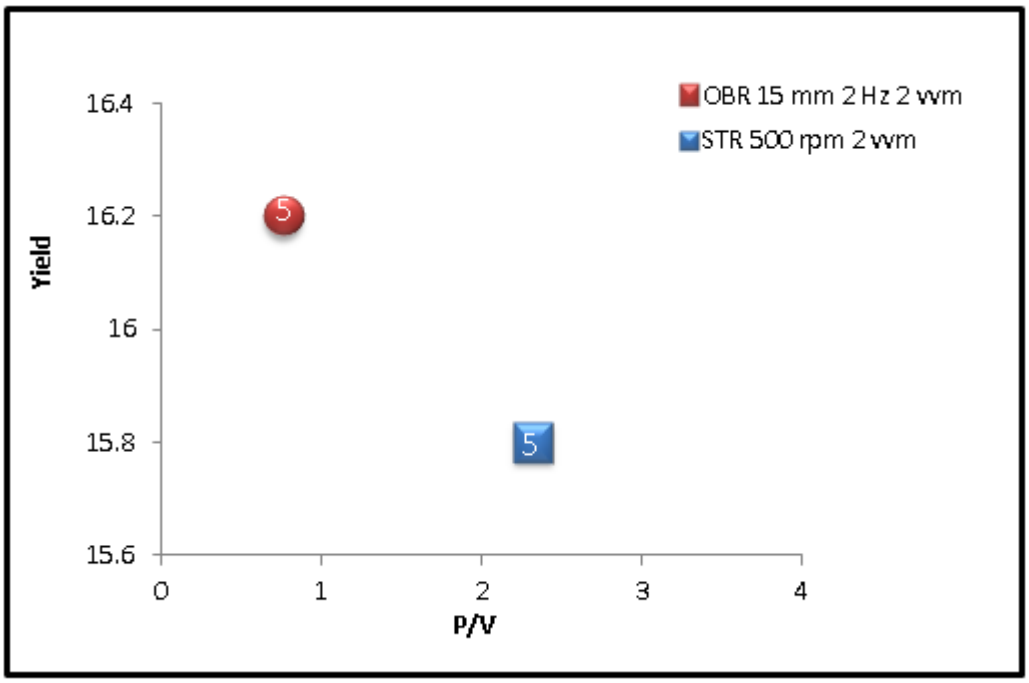

Figure 4.41: Power density vs. maximum xanthan gum yield for all the OBR runs under different conditions of frequency, amplitude and aeration vs. maximum xanthan gum yield of the all STR in different agitation and aeration rates.

Chapter 5

Discussion

5 Discussion

Chapter 6 presents the discussion of the experimental results for the production of xanthan gum in a shake flask, the production of xanthan gum in the STR, the production of xanthan gum in the OBR, the molecular weight results, and the comparisons of the results in the power consumption between the OBR, and the conventional workhorse STR.

5.1 The production of xanthan gum in a shake flask

5.1.1 The effect of the glucose concentration

In general, batch xanthan gum fermentation can be distinguished by two stages; the propagation and cell growth in trophophase, and the production of xanthan gum in idiophase (Fiedler and Behrens 1984). Both cell growth and xanthan formation have different nutrient requirements. Therefore, the optimal conditions for cell growth and xanthan formation are quite different. Many studies have been undertaken to define the nutritional requirements of *X. campestris* ATCC 13951 for optimal xanthan production (Davidson, 1978; Souw and Demain, 1979; Zhang and Greasham, 1999; Garcia *et al.,* 1992; Letisse *et al.,* 2001).

Leach *et al.* (1957), Lilly *et al*. (1958), Leela and Sharma (2000), Faria *et al.* (2009), Zhang and Chen (2010), and El Enshasy *et al.* (2011) studied various types of carbon sources during fermentation of the *X. campestris*. The resultant xanthan gum yield, given in declining order, was glucose, sucrose, maltose, and soluble starch. The most important factor in xanthan gum production would appear to be the initial concentration of the carbon source, which was glucose in the present study; because the initial glucose concentration is the driving force for glucose transfer from the medium into cells (Funahashi *et al.,* 1987; Zhang and Chen, 2010). It is generally believed that fast cell growth and high cell density is favoured by high nitrogen concentrations. However, xanthan production will be poor if the nitrogen

concentration in the medium is too high (Souw and Demain, 1979; Kennedy *et al.*, 1982; Woiciechowski *et al.*, 2004; Faria *et al.*, 2009). For good production, xanthan biosynthesis is favoured by a high concentration ratio of carbon to nitrogen source (C/N ratio) and an adequate supply of the other nutrients, which can be phosphorus, or sulphur (Davidson, 1978; Schweickart and Quinlan, 1989; Garcia-Ochoa *et al*., 1990; Lo *et al.,* 1997). The C/N ratio usually used in production media is more than that used during growth medium. The effect of the initial glucose concentration on *X. campestris* ATCC 13951 growth was studied and the results from this study are presented in Chapter 4.

In general results obtained were in good agreement with those of prior studies (Davidson, 1978; Souw and Demain, 1979; De Vuyst et al., 1987; Faria et al., 2009). However, most prior studies used different growth media for X. campestris ATCC 13951 such as Yeast Malt (YM) and Yeast Peptone Glucose (YPG). These considered the carbon and nitrogen effects separately and did not provide useful insights into the synergistic effects of glucose and yeast extract. Funahashi et al., (1987) suggested that the best C/N (glucose/yeast) ratio for the production of xanthan gum is 10:1.

In the present work yeast malt extract (YM) medium was used for the growth medium and the glucose concentrations were varied. The results show an agreement with Lo *et al.* (1997), where they used a glucose range of 25 - 50 g/l and yeast extract varied from 2 - 4 g/l. They found that both the xanthan yield and specific production rate increased with increasing C/N ratio in the medium, but the cell yield and specific

growth rate decreased as C/N ratio increase. While in this study, the glucose was varied from 2 - 8 g/l and Yeast was constant at 4 g/l. We found that an increase in glucose concentration up to C/N ratio 2:1 in YM medium enhanced cell growth, whereas xanthan gum was produced steadily regardless the C/N ratio up to 24 hours, this is may refer to the low initial glucose concentration unlike in Lo *et al.* (1997) study (Figure 4.1, 4.2 and 4.3).

The growth fell in the late stages of the process after a short period of stationary phase, although there was residual glucose source left in all experiments. This is suggesting that the microorganism uses the remaining glucose for producing extra xanthan gum and the fell in cell growth may have been due to cell lysis. Therefore, the production of xanthan gum continued towards the end of the run. The results showed that at C/N ratio 0.5:1 and 1:1 the glucose was exhausted after 48 hours with better growth and better xanthan gum production at C/N ratio 1:1. In addition, as can be seen from the same figures although the main carbon source was exhausted xanthan production was continued to the end of the fermentation, this is may suggesting that the microorganism may have been using another carbon sources, it might be either from malt extract or yeast extract to produce xanthan gum. This was apparent at the end of the fermentation where the total xanthan produced in addition to the biomass value was more than the initial glucose concentration. On the other hand at C/N ratio 1.5:1 and 2:1 there were an increase in biomass but also there were a remaining glucose of 25% and 50% respectively at 48 hours. From these findings the author proposes that the best C/N ratio for the inoculation medium is 1:1 where the glucose and yeast extract concentrations are equal at 4 g/l. This is because in the

experiment with C/N ration equal to 1:1 after 24 hours including trophophase, the dry cell weight was 1.2 - 1.4 g/l and had an optical density of 1.4 - 1.6 at (λ 600nm) and this appeared to be a suitable cell mass for inoculation purposes.

5.1.2 The effect of citric acid supplementation on the process

Souw and Demain (1979) found that the production of xanthan by *X. campestris* using synthetic media was stimulated by the addition of certain organic acids, such as succinate, pyruvate, and ketoglutarate. Conversely, excess concentrations of these organic acids inhibited xanthan formation. In addition, Jana and Ghosh (1995, 1997) found that xanthan production was affected by the addition of citric acid in fed batch mode. They concluded that the addition of up to 2.6 g/l citric acid under oxygen-limiting conditions improved cell viability as well as increasing xanthan yield. In contrast, at higher aeration conditions citric acid addition did not improve xanthan production. Moreover, increased citric acid concentration in the medium resulted in an increase in ATP production by cells which was used in the synthesis of xanthan (Jana and Ghosh, 1999).

It has been shown that citric acid metabolism by *X. campestris* ATCC 13951 can affect the composition of xanthan gum by increasing the pyruvic acid content of xanthan where, the presence of pyruvate increases viscosity of xanthan gum (Tako and Namawa,1989; Hassler and Doherty, 1990).

Peters *et al*. (1990) have shown that the addition of citric acid to the medium act as a chelating agent to prevent the precipitation of salts during heat sterilisation. This was in agreement with the results obtained in the present study. In addition we found that the addition of citric acid to a defined medium in shake flask fermentations reduced foam formation (Figure 4.4).

The results indicate that the added citric acid was totally consumed after 10 hours in all different concentration runs (data are not shown). Additionally the addition of citric acid to a defined production medium shifted the trophophase from 24 hours to 48 hours compared with growth medium.

As can be seen from figures 4.5 and 4.6 in the results (chapter 4) although citric acid was totally consumed in the first 10 hours, the results indicate the effect of the addition of citric acid to a defined medium, where biomass formation and xanthan gum production were increased when compared to the control. The addition of 2.0 g/l citric acid increased the growth 36% after 48 hours while 40 % increase in growth occurred when 4 g/l citric acid was added. These findings are in agreement with Jana and Ghosh (1995, 1997, and 1999). In addition, from the results presented in figure 4.7 in the results (Chapter 4), it can be seen that the addition of citric acid led to enhanced glucose consumption. Therefore, the author suggested the optimum citric acid concentration for the production of xanthan gum by the bacterium *X. campestris* ATCC 13951 in this synthetic medium is 2.0 g/l, which is supported by the findings of Jana and Ghosh (1997).

5.1.3 The effect of agitation rate on the production of xanthan in shake flask

Previous studies on the kinetics of growth and xanthan production by *X. campestris* ATCC 1395 at different agitation speeds were only studied in a laboratory fermenter. It is known that the production of xanthan gum in stirred tank reactors at lower stirring speeds encounters oxygen limitation earlier (Suh and Yang, 1990). In addition, xanthan gum is basically a slime secreted around the cells which implies the development of increasing rheological complexity throughout the time course of a xanthan fermentation process. As a result, mixing becomes less effective with time resulting in oxygen diffusional limitation. Such limitation may account for the change in the growth rate of the cultures (Dreveton *et al*., 1996).

Galindo *et al*. (1993) studied the effect of shake flask type on the production of xanthan gum and found that a Baffled Erlenmeyer flask was more suitable for scale-up than use of Fernbach flasks. Although the bacterial growth and xanthan production were similar in both types, on a weight basis xanthan produced in baffled flasks was up to three times more viscous and more pseudoplastic or 'shear thinning'.

In the present study the production of xanthan gum in Erlenmeyer shake flasks was examined at a range of stirrer rotational speeds to investigate the effects of agitation upon the process. The objective of this experiment was to systematically

investigate and quantify how the onset and extent of oxygen limitation impacted on the xanthan produced in a shake flask.

As can be seen in figure 4.8 and 4.9 in the results (Chapter 4) the biomass concentration increased steadily for all experiments during the course of fermentation. Agitation at 300 rpm seemed to provide the best growth conditions over the course of the fermentation, producing maximal growth and xanthan production by the end of the fermentation course. Papagianni (2001) also reported a similar growth profile at 150 and 300 rpm in a stirred tank reactor (STR) using medium viscosity fungi *Aspergillus niger*. Giavasis (2006) suggested that low biomass formation at low agitation rate in a *Sphingomonas paucimobolis* culture was caused by poor mixing in the vessel (STR), hence inadequate nutrient uptake by the bacterium.

At 300 rpm, mixing and oxygen transfer were clearly adequate in the present study, as at the end of the fermentation residual glucose was the lowest in all the other conditions examined in this experiment (Fig 4.10), whereas at 200 rpm the growth, xanthan production and glucose consumption were lower than those in 300 rpm process. Amanullah *et al*. (1997) found that under constant non-limiting dissolved oxygen concentration of 20% of air saturation using gas blending, the biological performance of the culture is independent of agitation speed as long as broth homogeneity could be ensured. From these findings it can be assumed that in shake flask fermentation, where there is an oxygen limitation the growth and xanthan production are dependent on the shaking speed.

5.2 The production of xanthan gum in the Stirred Tank Reactor STR

It is generally agreed upon in the literature that the process bottleneck in highly productive fermentations is related to two problems: poor bulk mixing and low oxygen transfer rates (Moraine and Rogovin, 1973; Nienow, 1984; Funahashi *et al*., 1988a, Nienow and Elson, 1988; 1992; Herbst *et al*., 1992; Galindo and Nienow, 1992, 1993; Flores *et al*., 1994; Zhao *et al*., 1994).

Both aeration and agitation are important, and affect both bulk mixing and the mass transfer rate, which in turn affects both dissolved oxygen and nutrient uptake. In order to examine the effects of aeration and agitation, these conditions were varied and their effect upon dissolved oxygen, pH, growth, production and glucose consumption were examined. In this study data was collected manually, however auto command software for the automatic log in of data would have been more beneficial.

5.2.1 The effect of agitation speed on the production of xanthan gum in STR

Agitation speed affects both the extent of motion (bulk mixing) and the rate of oxygen transfer in xanthan fermentation broth (Amanullah *et al*., 1998b). The rheological complexity of the fermentation broth causes the volumetric mass transfer coefficient k_La for oxygen concentration and its spatial uniformity to decrease with

increasing viscosity. Also a change in process agitation speed at some point can lead to oxygen limitation of the xanthan production rate. This was discussed previously in the literature review (Chapter 2). As the lower the stirring speed, the earlier oxygen limitation was encountered (Suh and Yang, 1990).

As can be seen in figure 4.11 in the results (Chapter 4), the dissolved oxygen profiles show the absence of a noticeable lag phase in these experiments, which is characterised by a rapid decrease in dissolved oxygen even at low viscosities. At low agitation speeds; 100 rpm, 200 rpm and 300 rpm the higher the faster the onset of the oxygen limitation. In contrast, at high agitation speed of 500 rpm there was no oxygen limitation, this results are indicating the influence of the agitation speed on xanthan gum fermentation. Amanullah *et al*. (1998b) reported similar results for higher agitation rates, 500 rpm and 1000 rpm with controlled pH, which might indicate that above a stirrer threshold agitation, had no effect, but in that study, DOT was automatically controlled at 20%.

It is also clearly shown in figure 4.12 in the results (Chapter 4) with uncontrolled pH in the first 24 hours that there was a slight increase in the pH in all experiments, and it is possible that this may be caused by the consumption of citric acid as mentioned in section 4.1.2 in the results (Chapter 4). After 24 hours, toward the end of the exponential phase the pH decreases during the fermentation time, this may refer to the formation of organic acids. These acids could be acetic acid or pyruvic acid as there are used as branching groups in xanthan backbone or they could be other organic acids such as citric acid cycle (TCA) intermediate (Souw and Demain

1979, Cadmus *et al.,* 1978). In terms of organic acid produced by *X. campestris* ATCC 1395 strain there was significant evidence for acetic acid formation. An experiment was done to measure acetic acid formation throughout the fermentation run. The results showed that the pH profile was broadly in alignment with the formation of acetic acid (Figure 4.36 and 4.37). It was also observed during the practical work by the end of the fermentation run there was an obvious odour of acetic acid coming from the medium. In the process at 500 rpm there was another increase in the pH at 48 hours which may be explained by re-use of those organic acids either as a carbon source or for more branching.

Esgalhado *et al.* (1995) determined the optimal range of the pH and temperature for xanthan production was 7·0 - 8·0 and 25 – 30 °C, respectively. While the pH of 6·0 - 7·5 and a temperature of 25 – 27 °C were optimal for growth. While if the process pH falls below 5.0 the formation of xanthan drastically reduces.

The influence of agitation speed on cell growth and xanthan production was determined in this experimant. Figure 4.13 in the results (Chapter 4) shows that cell growth was lower as the agitation speeds was slower, local oxygen transfer rates are likely to be responsible for the lower growth rate. At the higher agitation rates of (500 rpm) the dry cell weight increased exponentially with the highest specific growth rate in this fermentation. After 48 hour, growth rates were ceased in all agitation speeds, this may cause due to exhaustion of the nitrogen source. This finding is in agreement with Papagianni *et al*. (2001b). In a previous study, the production of xanthan gum was found to be partially growth related (Weiss and

Ollis, 1980). In the present study, during the initial growth phase polysaccharide accumulation starts and continues after growth. Figure 4.14 in the results (Chapter 4) shows xanthan concentrations over time at 100, 200, 300, and 500rpm. The production was slow and rather similar for the medium speeds of 200 and 300 rpm. Production was significantly lower at the lowest agitation speed 100 rpm. Xanthan production appeared slightly higher at the end of fermentation (96 hour). The results are similar to Papagianni *et al*., 2001b. On increasing the stirrer speed to 500 rpm, xanthan production increased significantly, indicating a relationship between stirrer speed and xanthan production. From the findings of Amanullah *et al*., (1997) increased in xanthan production at higher impeller speeds is probably related to enhanced oxygen transfer rates at this speed.

It was noticed in the present study that during biomass precipitation a slime layer was observed around the cells, this was part of xanthan co-precipitated with biomass, even when the samples were diluted by a dilution factor of up to 10 as proposed by Kalogiannis *et al*. (2003). Hence, the method was modified by the author as described in the materials and methods (Chapter 3) in order to avoid the observed co-precipitation of xanthan gum with biomass during centrifugation.

The similarity of the exponential growth phase and the production of xanthan gum at the lower agitation speeds are also reflected in the residual glucose concentration profiles that shown in figure 4.15 in the results (Chapter 4). The initial concentration of glucose used in the medium was 20 g/l. In this experiment *X. campestris* ATCC 13951 had consumed around 5 g/l of glucose within 24 hours at the lower agitation

rates, which was probably utilised for growth and starting producing xanthan. But at the higher agitation speed 500 rpm almost half of the glucose was used in the same time (24 hour) corresponding to half of the total production of xanthan gum, indicating that the efficiency of high speed agitation rate on the production of xanthan gum. From figure 4.14 in the results (Chapter 4) xanthan was produced starting from the exponential phase, the latter was strikingly similar at the lower agitation speed (100, 200 and 300 rpm) until 48 h, when the residual glucose concentration was almost half the initial glucose concentration and xanthan concentration was around 6.5 g/l. Deviations in the glucose utilisation rate emerged beyond this time, resulting in differences in xanthan synthesis. Xanthan concentrations at 500 rpm were almost double the concentration at the lower agitation rates and substrate glucose was almost fully utilized by the microorganism. It was noticed from the residual glucose trend that at 500 rpm although the glucose was completely utilised at 48 hours, the microorganism continued xanthan gum formation toward the end of the fermentation course at 96 hours where xanthan concentration was 15.36 g/l. This may explain the increase in the pH that happened after 48 hours into the process. Beyond this point it could be that the microorganism reused the organic acids secreted at the end of the exponential phase to produce more xanthan gum for a protection. The data for the acetate level were not shown in the present study, due the difficulties for the separation of biomass from the broth and the length of the process of separation cause the evaporation of acetate and thus incorrect analysis. In addition, the small concentration of the acetate was difficult to be determined. Therefore there were only one condition of each fermenter was done to estimate acetic acid formation (Figure 4.37).

5.2.2 The effect of aeration on the production of xanthan gum in (STR)

Xanthan gum production is dependent on the volumetric mass transfer coefficient for oxygen, while biomass formation is reportedly not affected (Borges *et al*., 2008). This is not likely to be accurate as *Xanthomonas* is a highly aerobic microorganism, and it is therefore reasonable to assume it would grow faster when oxygen supply is adequate. The increase in viscosity during xanthan production decreases the volumetric mass transfer coefficient for oxygen, at some point leading to oxygen limitation of the xanthan production rate (Peters *et al*., 1989). Technically growth and production are limited by 2 factors; oxygen limitation and nutrient depletion. As mentioned in the previous section oxygen limitation was encountered at low stirring speeds in xanthan batch fermentations. 4 set of experiments has been done to declare the effect of aeration on xanthan production in STR in 2 different agitation speeds. At low agitation speed 200 rpm oxygen limitation was reduced by sparging at a rate and of 2vvm. Figures 4.16, 4.18 and 4.19, show that the growth and xanthan production were influenced by aeration rate at lower agitation rate 200 rpm. In contrast, there were not major differences at the higher agitation rate 500 rpm at 48 hours. At high aeration rates (2vvm) although the production of the lower agitation rate 200 rpm was closer to the production of the higher agitation rate 500 rpm, the glucose consumption rate was higher at the higher agitation rate 500 rpm (Figure 4.20). Moreover, the experiments started at neutral pH with an increase in the first 24 ours followed by slightly decrease to go back to ± neutral pH within 48 hours at all conisations of this experiment. Beyond that point (48 hours) different behaviour in

terms of the process pH was observed depending on the agitation speed. At low agitation rate 200 rpm for both aeration rates 2vvm and 1vvm, the pH continued to decrease, ending the process at acidic pH medium. While, at higher agitation rate 500 rpm, the pH increased slightly, ending the process at almost neutral pH medium (Figure 4.17). This could be explained by the production of organic acids as indicated by the production of acetate observed (Figure 4.36 and 4.37) that reduce the pH, this was a novel study for the pH profile change related to the acetate production in xanthan gum production. An increase in pH may refer to the consumption of the secreted organic acid to produce xanthan or for cell maintenance due to the exhaustion of glucose under the higher agitation rate conditions (Wolfe 2005).

5.3 The production of xanthan gum in the Oscillatory Baffled Reactor (OBR)

STR technology has been the workhorse of industrial bio-processing worldwide. Such fermenters, although generally considered well-characterised, are acknowledged to have a number of drawbacks and limitations (Popovic and Robinson, 1993; Leib *et al*., 2001) including poor bulk mixing and a tendency for gas channelling to occur, leading to inadequate gas dispersion especially for viscous systems. Alternatively, a robust fermenter has been developed using an oscillatory baffled reactor (OBR) technology, which offers enhanced and uniform global mixing at very low shear rates with a similar power consumption compared to conventional STRs (Harrison and Mackley, 1992; Ni *et al*., 2000 Gaidhani *et al*., 2005).

Ni *et al.,* 1995 reported 75% higher mass transfer coefficients in an oscillatory baffled column in comparison with a stirred tank reactor involving yeast culture. Encouraging scientific results in applications of OBR to the fermentation of pullulan (Gaidhani, 2004) prompted this study to investigate the fermentation of higher viscosity polysaccharide xanthan using an oscillatory baffled Reactor.

The work in this section explores the way in which *X. campestris* ATCC 13951 behaves in the low and uniform shear environment of an oscillatory baffled reactor (OBR), and compares its growth rate and xanthan synthesis pattern to those in conventional STRs. A series of xanthan fermentation experiments were performed in the OBR with particular emphasis placed on the influence of aeration and agitation effects on xanthan and biomass production.

5.3.1 The effect of the sparger attitude

The OBR was provided with a ring sparger with 26 holes pointing in a downward direction (Figure 3.11) thus air bubbles were sparged downwards towards the bottom of the reactor. Several experiments were done using this sparger and it was noticed that there was a blockage in the sparger by the end of fermentation time due to accumulation of the highly viscous xanthan gum in the sparger holes; this problem could not be appreciated until the end of the fermentation due to the absence of any window to allow observation of the process. Therefore, the author suggested a new configuration sparger, where another sparger with 8 holes pointing in an upward direction was made by the mechanical engineering department at the University of

Strathclyde. In addition the new sparger (upward orientation) will be similar to sparger orientation in (STR). The comparative results of the two spargers (down ward and upward orientation) are given in this section.

Figure 4.21 in the results (Chapter 4) shows the differences in dissolved oxygen profile between the two spargers (downward and upward) at different aeration rates (2vvm and 1vvm) agitated at the same amplitude and frequency (25 mm 2 Hz). This figure clearly shows the interaction effect of the sparger direction and aeration rate on the oxygen transfer rate in the production of xanthan gum by the bacterium *X. campestris* ATCC 1395 within the OBR system. The downward oriented sparger showed higher availability of oxygen in the medium than upward oriented sparger. This availability of the oxygen in lower aeration rate (1vvm) may refer to slower growth therefore lower production, whereas in higher aeration rate (2vvm) the growth was as good as the upward orientation but with lower production (Figures 4.21, 4.23 and 4.24). In addition, the direction of sparged air in downward oriented sparger may support the availability of the oxygen in the area around the DO probe where it is located under the second baffle hole toward the middle of the vessel (Figure 5.1). Generally, an increase of the aeration rate from (1vvm) to (2vvm) increased the oxygen transfer rate in both spargers. This finding suggesting that increasing in aeration rate increases the availability of air by speeding up eddies formation during the movement of the baffles, leading to better oxygen distribution in the medium (Gaidhani *et al.*, 2004, 2005).

Figure 4.22 in the results (Chapter 4) shows the pH profiles of these experiments, where the pH value in the process with the upward oriented sparger in both aeration rates (1vvm) and (2vvm) declined faster than those in the downward orientation processes, although all processes ended with the same acidic pH values. The faster decline in the pH may be due to the accumulation of CO_2 which causes a longer hold up between two baffles. In addition, a low pH medium may suggest the presence of organic acids that are not been reused unlike those in STR experiments, which may result in lower molecular weight or less branching molecules than those in STR. Moreover, the sparger orientation showed clear effects on the growth and biomass formation especially under the low aeration rate (1vvm). At 48 hours the biomass value in the upward orientation sparger was almost the double that of the downward oriented sparger process. By contrast, there was slightly increase in biomass formation in upward orientation sparger at the higher aeration rate (2vvm) than the lower aeration for the same sparger.

From these results it can conclude that upward oriented sparger with high aeration rate (2vvm) or more aeration rates are better for growth and biomass formation (Figure 4.23 and 4.24). This is due to the downward orientation sparger was sparging the air toward the bottom of the vessel and then the air bubbles hit the vessel base and then reflect to upward direction. This process did not take place with the upward orientation sparger, where the holes were pointing upward. Figure 5.1 demonstrates a proposed movement of the medium bulk between the two baffles in both spargers downward and upward. While, the interesting results appeared when both processes downward orientation sparger at the higher aeration rate (2vvm) and upward

orientation sparger at the lower aeration rate (1vvm) showed similar growth and xanthan production throughout all the fermentation time. But these two processes showed different glucose consumption rates (Figure 4.25) indicating that there is a clear interaction between the sparger orientation and aeration rate. Additionally, it can be seen from this figure that after 48 hours fermentation time at the lower aeration rate (1vvm) upward oriented sparger process consumed double the carbon source of the processes where downward oriented sparger process was used. This increased glucose consumption was associated with improved biomass formation and xanthan synthesis showing the superiority of the upward oriented sparger for this process at low aeration rate. At the higher aeration rate (2vvm) there were no differences in the glucose consumption profile in both orientation, between the two sparger geometries suggesting that above a threshold level superficial gas velocity is high enough to avoid sparger blockage (Kang *et al*., 2000).

From these findings it can be assumed that in such a viscous medium sparger orientations is working with the aeration rate, where the speed of eddies is the most important parameter to distribute oxygen through the medium. This finding is in agreement with Oliveira and Ni (2004) where their experimental study results on mass transfer of oxygen into water in an oscillatory baffled column (OBC) showed that the gas holdup is the most important factor. In addition, above a critical level of fluid oscillation, the oscillatory operating conditions are the main factor governing the mass transfer coefficients.

The changes to the sparger geometry proposed and implemented by the author made the OBR much more suitable for the production of highly viscous products like xanthan gum. It also illustrates the profound differences between production of a moderate viscosity product such as pullulan in the OBR (Gaidhani *et al*., 2004, 2005) and the much more challenging production a high viscosity product.

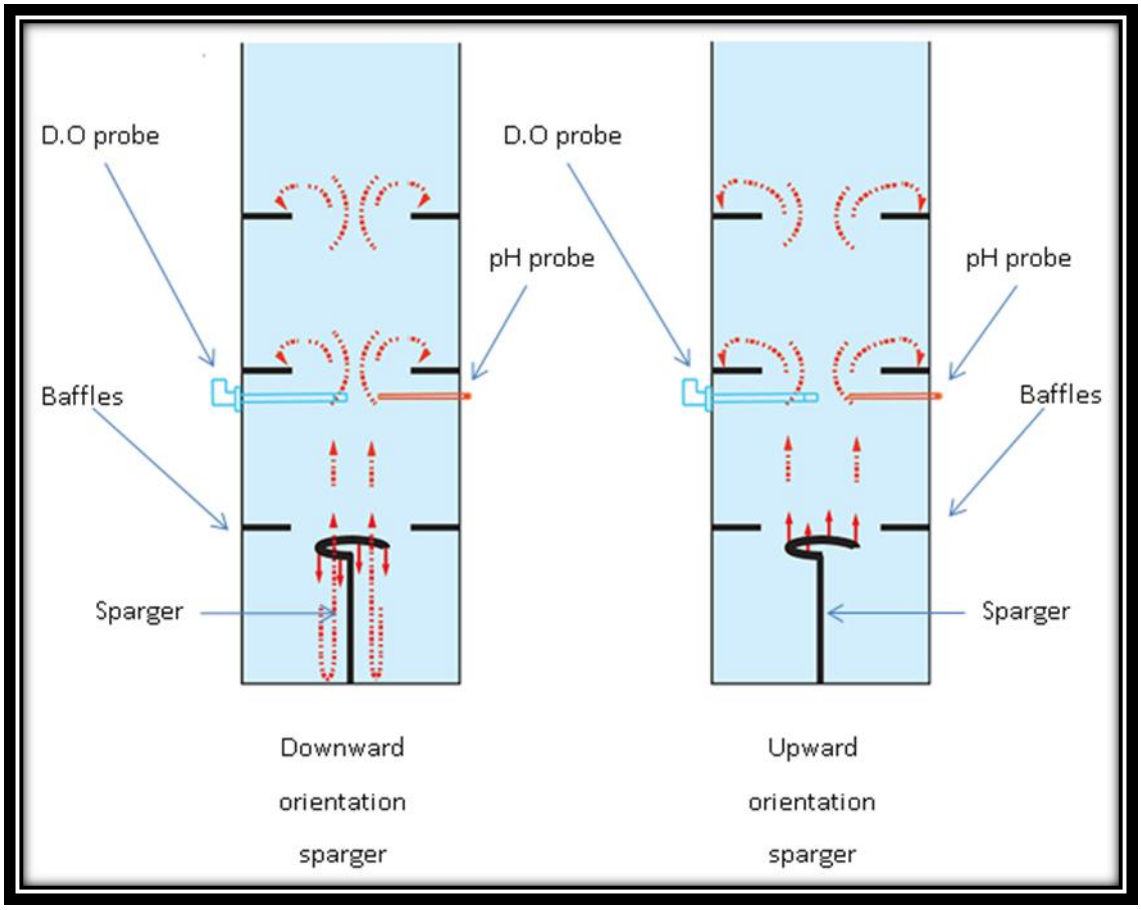

Figure 5.1: A proposed movement of the medium bulk in downward and upward orientation sparger.

5.3.2 The interaction between aeration, frequency and amplitude in xanthan production process in OBR

Ni *et al.,* 1998 found that the uniformity of methylmethacrylate suspensions droplets in a batch oscillatory baffled reactor (OBR) can be controlled by changing in oscillation frequency and amplitude leading to changes in the air bubble droplet size and air size distribution. The aim of this section is to discuss the effects of different amplitudes and frequencies, and their interaction with aeration on oxygen supply and xanthan gum production in the OBR. Two sets of experiments have been done in this section: one, high amplitude low frequency and, the other, low amplitude and high frequency, two levels of aeration rate (1vvm) and (2vvm), and only upward orientation sparger was used for each combination of amplitude and frequency.

5.3.2.1 The effect of interaction of aeration with low frequency and high amplitude

Due to the physical differences between the STR and OBR vessels (Table 4.2) differences in diameter and length of the broth medium occurred and the dissolved oxygen probe was located at different height in the vessels (See Figure 3.2 and 3.3 in the materials and method chapter 3). Additionally the mixing pattern between the two systems was different. Although, air bubbles were sparged into the bottom of the reactor in both systems, within the STR, air was distributed through the impeller in a turbulent motion and gas dispersion was dominated by impeller speed and the baffles. However, within the OBR, air distribution occurred between the baffles as

eddies were generated within compartments and were dominated by the oscillation amplitude and frequency of the baffles (Ni *et al.*, 1998 Gaidhani *et al.*, 2004, 2005).

For these reasons it is unsurprising that dissolved oxygen profiles are different in both systems. In this section two oscillation amplitudes were used: 25 mm and 15 mm at a fixed oscillation frequency (2 Hz). An experiment was carried out at the same oscillation amplitude but at a higher frequency (3 Hz). Unfortunately, the baffles were broken and pulled apart from their supporting stainless steel rods. This may have been caused due to the high viscosity of xanthan gum; which at higher frequency seems to cause higher pressures to be applied on the baffle discs. Therefore, the maximum safe frequency for xanthan gum production at oscillation amplitude 25 mm using the current OBR geometry is 2 Hz.

It can be noticed that in figure 4.26 in the results (Chapter 4) from the D.O profile that at a lower oscillation amplitude (15 mm) and at a lower aeration rate, 1vvm, there was almost no oxygen limitation, whereas at a higher aeration rate of 2vvm, dissolved oxygen limitation was greater for a smaller oscillation amplitude (15 mm) than that seen for the larger one (25 mm). These findings are the similar to those of Gaidhani (2004), where a range of amplitudes (10 mm, 20 mm and 30 mm) and a range of frequencies (1-4 Hz) were used. These results showed the best combination of amplitude and frequency for the production of pullulan was at 20 mm 3Hz.

There is no limitation period in the process where lower amplitude with a low aeration rate (15 mm 1vvm) was used. This may be due to greater availability of

dissolved oxygen in the medium of the OBR in the middle of the vessel where the dissolved oxygen probe is located. It should be noticed that the location of the dissolved oxygen probe had been changed from that described by Gaidhani (2004) (see 3.7 materials and methods chapter 3). As well as this, the most important reason that this may have occurred is the high viscosity of the medium broth which may affected the size and speed of the eddies (Gaidhani *et al.*, 2004 and 2005).

The pH profile of figure 4.27 in the results (chapter 4) shows that at higher oscillation amplitude (25 mm) at both aeration levels (1vvm and 2vvm) there was a sharper decrease in the pH level than at the lower oscillation amplitude. This occurred between 24 - 72 hours, ending with an even lower pH. These results are in agreement with the results in the previous section (5.3.1), which showed that there is a close relationship between the decrease in dissolved oxygen (oxygen limitation) in the medium and the decrease in pH due to acid formation. Additionally, these results may suggest that the molecular weight of the produced xanthan gum from OBR could be smaller than that produced from STR due to much less branching.

The effects of oscillation frequency and aeration on the total biomass are given in figure 4.28 in the results (chapter 4). Although the dissolved oxygen level had been shown to fall to zero at a high oscillation amplitude (25 mm) at both low and high aeration rates (2vvm and 1vvm) in the period between 24 - 72 and 24 - 48 hours respectively, the biomass levels were higher than those at a low oscillation amplitude (15 mm) and low aeration rate (1vvm) where no oxygen limitation was experienced during the fermentation time. On the other hand, at a low oscillation amplitude (15

mm) and a high aeration rate (2vvm), the longest oxygen limitation period occurred and the best biomass level was reached. These results may indicate that lower amplitude is better for eddy formation size but a higher speed (superficial gas velocity) is necessary to push them to the side of the vessel. This is where a higher aeration rate improves biomass formation.

The pattern of polysaccharide synthesis in the OBR can be seen in figure 4.29. Xanthan gum concentration was highest (16.2 g/l) with oscillation an amplitude of 15 mm at the higher aeration rate of 2vvm. However at the same frequency with a lower aeration rate (1vvm) xanthan gum concentration reached only 9.5 g/l. Similarly, at the higher oscillation frequency of 25 mm, the production of the polysaccharide was clearly affected by the aeration rates of 2vvm and 1vvm, as the concentration of xanthan gum was 15.3 g/l and 11.0 respectively. In addition, glucose was consumed at a similar rate in both processes at low oscillation amplitude up to 72 hours. Beyond 72 hours, at an amplitude of 15 mm and a high aeration rate (2vvm), the glucose continued to be consumed by the microorganisms. By contrast, 49% of the glucose remained at an amplitude of 15 mm at the lower aeration rate (1vvm) (Figure 4.30).

From these results it can be assumed that there is an interactive effect between the three parameters; oscillation amplitude, frequency and the aeration rate. These three parameters influence the eddy size and speed and therefore effect gas hold up and oxygen transfer within the OBR. This is clearly a highly complex system and the

relationship between the parameters in such non-mechanically agitated systems is not as simple as reported by Kang *et al*., (2001).

Ni *et al*., (1995) stated that the mass transfer coefficient in the OBR is a function of aeration-agitation intensity and of the physical and chemical properties of the fermenter. This again points to the highly complex nature of the interactions between process parameters in a relatively lightly characterised reactor system such as the OBR.

These results show that the main parameter that is controlling the mixing in the OBR is the aeration rate. In addition, there are an optimal set of oscillation conditions for xanthan gum production in the current OBR. The enhancement of biomass formation and polysaccharide synthesis by improving the mixing and aeration conditions (in terms of high frequency/low amplitude) is best at oscillation amplitude of 15 mm, a frequency of 2 Hz and an aeration rate of 2vvm.

5.3.2.2 The effect of interaction of aeration with high frequency and low amplitude

Ni *et al.,* (1998) reported that an increase in either oscillation amplitude or oscillation frequency decreased the droplet size and narrowed the size distribution. Similarly, in the production of xanthan gum, an increase in the oscillation amplitude seems to be decreasing the size distribution and the uniformity of the air bubbles. In addition, in the previous section it was shown that lower oscillation amplitude with a higher speed that was caused by a higher aeration rate of 2vvm was preferable for biomass

and polysaccharide production. In this section, the oscillation amplitude was reduced to 5 mm and the frequency was increased to 5 Hz so the effect of the aeration rate on the biomass formation and the xanthan gum production in the OBR could be studied.

Figure 4.31, dissolved oxygen profiles for both low oscillation amplitude and high frequency at the 2 aeration rates are shown. A clear increase in the dissolved oxygen level at a high oscillation amplitude with a low frequency is apparent; this is reflected in the delay of the dropping of the oxygen level at the beginning of the process and oxygen limitation in both processes. Again at the higher aeration rate (2vvm) the increase in the oxygen level was more apparent than at the lower aeration rate. These results and the pH results (figure 4.32) support the findings in the previous section, that as the pH in the medium is reduced, a reduction in dissolved oxygen levels generally follow. This is broadly similar to the effect of dissolved oxygen upon acetate synthesis in *Escherichia coli.* (Voulgaris *et al*., 2010). It was noticed that both dissolved oxygen and pH profiles in the processes with a low oscillation amplitude and a high frequency at a high aeration rate (2vvm) had very similar overall trends to the process at 500 rpm in the STR. Here, pH slightly increased in the exponential phase and then declined up until the stationary phase, finally returning to a near neutral pH. Whereas at the lower aeration rate process (1vvm) the pH continued to decline and at the process end, the medium pH was still somewhat acidic. This is consistent with poorer oxygen transfer leading to acetate synthesis but without the re-uptake and utilisation as noted in E.coli (Luli and Strohl, 1990; Farmer and Liao, 1997; Vougaris *et al*., 2010). The lower oxygen transfer leads to quicker saturation of the respiratory pathway and a more rapid synthesis of

acetate. In turn, this acetate is less likely to be re-used due to the greater amount of residual glucose and other sugars remaining and to the lower oxygen supply. The results displayed in figures 4.33 and 4.34 (in the results, chapter 4) for biomass and xanthan respectively clearly show that a lower oscillation amplitude and a high frequency with a high aeration rate are the best combination of conditions for production of xanthan gum in the current geometry of the OBR. These settings gave a biomass formation of 1.6 g/l and xanthan gum production of 15.8 g/l which were the highest levels in all processes operated in the OBR. In addition, figure 4.35 showed the effectiveness of these settings in achieving high glucose consumption during the fermentation.

5.4 Molecular weight

Unfortunately not all the samples were applied to the molecular weight estimation due to the high cost of the analysis, therefore, only a limited number of samples were done. It can be seen from table 4.1 in the results (Chapter 4) the influence of the process conditions on the average molecular weight. The STR samples showed that at a low agitation rate (100 rpm) the average molecular weight was the lowest of 2940 kDa while the highest average molecular weight of 5470 kDa was shown at the agitation rate of 200 rpm. However, an increase in the agitation rate from 200 rpm to 500 rpm reduced the average molecular weight to 3890 kDa as well as the polydispersity. This result appears to be similar to those of Casas *et al.,* (2000), who used several operational conditions for xanthan gum production including a range of agitation speeds (100 rpm, 300 rpm, 500 rpm and 800 rpm). Their results showed the lowest average molecular weight (3.6 MMDa) occurred at the lower agitation rate of

100 rpm. Similarly, when the agitation rate increased from 300 rpm to 500 rpm, the average molecular weight increased to 4.3 MMDa and 4.2 MMDa respectively and the highest acetate content was seen. This may explain the increase in the pH level at the agitation rate of 500 rpm, while beyond that agitation rate, the average molecular weight decreased to the minimum seen (3.1 MMDa) at the agitation rate of (800 rpm).

In OBR, the aeration does not show any clear influence over the average molecular weight of xanthan. In contrast, the other parameters (oscillation amplitude and frequency) did show a clear influence on the average molecular weight of xanthan. The average molecular weight at the high amplitude of 25 mm was higher than the average molecular weight at the lower amplitude of 5 mm. This result may suggest that the size and the speed of eddies that are caused and controlled by these two parameters (amplitude and frequency) have an influence on the average molecular weight of xanthan.

5.5 Power consumption

As can be seen from equations 4.1 and 4.2, aeration rate was not included, therefore the power consumption value will be aeration independent. Therefore, those processes of similar agitation speed with different aeration rates will have the same exact power consumption values.

Figure 4.40 shows a comparison of the power consumption values of the experimental conditions in the OBR and the STR vs. xanthan yield. While figure

4.41, shows the differences in the power consumption values of the best yield in both the OBR and the STR, at a high aeration rate of 2vvm. The results clearly show that the best yield in the OBR applied almost one third of the power consumption value of that produced from the STR. This result may suggest that the OBR is promising for a power consumption saver for the production of the highly viscous polysaccharide fermentation.

5.6 A comparison of the production of xanthan with the production of pullulan in the OBR.

The results presented and discussed in the previous sections make it clear that the OBR is suitable for the cultivation of *X. campestris* and can potentially be applied to the highly viscous bioprocesses. This section compares the pullulan production processes with the production of xanthan gum in the OBR.

Gaidhani (2004) studied the production processes of pullulan in the OBR and he compared his results with some studies done on the production of pullulan in the STR. The results showed that the production of pullulan in the OBR occurred much more rapidly with higher maximal concentration of pullulan than that in the STR. In addition, the quality of the product from the OBR is generally better, with a pullulan of higher molecular weight being elaborated. On the other hand the production of xanthan gum of the non-optimised OBR is at least equal to the traditional STR.

Two reasons could explain these differences in the production of these kinds of polysaccharides. Firstly, the morphology of both microorganisms is different. *X. campestris* is a single cell bacterium whereas *A. pullulans* is yeast-like fungus, therefore in the case of the STR, the baffles could trap the fungus during agitation which causes the accumulation of the microorganism on that area reducing the production of the polysaccharide but this does not occur in the OBR and therefore the production of pullulan is better in the OBR. Where in the case of xanthan, the baffles enhance the mixing; therefore, the production of xanthan in the STR is similar to that in the OBR. Secondly, xanthan has a high viscosity. It has been shown that the volume average shear rate in the OBR is generally of the order of 10-20 /s, which is significantly lower than that in the STR, where it is typically at least 100 /s or greater (Ni *et al*., 1999 b,c; 2000a). This feature of global mixing, coupled with very low and uniform shear rate is beneficial to the pullulan production but less advantageous for xanthan production where shear sensitive cultures may be involved.

5.7 Summary

This was first study of its kind, and the results indicate the positive potential of the OBR in the fermentation industry. Some improvements were recommended by the author resulted in reduced process variability need to be tested. This would make the OBR attractive to the biopolymer production industry.

Chapter 6

Conclusion and Recommendation

6 Conclusions

6.1 Conclusions

This thesis reports the first major experimental investigation into the application of an oscillatory baffled reactor (OBR) in comparison with the industrial housework fermenter the stirred tank reactor (STR) in the cultivation of xanthan gum. This work shows that there is scope for further optimisation of the OBR agitation and aeration systems. Each set of experiments provided information to better understand the cultivation of *X. campestris* ATCC 13951 in the reactors systems used. The major conclusions of this work are summarised as follows:

1. To inoculate *X. campestris* in YM medium the best C/N ratio is one, where glucose and yeast extract concentrations are equal at 4 g/l. This generated suitable inoculums in 24 hours at 30 °C at 200 rpm, and the optimum citric acid concentration in a synthetic medium for the production of xanthan gum is 2.0 g/l.
2. It was noticed that in uncontrolled pH fermentations, some organic acids produced in both STR and OBR were sometimes re-utilised.
3. In xanthan gum production in STR the production of xanthan gum was related to the aeration rate at lower agitation rate but not at the higher agitation rate.
4. Upward orientation sparger is better than downward orientation for the production of xanthan gum in the current geometry of the OBR.

5. Lower oscillation amplitude and high frequency with high aeration rate are the best combination for production of xanthan gum in the current geometry of the OBR.
6. In the STR the molecular weight and degree of branching of xanthan influenced by agitation and aeration rates.
7. Due to the viscosity and high molecular weight of xanthan gum there was a great challenge in the estimation of xanthan molecular weight. Poorest recovery occurred with lowest molecular weight and vice versa.
8. In xanthan gum production in OBR oscillation amplitude and frequency have an influence on produced xanthan molecular weight.
9. According to the equation applied in both systems STR and OBR the variety of impeller speeds and oscillation frequencies as set out show different power densities but these equations did not consider the aeration rate effect. In the OBR the oscillation amplitude is the main parameter that increases the power consumption in the OBR not the frequency.
10. The results of the study clearly indicate that the OBR is readily suitable for the cultivation of microorganisms for the synthesis of useful products with highly viscous polysaccharide and the performance of the non-optimised OBR is at least equal to the traditional STR.

6.2 Recommendations for future work

This work shows that there is a scope for optimisation of fermentation agitation and aeration with the constraints and was given a set of optimum production conditions for the production of xanthan gum in both STR and OBR.

During the study new questions arose and some problems were encountered which clearly needed further detailed study, which could form the basis of the recommendations for future studies. These include:

- In this study two wild type strains ATCC 13951 and ATCC 33913 (*X. campestris*) were used. Other strains should be studied, in particular genetically modified strains are highly recommended as well.
- Due to technical difficulties in controlling the pH in the OBR, all fermentation were done in uncontrolled pH condition, and the results showed that there were a significant effect of the operational condition on the pH profile during the fermentation time; Three recommendations arise from this:
    - To study the effect of the controlled pH fermentation on the production of xanthan gum in the OBR.
    - To examine the organic acids that were produced during biosynthesis of xanthan gum, including their re-uptake and utilisation.
    - To study the effect of the different operational conditions on the production of these organic acids.

- Many modifications have been done to the OBR in this study which had previously only been used to study low to moderate viscosity systems. But there are many more to add to improve the OBR function especially for the production of high viscous polysaccharides.
- Sparger orientation had a profound effect on the oxygen dispersion and therefore the production of xanthan in the OBR. Further studies to enhance sparger efficiency are important.
- Inserting multiple DO probes that will explain the oxygen profile in the reactor much better.
- In terms of molecular weight analysis the number of samples which could be processed was not enough to give a clear idea on the effect of the operational condition in OBR on xanthan molecular weight and the degree of branching, therefore more studies should be done in this area.
- The power density equations in both STR and OBR were describing the effect of agitation speed on the power consumption but not the aeration, therefore, the suggestion of new equation for the power density can be studied.
- The mechanism of xanthan production needs further study especially into the relationship between operational condition and molecular weight distribution. The factors affecting control of molecular weight in microbial polysaccharides are very poorly understood and this makes any systematic approach to manipulation of functional properties of such polymers very difficult. Such investigations are long overdue.

- The use of a novel magnetically coupled agitation system in the OBR should be investigated with viscous products. Such a coupling system would help reduce contamination.
- In the present study all the data were taken manually, the use of a programme to collect the data automatically is highly recommended for scanning the whole fermentation run.

References

7 References

Ahmann, D. (1997). Bioremediation of metal-contaminated soil. *Society for Industrial Microbiology News , 47*, 218–233.

Alves, S. S., Vasconcelos, J. M. (1996). Optimisation of agitation and aeration in fermenters. *Bioprocess and Biosystems Engineering , 14* (3), 119-123.

Amanullah, A., Carreon-Serrano, L., Galindo, E., Nienow, A. W. (1996). Reproducibility of pilot scale Xanthan fermentations. *Biotechnology Progress , 12*, 466-473.

Amanullah, A., Serrano-Carreon, L., Castro, B., Galindo, E., Nienow, A. (1998a). The Influence of Impeller Type in Pilot Scale Xanthan Fermentations. *Biotechnology and Bioengineering , 57* (1), 95-108.

Amanullah, A., Tuttiett, B., Nienow, A. W. (1998b). Agitator speed and dissolved oxygen effects in xanthan fermentations. *Biotechnology and Bioengineering , 57* (2), 198-210.

Atkinson, B., Mavituna, F. (1991). *Biochemical engineering and biotechnology handbook.* New York: Stockton Press.

Baird, J. K., Sandford, P. A., Cottrell, I. W. (1983). Industrial Applications of Some New Microbial Polysaccharides. *Biotechnology , 1*, 778 - 783.

Baird, M. H., Garstang, J. H. (1972). Gas absorption in a pulsed bubble column . *Chemical Engineering Science , 27* (4), 823-833.

Baird, M. H., Garstang, J. H. (1967). Power consumption and gas hold-up in a pulsed column. *Chemical Engineering Science , 22* (12), 1663-1673.

Baird, M. H., Rao, N. V., Prochazka, J., Sovova, H. (1994). Reciprocating Plate Columns. In M. J. Slater, J. Godfrey, *Solvent Extraction Equipment Design* (pp. 311-362). Chichester: Wiley.

Baradossi, G., Brant, D. A. (1982). Light scattering study of a series of xanthan fractions in aqueous solution. *Macromolecules , 15* (3), 874–879.

Barreras, M., Bianche, M. A., Ielpi, L. (2006). Crystallization and preliminary crystallographic characterization of GumK, a membrane-associated glucuronosyltransferase from *Xanthomonas campestris* required for xanthan

polysaccharide synthesis. *Acta Crystallographica Section F: Structural Biology and Crystallization Communications , 62* (9), 880–883.

Becker, A., Katzen, F., Pühler, A., Ielpi, L. (1998). Xanthan gum biosynthesis and application: a biochemical/genetic perspective. *Applied microbiology and biotechnology , 50* (2), 145-52.

Beeton, S., Millward, H. R., Bellhouse, B. J., Nicholson, A. M., Jenkins, N., Knowles, C. J. (1991). Gas transfer characteristics of a novel membrane bioreactor. *Biotechnology Bioengineering , 38* (10), 1233-1238.

Bellhouse, B. J., Bellhouse, F., Curl, C. M., MacMillan, T. I., Gunning, A. J., Spratt, E. H., *et al*. (1973). A high efficiency membrane oxygenator and pulsatile pumping system, and its application to animal trials. *Transactions - American Society for Artificial Internal Organs , 19*, 72-79.

Bindal, A., Narsimhan, G., Hem, S. L., Kulshreshtha, A. (2007). Structural changes in xanthan gum solutions during steam sterilisation for sterile preparations. *Pharmaceutical Development and Technology , 12* (2), 159-167.

Blanch, M., Legaz, M.-E., Vicente, C. (2008). Xanthan production by *Xanthomonas albilineans* infecting sugarcane stalks. *Journal of Plant Physiology , 165* (4), 366-374.

Booth, A. N., Hendrickson, A. P., DeEds, F. (1963). Physiologic effects of three microbial polysaccharides on rats. *Toxicology and Applied Pharmacology , 5* (4), 478-484.

Booth, A. N., Hendrickson, A. P., DeEds, F. (1968). *Rat feeding study of whole dried ferment containing polysaccharide B-1459 (xanthan gum).* Paris: Marinalg International.

Borges, C. D., da Moreira, A. S., Vendruscolo, C. T., Ayub, M. A. (2008). Influence of agitation and aeration in xanthan production by *Xanthomonas campestris pv. pruni* strain 101. *Revista Argentina de microbiología , 40* (2), 81-85.

Borges, C. D., M., d. P., Feitosa, J. P., Vendruscolo, C. T. (2009). The influence of thermal treatment and operational conditions on xanthan produced by X. arboricola pv pruni strain 106. *Carbohydrate Polymers , 75* (2), 262-268.

Born, K., Langendorff, V., Boulenguer, P. (2005). Xanthan. In A. Steinbuchel, S. K. Rhee, *Polysaccharides and Polyamides in the Food Industry: Properties, Production, and Patents* (pp. 259-291). London: Wiley.

Bradbury, J. (1984). Genus 11. *Xanthomonas*. In N. Krieg, J. Holt, *Bergey's manual of systematic bacteriology*, (Vol. 1, pp. 199-210). Baltimore.: The Williams Wilkins Co.

Bradshaw, I. J., Nisbet, B. A., Kerr, M. H., Sutherland, I. W. (1983). Modified xanthan its preparation and viscosity. *Carbohydrate Polymer , 3*, 23-38.

Bradshaw, J. F. (1987). A comparison of the poly(hexamethylenebiguanidinium chloride) assay and a neutral equivalent method for the determination of alginates in industrial liquors extracted from brown seaweed. *Carbohydrate Polymers , 7* (6), 409-419.

Bretschneider, K., Gonella, M., Robeson, D. (1989). A comparative light and electron microscopical study of compatible and incompatible interactions between *Xanthomonas campestris pv. campestris* and cabbage (Brassica oleracea). *Physiological and Molecular Plant Pathology , 34* (4), 285-297.

Brotherton, J., Chau, P. (1996). Modeling of Axial-Flow Hollow Fiber Cell Culture Bioreactors. *Biotechnology Progress , 12* (5), 575-590.

Brunold, C., Hunns, J., Mackley, M., Thompson, J. (1989). Experimental observations on flow patterns and energy losses for oscillatory flow in ducts containing sharp edges. *Chemical Engineering Science , 44* (5), 1227-1244.

Byong, H. L. (1996). *Fundamentals of food biotechnology.* New York: VCH .

Cadmus, M. C., Knutson, C. A., Lagoda, A. A., Pittsley, J. E., Burton, K. A. (1978). Synthetic media for production of quality xanthan gum in 20 liter fermentors. *Biotechnology and Bioengineering , 20* (7), 1003-1014.

Cadmus, M. C., Rogovin, S. P., Burton, K. A., Pittsley, J. E., Knutson, C. A., Jeanes, A. (1976). Colonial variation in *Xanthomonas campestris* NRRL B-1459 and characterization of the polysaccharide from a variant strain. *Canadian Journal of Microbiology , 22* (7), 942-948.

Callet, F., Milas, M., Rinaudo, M. (1987). Influence of acetyl and pyruvate contents on rheological properties of xanthan in dilute solution. *International Journal of Biological Macromolecules , 9*, 291–293.

Camesano, A. T., Wilkinson, K. J. (2001). Single molecule study of xanthan conformation using atomic force microscopy. *Biomacromolecules , 2* (4), 1184-1191.

Casasa, J. A., Santosa, V. E., Garcia-Ochoa, F. (2000). Xanthan gum production under several operational conditions: molecular structure and rheological properties. *Enzyme and Microbial Technology , 26*, 282-291.

Charles, M. (1985). Fermentation scale-up: Problems and possibilities. *Trends in Biotechnology , 3* (6), 134-139.

Chen, C., Huang, Y., Yang, S. (2002). A fibrous-bed bioreactor for continuous production of developmental endothelial locus-1 by osteosarcoma cells. *Journal of Biotechnology , 97* (1), 23-29.

Crescenzi, V., Dea, I., Paoletti, S. (1989). *Biomedical and biotechnological advances in industrial polysaccharides.* New York: Gordon and Breatch.

Crossman, L., Dow, J. (2004). Biofilm formation and dispersal in *Xanthomonas campestris*. *Microbes and Infection , 6* (6), 623-629.

Daniels, M. J., Leach, J. E. (1993). Genetics of *Xanthomonas*. In J. G. Swings, E. L. Civerolo, *Xanthomonas* (pp. 301–339). London: Chapman and Hall.

Davidson, I. W. (1978). Production of polysaccharide by *Xanthomonas campestris* in continuous culture. *FEMS Microbiology Letters , 3* (6), 347-349.

Dea, I. C., Morris, E. R., Reesa, D. A., Welsha, E. J., Barnes, H. A., Price, J. (1977). Associations of like and unlike polysaccharides: Mechanism and specificity in galactomannans, interacting bacterial polysaccharides, and related systems. *Carbohydrate Research , 57*, 249-272.

Demain, P., Souw, A. L. (1979). Nutritional Studies on Xanthan Production by *Xanthomonas campestris* NRRL B1459. *Applied and Environmental Microbiology , 37* (6), 1186–1192.

Dentini, M., Crescenzi, V., Blasi, D. (1984). Conformational properties of xanthan derivatives in dilute aqueous solution. *International Journal of Biological Macromolecules , 6* (2), 93-98.

Dickens, A., Mackley, M., Williams, H. (1989). Experimental residence time distribution measurements for unsteady flow in baffled tubes. *Chemical Engineering Science , 44* (7), 1471-1479.

Dintzis, F. R., Babcock, G. E., Tobin, R. (1970). Studies on dilute solutions and dispersion of the polysaccharide from *Xanthomonas campestris* NRRL B-1459. *Carbohydrate Research , 13* (2), 257-267.

Dow, J. M., Daniels, M. J. (1994). Pathogenicity determinants and global regulation of pathogenicity of *Xanthomonas campestris* pv. *campestris* . *Current Topics in Microbiology and Immunology , 192*, 29-41.

Dow, J., Crossman, L., Findlay, K., He, Y., Feng, J., Tang, J. (2003). Biofilm dispersal in *Xanthomonas campestris* is controlled by cell-cell signaling and is required for full virulence to plants. *Proceedings of the National Academy of Sciences of the United States of America. , 100* (19), 10995-1000.

Dreveton, E., Monot, F., Ballerini, D., Lecourtier, J., Choplin, L. (1996). Influence of fermentation hydrodynamics on gellan gum physico-chemical characteristics. *Journal of Fermentation and Bioengineering , 82* (3), 272-276.

Dunger, G., Relling, V. M., Tondo, M., Barreras, M., Ielpi, L., Orellano, E. G., *et al*. (2007). Xanthan is not essential for pathogenicity in citrus canker but contributes to *Xanthomonas* epiphytic survival. *Archives of Microbiology , 188* (2), 175-135.

Dye, D. W., Bradbury, J., Goto, M., Hayward, A. C., Lelliott, R. A., Schroth, M. N. (1980). International standards for naming pathovars of phytopathogenic bacteria and a list of pathovar names and pathotype strains. *Review of Plant Pathology , 59*, 153-168.

Easson, D. J., Peoples, O. P., Sinskey, A. J. (1987). Biopolymer engineering: genetic control of exopolysaccharide biosynthesis. In M. Yalpani, *Industrial Polysaccharides: Genetic Engineering, Structure/Property Relations and Applications* (pp. 57–64). Amsterdam:: Elsevier Science Publishers B.V.

Eastwood, M. A., Brydon, W. G., Anderson, D. M. (1986). The Dietary Effects of Xanthan Gum in Man. *Food Additives and Contaminants , 4* (1), 17-26.

El Enshasy, H., Then, C., Othman, N. Z., Al Homosany, H., Sabry, M., Sarmidi, M. R., et al. (2011). Enhanced xanthan production process in shake flasks and pilot scale bioreactors using industrial semidefined medium. *African Journal of Biotechnology , 10* (6), 1029-1038.

Elson, T. P. (1990). The growth of caverns formed around rotating impellers during the mixing of a yield stress fluid. *Chemical Engineering Communications , 96* (1), 303 – 319.

Elson, T. P., Cheesman, D. J., Nienow, A. W. (1988). Aspects of mixing rheologically complex fluids. *Chemical Engineering Research and Design , 66*, 5-15.

Elson, T. P., Cheesman, D. J., Nienow, A. W. (1986). X-ray studies of cavern sizes and mixing performance with fluids possessing a yield stress . *Chemical Engineering Science , 41* (10), 2555-2562.

Esgalhado, M. E., Roseiro, J. C., Collaço, M. T. (1995). Interactive Effects of pH and Temperature on Cell Growth and Polymer Production by *Xanthomonas campestris* . *Process Biochemistry , 30* (7), 667-671.

Etoc, A., Delvigne, F., Lecomte, J. P., Thonar, t. P. (2006). Foam control in fermentation bioprocess: from simple aeration tests to bioreactor. *Biotechnology and Applied Biochemistry , 129*, 392-404.

Evans, C. G., Yeo, R. G., Ellwood, D. C. (1978). Continuous culture studies on the production of extracellular polysaccharides by *Xanthomonas juglandis*. In R. C. Berkeley, G. W. Gooday, D. C. Ellwood, *Microbial Polysaccharides and Polysaccharases* (pp. 51-67). London: Academic Press.

Faria, S., Vieira, P. A., Resende, M. M., França, F. P., Cardoso, V. L. (2009). A Comparison Between Shaker and Bioreactor Performance Based on the Kinetic

Parameters of Xanthan Gum Production. *Applied Biochemistry and Biotechnology , 156* (1-3), 45-58.

Farmer, W. R., Liao, J. C. (1996). Progress in metabolic engineering. *Current Opinion in Biotechnology , 7*, 198-204.

Feng, Y., Heb, Z., Onga, S. L., Hua, J., Zhang, Z., Nga, W. J. (2003). Optimization of agitation, aeration, and temperature conditions for maximum β-mannanase production. *Enzyme and Microbial Technology , 32* (2), 282-289.

Fiedler, S., Behrens, U. (1984). Growth of *Xanthomonas campestris* and xanthan accumulation. *Allgemeine Mikrobiologie , 24*, 223-230.

Floresa, F., G, T. L., Galindo, G. (1994). Effect of the dissolved oxygen tension during cultivation of *X. campestris* on the production and quality of xanthan gum. *Journal of Biotechnology , 34* (2), 165-173.

Funahashi, H., Hirai, K. I., Yoshida, T., Taguchi, H. (1988a). Mechanistic analysis of xanthan gum production in a stirred tank . *Journal of Fermentation Technology , 66* (3), 355-364.

Funahashi, H., Hirai, K. I., Yoshida, T., Taguchi, H. (1988b). Mixing state of xanthan gum solution in an aerated and agitated fermentor—Effects of impeller size on volumes of mixing regions and circulation time distribution. *Journal of Fermentation Technology , 66* (1), 103-109.

Funahashi, H., Machara, M., Taguchi, H., Yoshida, T. (1987a). Effects of agitation by flat-bladed turbine impeller on microbial production of xanthan gum. *Journal of Chemical Engineering of Japan , 20* (1), 16-22.

Funahashi, H., Yoshida, T., Taguchi, H. (1987b). Effect of glucose concentrations on xanthan gum production by *Xanthomonas campestris . Journal of Fermentation Technology , 65* (5), 603-606.

Gaidhani, H. K. (2004). *An Experimental Investigation of Pullulan Fermentation in a Batch Oscillatory Baffled Fermenter.* Edinburgh: Heriot-Watt University.

Gaidhani, H. K., McNeil, B., Ni, X. (2005). Fermentation of Pullulan Using an Oscillatory Baffled Fermenter. *Chemical Engineering Research and Design , 83* (6), 640-645.

Galindo, E., Nienow, A. W. (1992). Mixing of highly viscous simulated xanthan fermentation broths with the Lightnin A-315 impeller. *Biotechnology Progress , 8* (3), 233-239.

Galindo, E., Nienow, A. W. (1993). Performance of the Scaba 6SRGT agitator in mixing of simulated Xanthan gum broths. *Chemical Engineering Technology , 16*, 102-108.

Gao, S., Ni, X., Cumming, R. H., Greated, C. A., Norman, P. (1998). Experimental Investigation of Bentonite Flocculation in a Batch Oscillatory Baffled Column . *Separation Science and Technology , 33* (14), 2143 - 2157.

Garcia-Ochoa, F., Santos, V. E., Fritsch, A. P. (1992). Nutritional study of *Xanthomonas campestris* in xanthan gum production by factorial design of experiments. *Enzyme and Microbial Technology , 14* (12), 991-996.

Garcia-Ochoa, F., and Gomez, E. (2009). Bioreactor scale-up and oxygen transfer rate in microbial processes : An overview. *Biotechnology advances , 27*, 153–176.

Garcia-Ochoa, F., Garcia-Leon, M. A., Romero, A. (1990). Kinetic modelling of xanthan production from sucrose. *Chemical and biochemical engineering quarterly , 4* (1), 15-20.

Garcia-Ochoa, F., Santosa, V. E., Casasb, J. A., Gómez, E. (2000). Xanthan gum: production, recovery, and properties. *Biotechnology Advances , 18* (7), 549-579.

Giavasis, I., Harvey, L. M., McNeil, B. (2006). The effect of agitation and aeration on the synthesis and molecular weight of gellan in batch cultures of Sphingomonas paucimobilis. *Enzyme and Microbial Technology , 38*, 101–108.

Gunning, A. P., McMaster, T. J., Morris, V. J. (1993). Scanning tunnelling microscopy of xanthan gum. *Carbohydrate Polymers , 21* (1), 47-51.

Harrison, S. T., Mackley, M. R. (1992). A pulsatile flow bioreactor. *Chemical Engineering Science , 47* (2), 490-493.

Hassler, A., Doherty, D. (1990). Genetic engineering of polysaccharide structure: production of variants of xanthan gum in *Xanthomonas campestris* . *Biotechnology Progress , 6* (3), 182-187.

Hayward, A. C. (1993). The host of *Xanthomonas*. In J. G. Swings, E. Civerolo, *Xanthomonas* (pp. 1-119). London: Chapman Hall.

Herbst, H., Peters, H. U., Suh, I. S., Schumpe, A., Deckwer, W. D. (1987). Monitoring xanthan quality during fermentation by size exclusion chromatography. *Biotechnology Techniques , 2* (2), 101-104.

Herbst, H., Schumpe, A., Deckwer, W. (1992). Xanthan production in stirred tank fermenters: Oxygen transfer and scale-up. *Chemical Engineering Technology , 15* (6), 425-434.

Hewgill, M., Mackley, M., Pandit, A., Pannu, S. (1993). Enhancement of gas-liquid mass transfer using oscillatory flow in a baffled tube . *Chemical Engineering Science , 48* (4), 799-809.

Ho, C. S., Oldshue, J. Y. (1988). *Biotechnology Processes: Scale-up and Mixing* (Vol. 4). USA: American Institute of Chemical Engineers (AIChE).

Hoefler, A. C. (2004). *Hydrocolloids.* Minnesota: Eagan Press.

Holzwarth, G. (1976). Conformation of the extracellular polysaccharide of *Xanthomonas campestris* . *Biochemistry , 15* (19), 4333-4339.

Holzwarth, G., Prestridge, E. B. (1977). Multistranded helix in xanthan polysaccharide. *Science , 197*, 757-759.

Howes, T. (1988). *On the Dispersion of Unsteady Flow in Baffled Tubes.* Cambridge: Cambridge Universirty.

Howes, T., Mackley, M. (1990). Experimental axial dispersion for oscillatory flow through a baffled tube . *Chemical Engineering Science , 45* (5), 1349-1358.

Howes, T., Mackley, M., Roberts, E. (1991). The simulation of chaotic mixing and dispersion for periodic flows in baffled channels . *Chemical Engineering Science , 46* (7), 1669-1677.

Hui, P. A., Neukom, H. (1964). Properties of galactomannans. *Tappi , 47*, 39–42.

Ielpi, L., Couso, R. O., Dankert, M. A. (1993). Sequential assembly and polymerization of the polyprenol-linked pentasaccharide repeating unit of the xanthan polysaccharide in *Xanthomonas campestris* . *Journal of Bacteriology , 175* (9), 2490-2500.

Ielpi, L., Couso, R., Dankert, M. (1981). Lipid-linked intermediates in the biosynthesis of xanthan gum. *FEBS Letters , 130*, 253-256.

Jana, A. K., Ghosh, P. (1997). Stimulation of xanthan production by *Xanthomonas campestris* using citric acid. *World Journal of Microbiology and Biotechnology , 13* (3), 261-264.

Jana, A. K., Ghosh, P. (1995). Xanthan biosynthesis in continuous culture: Citric acid as an energy source. *Journal of Fermentation and Bioengineering , 80* (5), 485-491.

Jana, A. K., Ghosh, P., Valadares-Inglis, M. C. (1999). Effect of citric acid on the biosynthesis and composition of xanthan. *The Journal of General and Applied Microbiology , 45* (3), 115-120.

Jarman, T. R., Pace, G. W. (1984). Energy requirements for microbial exopolysaccharide synthesis. *Archives of Microbiology , 137* (3), 231-235.

Jaworski, Z., Pacek, A. W., Nienow, A. W. (1994). On flow close to cavern boundaries in yield stress fluids. . *Chemical Engineering Science , 49* (19), 3321-3324.

Kalogiannis, S., Iakovidou, G., Kyriakides, M. L., Kyriakidis, D. A., Skaracis, G. N. (2003). Optimization of xanthan gum production by *Xanthomonas campestris* grown in molasses. *Process Biochemistry , 39* (2), 249-256.

Kang, K. S., Pettitt, D. J. (1992). Xanthan, Gellan, Wellan and Rhamsan. In R. L. Whistler, J. N. Bemiller, *Industrial gums: Polysaccharides and their derivatives* (pp. 341–397). New York: Academic Press.

Kang, X., Wang, H., Wang, Y., Harvey, L., McNeil, B. (2001). Hydrodynamic characteristics and mixing behaviour of *Sclerotium glucanicum* culture fluids in an airlift reactor with an internal loop used for scleroglucan production. *Journal of Industrial Microbiology and Biotechnology , 27* (4), 208-214.

Kang, Y., Cho, Y. J., Woo, K. J., Kim, K. I., Kim, S. D. (2000). Bubble properties and pressure fluctuations in pressurized bubble columns. *Chemical Engineering Science , 55* (2), 411-419.

Kapat, A., Jung, J. K., Park, Y. H., Hong, S. Y., Choi, H. K. (1998). Effects of agitation and aeration on the production of extracellular glucose oxidase from a recombinant *Saccharomyces cerevisiae*. *Bioprocess and Biosystems Engineering , 18* (5), 347-351.

Karr, A. (1959). Performance of a Reciprocating-Plate Extraction Column. *AIChE Journal , 5* (4), 446-452.

Katzen, F., Ferreiro, D. U., Oddo, C. G., Ielmini, M. V., Becker, A., Pühler, A., *et al*. (1998). *Xanthomonas campestris* pv. *campestris* gum Mutants: Effects on Xanthan Biosynthesis and Plant Virulence. *Journal of Bacteriology , 180* (7), 1607-1617.

Kennard, M., Janekeh, M. (1991). Two- and three-phase mixing in a concentric draft tube gas-lift fermentor. *Biotechnology and Bioengineering , 38* (11), 1261–1270.

Kennedy, J. F., Bradshaw, I. J. (1987). A comparison of the poly (hexamethylenebiguanidinium chloride) assay and a neutral equivalent method for the determination of alginates in industrial liquors extracted from brown seaweed. *Carbohydrate Polymers , 7* (6), 409-419.

Kennedy, J. F., Bradshaw, I. J. (1984). Production, properties and applications of xanthan. *Progress in Industrial Microbiology , 19*, 319–371.

Kennedy, J. F., Jones, P., A., B. S., Banks, G. T. (1982). Factors affecting microbial growth and polysaccharide production during the fermentation of *Xanthomonas campestris* cultures. *Enzyme and Microbial Technology , 4* (1), 39-43.

Kiosseoglou, A., Papalamprou, E., Makri, E., Doxastakis, G., Kiosseoglou, V. (2003). Functionality of medium molecular weight xanthan gum produced by *Xanthomonas Campestris* ATCC 1395 in batch culture. *Food Research International , 36* (5), 425-430.

Kuboi, R., and Nienow, A. (1986). Intervortex mixing rates in high viscosity liquids agitated by high speed dual impellers. *Chemical Engineering Science , 41*, 123-134.

Lasko, D. R., Schwerdel, C., Bailey, J. E., Sauer, U. (1997). Acetate-specific stress response in acetate-resistant bacteria: an analysis of protein patterns. *Biotechnology Progress , 13* (5), 519-523.

Leach, J. G., Lilly, V., Wilson, H. A., Purvis, M. R. (1957). Bacterial polysaccharides: the nature and function of the exudate produced by *Xanthomonas phaseoli*. *Phytopathology , 47*, 113-120.

Lee, B. H. (1996). *Fundamentals of food biotechnology*. New York: VCH.

Lee, P. K., Chang, H. N., Kim, B. H. (1989). Xanthan production by*Xanthomonas campestris* in continuous fermentation. *Biotechnology Letters , 11* (8), 573-578.

Leela, J. K., Sharma, G. (2000). Studies on xanthan production from *Xanthomonas campestris* . *Bioprocess and Biosystems Engineering , 23* (6), 687-689.

Leib, T. M., Pereiraa, C. J., Villadsen, J. (2001). Bioreactors: a chemical engineering perspective. *Chemical Engineering Science , 56* (19), 5485-5497.

Leigh, J. A., Coplin, D. L. (1992). Exopolysaccharides in Plant-Bacterial Interactions. *Annual Review of Microbiology , 46*, 307-346.

Letisse, F., Chevallereau, P., Simon, J. L., Lindley, N. D. (2001). Kinetic analysis of growth and xanthan gum production with *Xanthomonas campestris* on sucrose, using sequentially consumed nitrogen sources. *Applied Microbiology and Biotechnology , 55* (4), 417-422.

Leyns, F., DeCleene, M., Swings, J. G., Deley, J. (1984). The host range of the genus *Xanthomonas*. *The Botanical Review , 50* (3), 308-356.

Li, H., Rief, M., Oesterhelt, F., Gaub, H. E. (1999). Force spectroscopy on single xanthan molecules. *Applied Physics A: Materials Science Processing , 68* (4), 407-410.

Lilly, V. G., Wilson, H. A., Leach, J. G. (1958). Bacterial polysaccharides. II. Laboratory-scale production of Polysaccharides by Species of *Xanthomonas*. *Applied and Environmental Microbiology , 6*, 105-108.

Liu, L., Wang, M., Sun, J., Du, G., Chenb, J. (2010). Application of a novel cavern volume controlled culture model to microbial hyaluronic acid production by batch

culture of Streptococcus zooepidemicus. *Biochemical Engineering Journal , 48* (2), 141-147.

Liu, S., Ni, X., Greated, C., Fruer, P. (1995). Measurements of velocities of single particles for steady and oscillatory flows in plain and baffled tubes. *the Chemical Engineering Research and Design , 73*, 727-732.

Lo, T., Prochazka, J. (1983). Reciprocating Plate Extraction Columns. In H. o. Extraction, *Lo, T. C.; Baird, M. H. I.; Hanson, C.* (pp. 373-389). New York: Wiley Interscience.

Lo, Y.-M., Yang, S.-t., and Min, D. B. (1997). Effects of yeast extract and glucose on xanthan production and cell growth in batch culture of *Xanthomonas campestris. Applied Microbiology Biotechnology* , 689-694.

Liu, L., Wang, M., Sun, J., Du, G., Chenb, J. (2010). Application of a novel cavern volume controlled culture model to microbial hyaluronic acid production by batch culture of Streptococcus zooepidemicus. *Biochemical Engineering Journal , 48* (2), 141-147.

Luli, G. W., Strohl, W. R. (1990). Comparison of growth, acetate production, and acetate inhibition of *Escherichia coli* strains in batch and fed-batch fermentations. *Applied and Environmental Microbiology , 56* (4), 1004-1011.

Mackley, M. (1991). Process innovation using oscillatory flow within baffled tubes. *Chemical engineering research design , 69*, 197-199.

Mackley, M. R., Stonestreet, P. (1995). Heat transfer and associated energy dissipation for oscillatory flow in baffled tubes. *Chemical Engineering Science , 50* (14), 2211-2224.

Mackley, M., Ni, X. (1993). Experimental fluid dispersion measurements in periodic baffled tube arrays. *Chemical Engineering Science , 48* (18), 3293-3305.

Mackley, M., Ni, X. (1991). Mixing and dispersion in a baffled tube for steady laminar and pulsatile flow . *Chemical Engineering Science , 46* (12), 3139-3151.

Mackley, M., Smith, K., Wise, N. (1993). The mixing and separation of particle suspensions using oscillatory flow in baffled tubes. *Chemical engineering research design , 71*, 649-656.

Mackley, M., Tweddle, G., Wyatt, I. (1990). Experimental heat transfer measurements for pulsatile flow in baffled tubes. *Chemical Engineering Science , 45* (5), 1237-1242.

Marudova-Zsivanovits, M., Jilov, N., Gencheva, E. (2006). Rheological investigation of xanthan gum–chromium gelation and its relation to enhanced oil recovery. *Journal of Applied Polymer Science , 103* (1), 160-166.

Matsuda, Y., Biyajima, Y., Sato, T. (2009). Thermal Denaturation, Renaturation, and Aggregation of a Double-Helical Polysaccharide Xanthan in Aqueous Solution. *Polymer Journal , 41*, 526–532.

McLean, J. . (2001). Chromate reduction by a pseudomonad isolated from a site contaminated with chromated copper arsenate. *Applied and Environmental Microbiology , 67*, 1076–1084.

Milas, M., Rinaudo, M. (1984). On the existence of two different secondary structures for the xanthan in aqueous solutions. *Polymer Bulletin , 12*, 507-514.

Milas, M., Rinaudo, M. (1986). Properties of xanthan gum in aqueous solutions: Role of the conformational transition. *Carbohydrate Research , 158*, 191-204.

Milas, M., Rinaudo, M., Tinland, B. (1985). The viscosity dependence on concentration, molecular weight and shear rate of xanthan solutions. *Polymer Bulletin , 14* (2), 157-164.

Milas, M., Rinaudo, M., Tinland, B., Murcia. (1988). Evidence for a single stranded xanthan chain by electron microscopy. *Polymer Bulletin , 19*, 567-572.

Milas, M., Rinaudo, M. (1979). Conformational investigation on the bacterial polysaccharide xanthan. *Carbohydrate Research , 76* (1), 189-196.

Misra, T. K., Barnett, S. M. (1987). Evaluation of a Novel Foam Fermentor in the Production of Xanthan Gum. *Biotechnology Processes* , 227-237.

Moorhouse, R., Walkinshaw, M. D., Arnott, S. (1977). Xanthan gum-molecular conformation and interactions In P. A. Sandford, *Extracellular Microbial Polysaccharides* (pp. 90–102). Washington: American Chemical Society.

Moo-Young, M. (1985). *Comprehensive biotechnology* (pp. 1005-1041). Oxford: Pergamon Press .

Moraine, R. A., Rogovin, R. (1973). Kinetics of the xanthan fermentation. *Biotechnology and Bioengineering , 15* (2), 225-237.

Morris, E. R. (1995). Polysaccharide rheology and in mouth perception. In P. A. Williams, G. O. Philips, A. M. Stephen, *Food Polysaccharides and Their Applications* (pp. 517-546). New York: Marcel Dekker.

Morris, E. R. (1996). Polysaccharide synergism - more questions than answers. In S. E. Harding, S. E. Hill, J. R. Mitchell, *Biopolymer Mixtures* (pp. 247-288). Nottingham: Nottingham University Press.

Morrisa, E. R., Cutlera, A. N., Ross-Murphya, S. B., Reesa, D. A., Priceb, J. (1981). Concentration and shear rate dependence of viscosity in random coil polysaccharide solutions. *Carbohydrate Polymers , 1* (1), 5-21.

Morrisa, E. R., Reesa, D. A., Younga, G., Walkinshawa, M. D. (1977). Order-disorder transition for a bacterial polysaccharide in solution. A role for polysaccharide conformation in recognition between *Xanthomonas* pathogen and its plant host. *Journal of Molecular Biology , 110* (1), 1-16.

Mullera, G., Aurhourrachea, M., Lecourtierb, J., Chauveteau, G. (1986). Salt dependence of the conformation of a single-stranded xanthan. *International Journal of Biological Macromolecules , 8* (3), 167-172.

Nasr, S., Soudi, M. R., Haghighi, M. (2007). Xanthan production by a native strain of *X. campestris* and evaluation of application in EOR. *Pakistan Journal of Biological Sciences , 10* (17), 3010-3013.

Ni, X. (1994). Residence time distribution measurements in a pulsed baffled tube bundle. *Journal of Chemical Technology Biotechnology , 59* (3), 213-221.

Ni, X., Gao, S. (1996). Scale-up correlation for mass transfer coefficients in pulsed baffled reactors. *The Chemical Engineering Journal and the Biochemical Engineering Journal , 63* (3), 157-166.

Ni, X., Gough, P. (1997). On the discussion of the dimensionless groups governing oscillatory flow in a baffled tube. *Chemical Engineering Science , 52* (18), 3209-3212.

Ni, X., Mackley, M. (1993). Chemical reaction in batch pulsatile flow and stirred tank reactors. *The Chemical Engineering Journal , 52* (3), 107-114.

Ni, X., Pereira, N. (2000). Parameters affecting fluid dispersion in a continuous oscillatory baffled tube. *AIChE Journal , 46* (1), 37–45.

Ni, X., Cosgrovea, J. A., Arnottb, A. D., Greatedb, C. A., Cumming, R. H. (2000). On the measurement of strain rate in an oscillatory baffled column using particle image velocimetry. *Chemical Engineering Science , 55* (16), 3195-3208.

Ni, X., Gao, S., Pritchard, D. (1995). A study of mass transfer in yeast in a pulsed baffled bioreactor. *Biotechnology and bioengineering , 45* (2), 165-75.

Ni, X., Gao, S., Cumming, R. H., Pritchard, D. W. (1995). A comparative study of mass transfer in yeast for a batch pulsed baffled bioreactor and a stirred tank fermenter . *Chemical Engineering Science , 50* (13), 2127-2136.

Ni, X., Jian, H., Fitch, A. W. (2002). Computational fluid dynamic modelling of flow patterns in an oscillatory baffled column . *Chemical Engineering Science , 57* (14), 2849-2862.

Ni, X., Liu, S., Grewal, P., Greated, C. (1995). A study of velocity vector profile anf strain rate distribution for laminar and oscillatory flows in a baffled tube using particle image velocimetry . *Journal of Flow Visualization and image Processing* , 135-147.

Ni, X., Zhang, Y., Mustafa, I. (1998). An investigation of droplet size and size distribution in methylmethacrylate suspensions in a batch oscillatory-baffled reactor. *Chemical Engineering Science , 53* (16), 2903-2919.

Ni, X., Zhang, Y., Mustafa, I. (1999). Correlation of polymer particle size with droplet size in suspension polymerisation of methylmethacrylate in a batch oscillatory-baffled reactor. *Chemical Engineering Science , 54* (6), 841-850.

Nienow, A. (1984). Mixing studies on high viscosity fermentation processes xanthan gums. *The World Biotechnology Report , 1*, 293-304.

Nienow, A. W., Elson, T. P. (1988). Aspects of mixing in rheologically complex fluids. *Chemical Engineering Research and Design , 66*, 5-15.

Nienow, A. W., Miles, D. (1969). A dynamometer for the accurate measurement of mixing torque. *Journal of Physics E: Scientific Instruments , 2* (11), 994-995.

Nienow, A., Wisdom, D., Solomon, J., Machon, V., Vlcek, J. (1983). The effect of rheological complexities on power consumption in an aerated, agitated vessel. *Chemical Engineering Communications , 19* (4-6), 273 – 293.

Norton, I. T., Goodall, D. M., Frangou, S. A., Morris, E. R., Rees, D. A. (1987). Effects of agitation by flat -bladed turbine impeller on microbial production of xanthan gum. *Journal of Chemical Engineering of Japan , 20*, 16-22.

Norton, I. T., Goodall, D., Frangou, S., Morris, E., Rees, D. A. (1984). Mechanism and dynamics of conformational ordering in xanthan polysaccharide. *Journal of Molecular Biology , 175* (3), 371-394.

Oldshue, J. Y. (1960). Fluid mixing in fermentation processes. *Journal of Industrial and Engineering Chemistry , 52*, 60-62.

Oliveira, M. S., Ni, X.-W. (2004). Effect of hydrodynamics on mass transfer in a gas–liquid oscillatory baffled column. *Chemical Engineering Journal , 99* (1), 59-68.

Paoletti, S., Cesaro, A., Delben, F. (1983). Thermally induced conformational transition of xanthan polysaccharide. *Carbohydrate Research , 123*, 173-178.

Papagianni, M., Nokes, S. E., Filer, K. (2001). Submerged and Solid-State Phytase Fermentation by *Aspergillus niger*: Effects of Agitation and Medium Viscosity on Phytase Production, Fungal Morphology and Inoculum Performance. *Food Technology and Biotechnology , 39* (4), 319–326.

Papagianni, M., Psomas, S. K., Batsilas, L., Paras, S. V., Kyriakidis, D. A., Liakopoulou-Kyriakides, M. (2001). Xanthan production by *Xanthomonas campestris* in batch cultures. *Process Biochemistry , 37* (1), 73-80.

Paradossi, G., Brant, D. B. (1982). Light scattering study of a series of xanthan fractions in aqueous solution. *Macromolecules , 15* (3), 874-879.

Patton, J., Dugar, S. (1981). Growth kinetics of *Xanthomonas campestris* . B-1459. *Process Biochemistry , 33*, 46-49.

Peters, H. U., Herbst, H., Heselink, P. G., Lunsdorf, H., Schumpe, A., Deckwer, W. (1989). The influence of agitation rate on Xanthan production by *Xanthomonas campestris* . *Biotechnology and Bioengineering , 34*, 1393-1397.

Peters, H. U., Suh, I. S., Schumpe, A., Deckwer, W. D. (1992). Modeling of batchwise xanthan production. *The Canadian Journal of Chemical Engineering , 70* (4), 742-750.

Petersen, G. I., Nelson, G. A., Cathey, C. A., Fuller, G. G. (1989). Rheologically interesting polysaccharides from yeasts. *Applied Biochemistry and Biotechnology , 20*, 845–867.

Pinches, A., Pallent, L. J. (1986). Rate and yield relationships in the production of xanthan gum by batch fermentations using complex and chemically defined growth media. *Biotechnology and Bioengineering , 28*, 1484-1496.

Pollock, T., Mikolajczak, M., Yamazaki, M., Thorne, L. and Armentrout, R. (1997). Production of xanrthan gum by Sphingomonas Bacteria crrying genes from Xanthomonas campestris. *The Journal of Industrial Microbiology and Biotechnology , 19*, 92-97.

Poplawsky, A. R., Urban, S. C., Chun, W. (2000). Biological Role of Xanthomonadin Pigments in *Xanthomonas campestris* pv. *Campestris* . *Applied and Environmental Microbiology , 66* (12), 5123-5127.

Popovic, M. K., Robinson, C. W. (1993). Mixing characteristics of external-loop airlifts: non-Newtonian systems. *Chemical Engineering Science , 48* (8), 1405-1413.

Rajagopal, L., Sundari, C., Balasubramanian, D., Sonti, R. (1997). The bacterial pigment xanthomonadin offers protection against photodamage. *FEBS Letters , 415* (2), 125-128.

Rajeshwari, R., Sonti, R. (2000). Stationary-Phase Variation Due to Transposition of Novel Insertion Elements in *Xanthomonas oryzae* pv . *oryzae*. *Journal of Bacteriology , 182* (17), 4797-4802.

Rinaudo, M. (2004). Role of Substituents on the Properties of Some Polysaccharides. *Biomacromolecules , 5* (4), 1155-1165.

Rochefort, W. E., Middleman, S. (1987). Rheology of xanthan gum: salt, temperature, and strain effects in oscillatory and steady shear experiments. *Journal of Rheology , 31* (4), 337-369.

Rodriguez, H. and Aguilar, L. (1997). Detection of Xanthomonas campestris mutants with increased xanthan production. *The Journal of Industrial Microbiology and Biotechnology , 18*, 232-234.

Rogovin, S. P., Anderson, R. F., Cadmus, M. C. (1961). Production of Polysaccharide with *Xanthomonas campestris* . *Journal of Biochemical and Microbiological Technology and Engineering , 3* (1), 51-68.

Rosalam, S., England, R. (2006). Review of xanthan gum production from unmodified starches by *Xanthomonas campestris* . *Enzyme and Microbial Technology , 39*, 197–207.

Rossi, G. (2001). The design of bioreactors. *Hydrometallurgy , 59* (2), 217-231.

Roux, M., Sarret, G., Pignot-Pointrand, I., Fontecave, M., Coves, J. (2001). Mobilization of selenite by Ralstonia metallidurans CH34. *Applied and Environmental Microbiology , 67*, 769–773.

Rushton, J. H., Costich, E. W., Everett, H. J. (1950). Power characteristics of mixing impellers. *Chemical Engineering Progress , 46* (8), 395–476.

Saeed, S., Ein-Mozaffari, F. (2008). Using dynamic tests to study the continuous mixing of xanthan gum solutions. *Journal of Chemical Technology and Biotechnology , 83*, 559-568.

Sanderson, G. R. (1981). Applications of Xanthan gum. *British Polymer Journal , 13* (2), 71-75.

Sandford, P. A., Cottrell, I. W., Pettitt, D. J. (1984). Microbial polysaccharides: new products and commercial applications. *Pure and Applied Chemistry , 56*, 879–892.

Sato, T., Norisuye, T., Fujita, H. (1984). Double-stranded helix of xanthan: dimensional and hydrodynamic properties in 0.1 M aqueous sodium chloride. *Macromolecules , 17* (12), 2696–2700.

Schweickart, R. W., Quinlan, A. V. (1989). Kinetics of xanthan production when NH3-N limits biomass synthesis and glucose limits polysaccharide synthesis. *Journal of Biomechanical Engineering , 111* (2), 166-172.

Scragg, A. (1991). *Bioreactors In Biotechnology: A Practical Approach* . Ellis Horwood Ltd.

Serieys, M., Goma, G., Durand, G. (1978). Design and Oxygen-Transfer Potential of a Pulsed Continuous Tubular Fermentor. *Biotechnology and Bioengineering , 20*, 1393-1406.

Suh, C. H., Yang, S. T. (1990). Effects of temperature on cell-growth and xanthan production in batch cultures of *Xanthomonas campestris* . *Biotechnology and Bioengineering , 35*, 454-468.

Suh, C.-H., Yang, S.-T. (1991). Kinetics and modeling of temperature effects on batch xanthan gum fermentation. *Biotechnology and Bioengineering , 37* (6), 567-574.

Suh, I.-S., Schumpe, A., Deckwer, W.-D. (1992). Xanthan Production in Bubble Column and Air-Lift Reactors. *Biotechnology and Bioengineering , 39*, 85-94.

Silman, R. W., Rogovin, P. (1970). Continuous fermentation to produce xanthan biopolymer: Laboratory investigation. *Biotechnology and Bioengineerig , 12* (1), 75-84.

Singh, V., Fuchs, R., Hensler, W., Constantinides, A. (1990). Scaleup and Optimization of Oxygen Transfer in Fermentors Newtonian and Non-Newtonian Systems. *Biochemical Engineering , 589*, 616-641.

Slodki, M. E., Cadmus, M. C. (1978). Production of microbial polysaccharides. *Advances in Applied Microbiology , 23*, 19-54.

Smith, H. I., Symes, K. C., Lawson, C. J., Morris, E. R. (1981). Influence of the pyruvate content of xanthan on macromolecular association in solution. *International Journal of Biological Macromolecules , 3* (2), 129-134.

Smith, I. H., Pace, G. W. (1982). Recovery of microbial polysaccharides. *Journal of Chemical Technology and Biotechnology , 32* (1), 119-129.

Smitha, I. H., Symesa, K. C., Lawsona, C. J., Morrisb, E. R. (1981). Influence of the pyruvate content of xanthan on macromolecular association in solution. *International Journal of Biological Macromolecules , 3* (2), 129-134.

Solomon, J., Elson, T. P., Nienow, A. W., Pace, G. W. (1981). Cavern sizes in agitated fluids with a yield stress. . *Chemical Engineering Communications , 11* (1-3), 143 – 164.

Souw, P., Demain, A. L. (1979). Nutritional Studies on Xanthan Production by *Xanthomonas campestris* NRRL B1459. *Applied and Environmental Microbiology , 37*, 1186-1192.

Souw, P., Demain, A. (1980). Role of citrate in xanthan production by *Xanthomonas campestris* . *Fermentation Technology , 58* (5), 411-416.

Starr, M., Jenkins, C., Bussey, L., Andrewes, A. (1977). Chemotaxonomic significance of the xanthomonadins, novel brominated aryl-polyene pigments produced by bacteria of the genus *Xanthomonas*. *Archives of microbiology , 113* (1-2), 1-9.

Steinbuchel, A., Rhee, S. K. (2005). *Polysaccharides and Polyamides in the Food Industry.* Weinheim: Wiley.

Stephen, A. M., Phillips, G. O., Williams, P. A. (2006). *Food Polysaccharides and Their Applications.* New York: Marcel Dekker.

Stokke, B. T., Elgsaeter, A., Smidsrod, O. (1986). Electron microscopic study of single-and double-stranded xanthan. *International Journal of Biological Macromolecules , 8* (4), 217-225.

Su, L., Ji, W. J., Lan, W. Z., Dong, X. Q. (2003). Chemical modification of xanthan gum to increase dissolution rate. *Carbohydrate Polymers , 53* (4), 497-499.

Sutherland, I. W. (1977b). Bacterial exopolysaccharide their nature and production. In I. W. Sutherland, *Surface carbohydrates of the prokaryotic cell* (pp. 27-96). London: Academic Press.

Sutherland, I. W. (1990). *Biotechnology of Microbial Exopolysaccharides.* Cambridge: Cambridge University Press.

Sutherland, I. W. (1977a). Microbial Exopolysaccharide Synthesis. In P. A. Sandford, A. Laskin, *Extracellular Microbial Polysaccharides* (pp. 40-57). Washington: American Chemical Society.

Sutherland, I. W. (2001). Microbial polysaccharides from Gram -negative bacteria. *International Dairy Journal , 11* (9), 663-674.

Sutherland, I. W. (1993). Xanthan. In J. G. Swings, E. Civerolo, *Xanthomonas* (pp. 363-388). London: Chapman Hall.

Tait, M. I., Sutherland, I. W., Clarke-Sturman, A. J. (1986). Effect of Growth Conditions on the Production, Composition and Viscosity of *Xanthomonas campestris* Exopolysaccharide. *Journal of General Microbiology , 132*, 1483-1492.

Tako, M., Namawa, S. (1989). Evidence of intracellular association in xanthan molecule in aqueous media. *Agricultural Biological Chemistry* , 1941-1946.

Tang, J., Liu, Y., Barber, C., Dow, J., Wootton, J., Daniels, M. (1991). Genetic and molecular analysis of a cluster of rpf genes involved in positive regulation of synthesis of extracellular enzymes and polysaccharide in Xanthomonas campestris pathovar campestris. *Molecular and General Genetics, 226*, 409–417.

Tako, M., Nakamura, S. (1985). Synergistic interaction between xanthan and guar gum. *Carbohydrate Research , 138* (2), 207-213.

Techapuna, C., Poosarana, N., Watanabeb, M., Sasaki, K. (2003). Optimization of aeration and agitation rates to improve cellulase-free xylanase production by thermotolerant Streptomyces sp. Ab106 and repeated fed-batch cultivation using agricultural waste. *Journal of Bioscience and Bioengineering , 95* (3), 2981-2301.

Therkelsen, G. H. (1995). Carrageenan. In R. L. Whistler, J. N. BeMiller, *Industrial gums. Polysaccharides and their Drerivatives* (pp. 145-180). San Diego: Academic Press.

Van den Mooter, M., Swings, J., Gossele, F., Kersters, K., De Ley, J. (1987). The taxonomy of *Xanthomonas* Dowson. In E. Civerolo, A. Collmer, R. Davis, A. Gillaspie, *Plant pathogenic bacteria* (pp. 795-796). Boston: Martinus Nijhoff.

Van Dijck, W. (1935). *Patent No. 2011186.* US.

Vant Riet, S.,and Smith, J. (1975). The trailing vortex system produced by Rushton turbine agitators. *Chemical Engineering Science , 30*, 1093-1105.

Vant Riet, K., Tramper, J. (1991). *Basic bioreactor design.* New York: Marcel Dekker.

Vashitz, O., Sheintuch, M. (1991). Analysis of polymer synthesis rates during steady state growth of *X. comprestris. Biotechnology and Bioengineering , 37*, 383-385.

Vojnov, A. Zorreguieta, A., Dow, J., Daniels, M., Dankert, M. (1998). Evidence for a role for the gumB and gumC gene products in the formation of xanthan from its pentasaccharide repeating unit by Xanthomonas campestris. *Microbiology, 144*, 1487–1493

Vorholter, F. J., Schneiker, S., Goesmann, A., Krause, L., Bekel, T., Kaiser, O., *et al*. (2008). The genome of *Xanthomonas campestris* pv . *campestris* B100 and its use for the reconstruction of metabolic pathways involved in xanthan biosynthesis. *Journal of Biotechnology , 134* (1-2), 33-45.

Voulgaris, I., Arnold, S. A., Speight, R., Harvey, L., McNeil, B. (2010). Effects of dissolved oxygen availability and culture biomass at induction upon the intracellular expression of monoamine oxidase by recombinant *E. coli* in fed batch bioprocesses . *Process Biochemistry* , Article in Press, Corrected Proof .

Vuyst, L. D., Loo, J. V., Vandamme, E. (1987). Two-step fermentation process for improved xanthan production by *Xanthomonas campestris* NRRL-B-1459. *Journal of Chemical Technology Biotechnology , 39* (4), 263-273.

Vuyst, L. D., Vermeire, A., Loo, J. V., Vandamme, E. (1987a). Nutritional, physiological and process-technological improvements of the xanthan fermentation

process. *Mededelingen van de Faculteit Landbouwwetenschappen Rijksuniversiteit Gent , 52* (4), 1881-1900.

Wang, Y., McNeil, B. (1992). A study of gas hold-up, liquid velocity, and mixing time in a complex high viscosity, fermentation fluid in an airlift bioreactor. *Chemical Engineering Technology , 19* (2), 143–153.

Weiss, R. M., Ollis, D. F. (1980). Extracellular Microbial Polysaccharides.I. Substrate, Biomass, and Product Kinetic Equations for Batch Xanthan Gum Fermentation. *Biotechnology and Bioengineering , 22*, 859-873.

Wernau, W. C. (1981). *Patent No. 4282321* . U.S.

Whitfield, C. (1988). Bacterial extracellular polysaccharides. *Canadian Journal of Microbiology , 34*, 415-420.

Whitfield, C., Sutherland, I. W., Cripps, R. E. (1982). Glucose Metabolism in *Xanthomonas campestris* . *Journal of General Microbiology , 128* (5), 981-985.

Whitman, W. G. (1923). Preliminary experimental confirmation of the two-film theory of gas absorption. *Chemical and Metallurgical Engineering , 29*, 146-148.

Wisdoma, J., D., Solomon, J., Machonb, V., *et al*. (1983). The effect of rheological complexities on power consumption in an aerated, agitated vessel. *Chemical Engineering Communications , 19*, 273-293.

Woiciechowski, A. L., Soccol, C. R., Rocha, S. N., Pandey, A. (2004). Xanthan gum production from cassava bagasse hydrolysate with *Xanthomonas campestris* using alternative sources of nitrogen. *Applied Biochemistry and Biotechnology , 118*, 305-312.

Wolfe, A. J. (2005). The acetate switch. *Microbiology and Molecular Biology Reviews , 69* (1), 12-50.

Yang, S., Lo, Y. M., Min, D. (1996). Xanthan Gum Fermentation by *Xanthomonas campestris* Immobilized in a Novel Centrifugal Fibrous-Bed Bioreactor. *Biotechnology Progress , 12* (5), 630-637.

Yoshida, T., Tanner, R. D. (1993). *Bioproducts and bioprocess* (Vol. 2). Berlin: Springer-Verlag.

Zaidi, A., Ghosh, P., Schumpe, A., Deckwer, W. (1991). Xanthan production in a plunging jet reactor. *Applied Microbiology Biotechnology , 35*, 330-333.

Zhang, J., Greasham, R. (1999). Chemically defined media for commercial fermentations. *Applied microbiology and biotechnology , 51* (4), 407-421.

Zhang, Z., Chen, H. (2010). Fermentation Performance and Structure Characteristics of Xanthan Produced by *Xanthomonas campestris* with a Glucose/Xylose Mixture. *Applied Biochemistry and Biotechnology , 160* (6), 1653-1663.

Zhao, X., Zongding, H., Nienow, A. W., Kent, C. A., Chatwin, S. (1994). Rheological characteristics, power consumption, mass and heat transfer during Xanthan gum fermentation. *The Chinese Journal of Chemical Engineering , 2* (4), 198-209.

Appendix

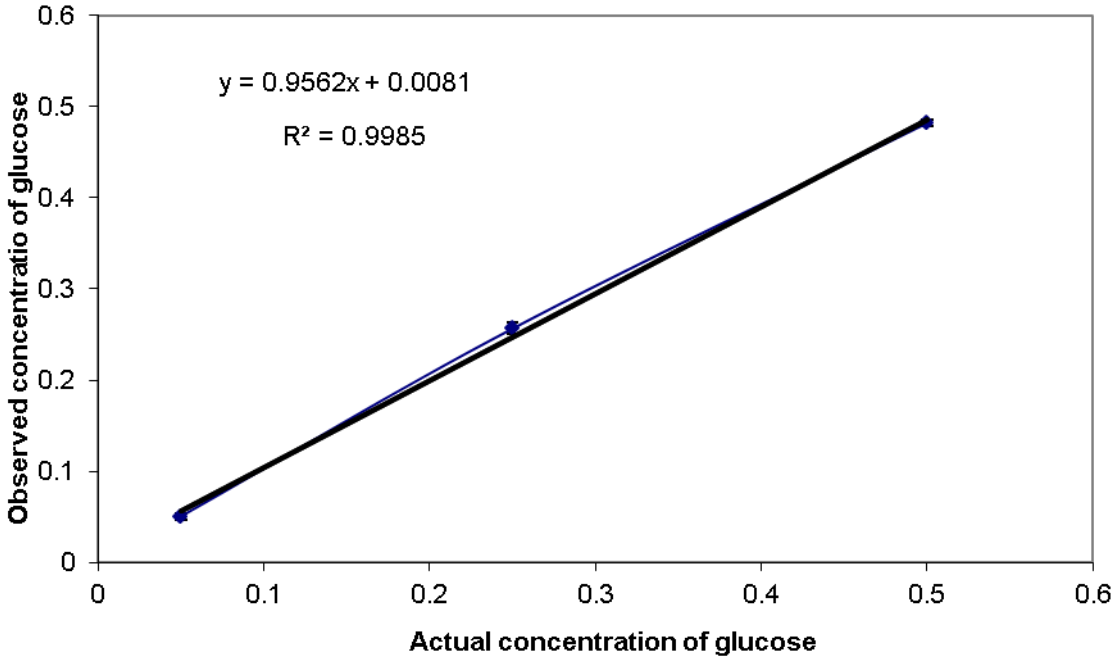

Figure I: Calibration curve for the estimation of Glucose concentration from the cell free extract of *X. campestris*.